DOE F 4600.2
(03/11)
All Other Editions Are Obsolete

U.S. Department of Energy
FEDERAL ASSISTANCE REPORTING CHECKLIST
AND INSTRUCTIONS FOR RD&D PROJECTS

1. Identification Number: **DE-FE0006821**	2. Program/Project Title: **Small Scale Field Test Demonstration CO2 Sequestration**

3. Recipient:
University of Kansas Center for Research, Inc.

4. Reporting Requirements:	Frequency	Addressees
A. MANAGEMENT REPORTING		
☒ Research Performance Progress Report (RPPR)	Q	FITS@NETL.DOE.GOV
☒ Special Status Report	A	FITS@NETL.DOE.GOV
B. SCIENTIFIC/TECHNICAL REPORTING		
(Reports/Products must be submitted with appropriate DOE F 241. The 241 forms are available at www.osti.gov/elink)		
Report/Product — Form		
☒ Final Scientific/Technical Report — DOE F 241.3	FG	http://www.osti.gov/elink-2413
☒ Conference papers/proceedings* — DOE F 241.3	A	http://www.osti.gov/elink-2413
☐ Software/Manual — DOE F 241.4		
☐ Other (see special instructions) — DOE F 241.3		
** Scientific and technical conferences only*		
C. FINANCIAL REPORTING		FITS@NETL.DOE.GOV
☒ SF-425 Federal Financial Report	Q, FG	
D. CLOSEOUT REPORTING		
☒ Patent Certification	FC	FITS@NETL.DOE.GOV
☒ SF-428 & 428B Final Property Report	FC	FITS@NETL.DOE.GOV
☐ Other		
E. OTHER REPORTING		See block 5 below for instructions.
☒ Annual Indirect Cost Proposal	O	
☐ Audit of For-Profit Recipients		FITS@NETL.DOE.GOV
☒ SF-428 Tangible Personal Property Report Forms Family	A	
☒ Other – see block 5 below	A	FITS@NETL.DOE.GOV

FREQUENCY CODES AND DUE DATES:

A - Within 5 calendar days after events or as specified.
FG- Final; 90 calendar days after the project period ends.
FC- Final; End of Effort.
Y - Yearly; 90 calendar days after the end of the reporting period.
S - Semiannually; within 30 calendar days after end of project year and project half-year.
Q - Quarterly; within 30 days after end of the reporting period.
Y180 – Yearly; 180 days after the end of the recipient's fiscal year
O - Other; See instructions for further details.

5. Special Instructions:

Annual Indirect Cost Proposal – If DOE is the Cognizant Federal Agency, then the proposal should be sent to FITS@NETL.DOE.GOV . Otherwise, it should be sent to the Cognizant Federal Agency.

Other – The Recipient shall provide all deliverables as contained in Section D of Attachment 2 Statement of Project Objectives.

QUARTERLY PROGRESS REPORT

To
DOE-NETL
Brian Dressel, Program Manager
Award Number: DE-FE0006821

SMALL SCALE FIELD TEST DEMONSTRATING CO_2 SEQUESTRATION IN ARBUCKLE SALINE AQUIFER AND BY CO_2-EOR AT WELLINGTON FIELD, SUMNER COUNTY, KANSAS

Project Director/Principal Investigator:
W. Lynn Watney
Senior Scientific Fellow
Kansas Geological Survey

Ph: 785-864-2184, Fax: 785-864-5317
lwatney@kgs.ku.edu

Joint Principal Investigator:
Jason Rush
Assistant Project Manager
Jennifer Raney
Prepared by Lynn Watney, Jennifer Raney, and Tiraz Birdie with contributions by Eugene Holubnyak, Jason Rush, George Tsoflias, Brandon Graham, Alex Nolte, John Victorine, John Doveton, Brent Campbell, Jason Bruns,

Date of Report: Feb.8, 2016
DUNS Number: 076248616

Recipient: University of Kansas Center for Research &
Kansas Geological Survey
1930 Constant Avenue
Lawrence, KS 66047

Project/Grant Period: 10/1/2011 through 9/30/2016
Seventeenth Quarterly Report
Period Covered by the Report: October 1, 2015 through December 31, 2015
Signature of Submitting Official:

W. Lynn Watney

Digitally signed by W. Lynn Watney
DN: cn=W. Lynn Watney, o=The University of Kansas, ou=Kansas Geological Survey, email=lwatney@kgs.ku.edu, c=US
Date: 2016.02.08 09:02:24 -06'00'

EXECUTIVE SUMMARY

Project Objectives

The objectives of this project are to understand the processes that occur when a maximum of 70,000 metric tonnes of CO_2 are injected into two different formations to evaluate the response in different lithofacies and depositional environments. The evaluation will be accomplished through the use of both *in situ* and indirect MVA (monitoring, verification, and accounting) technologies. The project will optimize for carbon storage accounting for 99% of the CO_2 using lab and field testing and comprehensive characterization and modeling techniques.

CO_2 will be injected under supercritical conditions to demonstrate state-of-the-art MVA tools and techniques to monitor and visualize the injected CO_2 plume and to refine geomodels developed using nearly continuous core, exhaustive wireline logs, and well tests and a multi-component 3D seismic survey. Reservoir simulation studies will map the injected CO_2 plume and estimate tonnage of CO_2 stored in solution, as residual gas, and by mineralization and integrate MVA results and reservoir models shall be used to evaluate CO_2 leakage. A rapid-response mitigation plan will be developed to minimize CO_2 leakage and provide comprehensive risk management strategy. A documentation of best practice methodologies for MVA and application for closure of the carbon storage test will complete the project. The CO_2 shall be supplied from a reliable facility and have an adequate delivery and quality of CO_2.

Scope of Work

Budget Period 1 includes updating reservoirs models at Wellington Field and filing Class II and Class VI injection permit application. Static 3D geocellular models of the Mississippian and Arbuckle shall integrate petrophysical information from core, wireline logs, and well tests with spatial and attribute information from their respective 3D seismic volumes. Dynamic models (composition simulations) of these reservoirs shall incorporate this information with laboratory data obtained from rock and fluid analyses to predict the properties of the CO_2 plume through time. The results will be used as the basis to establish the MVA and as a basis to compare with actual CO_2 injection. The small scale field test shall evaluate the accuracy of the models as a means to refine them in order to improve the predictions of the behavior and fate of CO_2 and optimizing carbon storage.

Budget Period 2 includes completing a Class II underground injection control permit; drilling and equipping a new borehole into the Mississippian reservoir for use in the first phase of CO_2 injection; establishing MVA infrastructure and acquiring baseline data; establishing source of CO_2 and transportation to the injection site; building injection facilities in the oil field; and injecting CO_2 into the Mississippian-age spiculitic cherty dolomitic open marine carbonate reservoir as part of the small scale carbon storage project.

In Budget Period 3, contingent on securing a Class VI injection permit, the drilling and completion of an observation well will be done to monitor injection of CO_2 under supercritical conditions into the Lower Ordovician Arbuckle shallow (peritidal) marine dolomitic reservoir. Monitoring during pre-injection, during injection, and post injection will be accomplished with MVA tools and techniques to visualize CO_2 plume movement and will be used to reconcile simulation results. Necessary documentation will be submitted for closure of the small scale carbon storage project.

Project Goals

The proposed small scale injection will advance the science and practice of carbon sequestration in the Midcontinent by refining characterization and modeling, evaluating best practices for MVA tailored to the geologic setting, optimize methods for remediation and risk management, and provide technical information and training to enable additional projects and facilitate discussions on issues of liability and risk management for operators, regulators, and policy makers.

The data gathered as part of this research effort and pilot study will be shared with the Southwest Sequestration Partnership (SWP) and integrated into the National Carbon Sequestration Database and Geographic Information System (NATCARB) and the 6th Edition of the Carbon Sequestration Atlas of the United States and Canada.

Project Deliverables by Task

1.5	Well Drilling and Installation Plan (Can be Appendix to PMP or Quarterly Report)
1.6	MVA Plan (Can be Appendix to PMP or Quarterly Report)
1.7	Public Outreach Plan (Can be Appendix to PMP)
1.8	Arbuckle Injection Permit Application Review go/no go Memo
1.9	Mississippian Injection Permit Application Review go/no go Memo
1.10	Site Development, Operations, and Closure Plan (Can be Appendix to PMP)
2.0	Suitable geology for Injection Arbuckle go/no go Memo
3.0	Suitable geology for Injection Mississippian go/no go Memo
11.2	Capture and Compression Design and Cost Evaluation go/no go Memo
19	Updated Site Characterization/Conceptual Models (Can be Appendix to Quarterly Report)
21	Commercialization Plan (Can be Appendix to Quarterly Report).
30	Best Practices Plan (Can be Appendix to Quarterly or Final Report)

ACCOMPLISHMENTS

1. Completed installation of on-site CO2 storage equipment and injection skid.
2. Begin CO_2 injection into the Mississippian reservoir.
3. Installed equipment to monitor injection and recovery of CO2.
4. Began systematic monitoring of brine and gases at Wellington to understand the behavior of CO2 and interaction with brine, oil, and reservoir rocks.
5. EPA's determination of the absence of a USDW for the Class VI permit application.

6. Submitted and received response from EPA refined conservative AoR model (Revised Section 5 of the Class VI permit.
7. Received portions of draft Class VI permit to review
8. Received requirements for the Financial Assurance and the Post Injection Site Care.
9. Refined and verified 18-seismometer array at Wellington with nearby earthquakes begin updating the earthquake catalog on a weekly basis.
10. Workflow in place to report notable earthquakes within 24 hours to ensure location and magnitude.
11. Participate in continued discussion and presentation on induced seismicity in the context of a safe and effective CO2 injection at Wellington.

Project Schedule

Schedule and costs for Arbuckle CO2 injection --

A no-cost-time extension (NCTE) will be filed in mid-February anticipating that a draft Class VI permit will be issued prior to April 2016.

Continuation Application (CA) for BP3 will be filed by April 2016 after receipt of the draft Class VI permit. The CA will include:

1) Summarize status and findings from the CO2-EOR injection in the Mississippian reservoir;
2) Review revised budget for the BP3 Arbuckle injection and PISC based on updated costs including financial responsibility and post injection site care;
3) review of the timeline, accomplishments, costs, and issues addressed during the course of the project;
4) review the draft Class VI permit and convey obligations and costs to the project as included in the financial assurance and post injection site care of the Class VI permit;
5) justify entering the budget period 3 to seek permission to proceed with preparations for the test injection - drilling #2-28, completing and testing #2-28 and #1-28;
6) Revise schedule and cost tables.

Wellington project will end on September 30, 2016 without a draft permit in the April 2016 timeframe. A time extension of the project will be needed to accommodate the Arbuckle CO2 injection now estimated to begin in February 2017 after #2-28 is drilled and CASSM and U-Tube are fabricated, installed and tested in the 2nd half of 2016 **(Figure 1**). A six-month long injection of CO2 at ~150 tonnes per day is anticipated based on the delivery from Linde for the Mississippian injection. The injection equipment and supply at this time suggest the injection could be done more quickly. The completion date anticipated for the CO2 injection is end of July 2017 so the one year post injection site care would begin in August 2017 and continue through August 2018 (**Figure 1**).

Figure 1. Revised timetable for DE-FE0006821.

MILESTONE STATUS REPORT

Task	Budget Period	Number	Milestone Description
Task 2.	1	1	Site Characterization of Arbuckle Saline Aquifer System - Wellington Field
Task 3.	1	2	Site characterization of Mississippian Reservoir for CO2 EOR - Wellington Field
Task 10.	2	3	Pre-injection MVA - establish background (baseline) readings
Task 13.	2	4	Retrofit Arbuckle Injection Well (#1-28) for MVA Tool Installation
Task 18.	3-yr1	5	Compare Simulation Results with MVA Data and Analysis and Submit Update of Site Characterization, Modeling, and Monitoring Plan
Task 22.	3-yr1	6	Recondition Mississippian Boreholes Around Mississippian CO2-EOR injector
Task 27.	3-yr2	7	Evaluate CO2 Sequestration Potential of CO2-EOR Pilot
Task 28.	3-yr2	8	Evaluate Potential of Incremental Oil Recovery and CO2 Sequestration by CO2-EOR - Wellington field

Task 2. Site Characterization of Arbuckle Saline Aquifer System – Wellington Field

Area of Review for EPA was refined substantially with the development of a conservative model that was resubmitted to EPA in December 2015. The revised Section 5 from the Class VI application is included in **Appendix A**. Central to the modeling and parameter definition is the distinct of 9 rock types (**Figure 2**). The rock type characterized by higher porosity and permeability in clearly distinguished in the Arbuckle model shown in **Figure 2**.

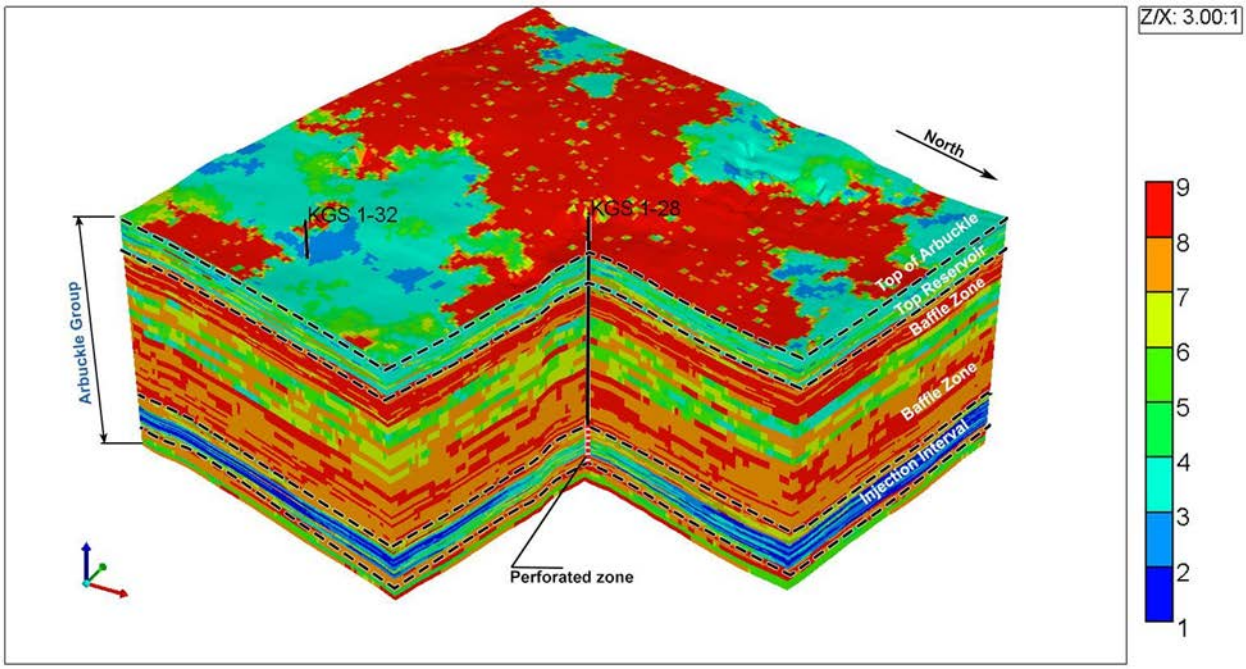

Figure 2. Rock type distribution model for the Arbuckle Group at Wellington Field.

The rock types illustrated in a west-to-east cross section thorugh the Arbuckle Group in Wellington Field delineates the zone to be perforated zone for the small scale CO2 injection (**Figure 3**). The interval consists of a succession of shallowing upward meter-scale peritidal cycles of primarily of porous packstones and grainstones. The cycles are capped by beds of breccia consisting of dissolved evaporite karst believed accumulated in shallow hypersaline ponds that were later dissolved when understaturated water returned. This led to the dissotuion of evaporite prior to the deposition of the next cycle as supported by early soft-sediment depositional fabrics intimately part of the karst breccia interval. This zone of higher transmissivity is clearly a stratiform bound interval that serves as a flow unit, bounded above and below by tighter less porous and permeable strata.

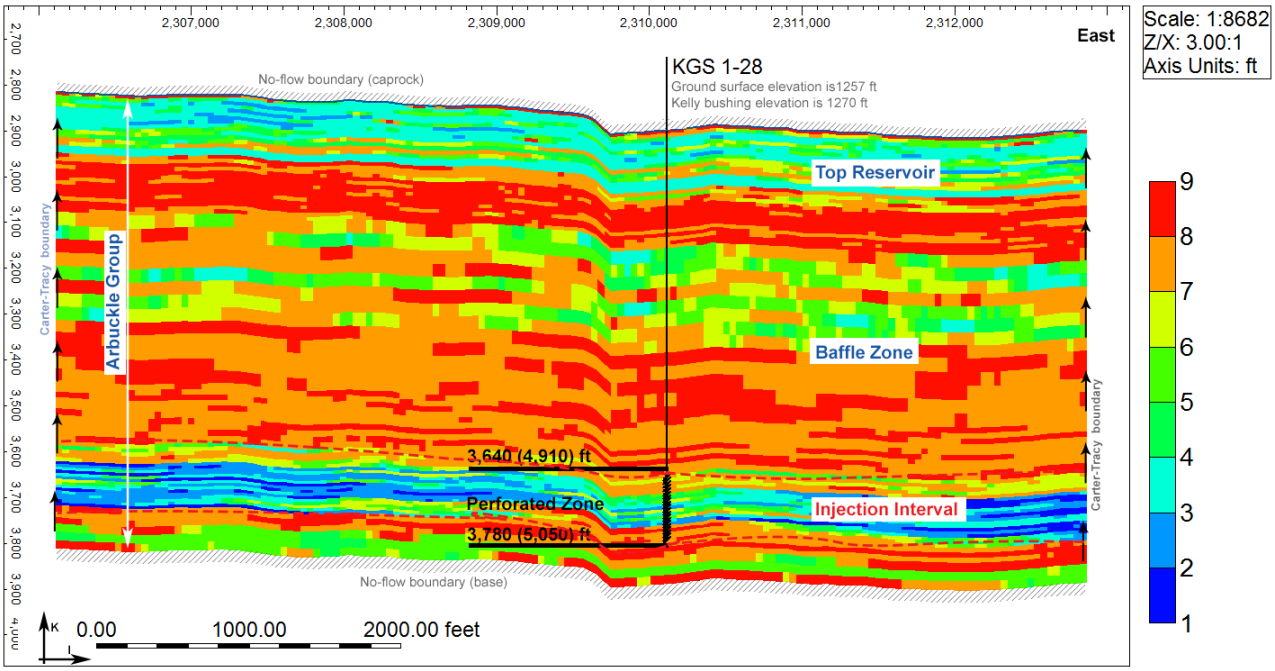

Figure 3. West to east cross section of the Arbuckle in Wellington Field with location of the CO2 injection well, #1-28 and perforation interval located in the lower Arbuckle. Index map is shown in Figure 5.

Each rock type with varying reservoir quality index includes differences in relative permeability and capillary pressure (**Figure 4** and **Table 1**).

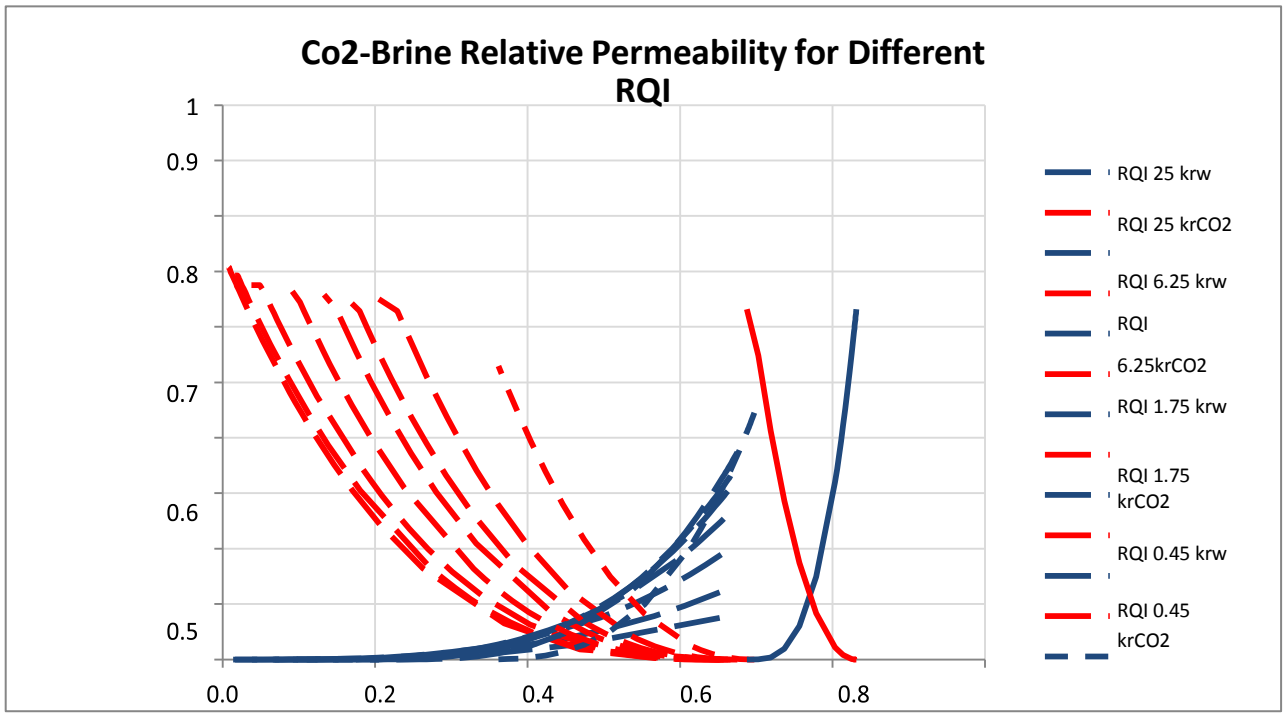

Figure 4. Calculated relative permeability for drainage (left) and imbibition (right) for full set of RQI.

Drainage Curves

RQI range from 0.3-0.4-AveRQI=0.35				
Pc	Sw	sCO_2	Krw	$krCO_2$
1	1.000	0.000	1.000	0.000
2	0.877	0.123	0.735	0.001
3	0.641	0.359	0.338	0.029
4	0.518	0.482	0.190	0.086
5	0.443	0.557	0.119	0.148
6	0.392	0.608	0.080	0.205
7	0.354	0.646	0.056	0.257
8	0.326	0.674	0.041	0.302
9	0.304	0.696	0.030	0.341
10	0.286	0.714	0.023	0.375
12	0.258	0.742	0.013	0.432
14	0.238	0.762	0.008	0.478
18	0.211	0.789	0.003	0.545
20	0.201	0.799	0.002	0.571
25	0.183	0.817	0.000	0.620
30	0.171	0.829	0.000	0.655
40	0.156	0.844	0.000	0.655
50	0.146	0.854	0.000	0.655
60	0.140	0.860	0.000	0.655
70	0.135	0.865	0.000	0.655
80	0.131	0.869	0.000	0.655
90	0.129	0.871	0.000	0.655
100	0.126	0.874	0.000	0.655
150	0.119	0.881	0.000	0.655
200	0.116	0.884	0.000	0.655
300	0.112	0.888	0.000	0.655

Imbibition Curves

RQI range from 0.3-0.4-AveRQI=0.35				
Pc	Sw	sCO_2	Krw	$krCO_2$
0	0.666	0.334	0.331	0.000
0.00	0.665	0.335	0.328	0.000
0.01	0.663	0.337	0.325	0.000
0.02	0.660	0.340	0.319	0.000
0.03	0.657	0.343	0.313	0.000
0.04	0.654	0.346	0.308	0.000
0.05	0.652	0.348	0.302	0.000
0.06	0.649	0.351	0.297	0.000
0.07	0.646	0.354	0.292	0.000
0.08	0.643	0.357	0.287	0.000
0.09	0.640	0.360	0.282	0.001
0.1	0.638	0.362	0.277	0.001
0.2	0.612	0.388	0.234	0.003
0.3	0.589	0.411	0.200	0.008
0.4	0.569	0.431	0.171	0.013
0.5	0.550	0.450	0.148	0.020
0.6	0.532	0.468	0.128	0.029
0.7	0.516	0.484	0.112	0.038
0.8	0.501	0.499	0.098	0.047
0.9	0.487	0.513	0.086	0.057
1	0.474	0.526	0.076	0.067
2	0.383	0.617	0.026	0.172
3	0.329	0.671	0.011	0.261
4	0.293	0.707	0.005	0.333
5	0.267	0.733	0.002	0.390
6	0.248	0.752	0.001	0.437
7	0.233	0.767	0.001	0.476
8	0.221	0.779	0.000	0.508
9	0.211	0.789	0.000	0.536
10	0.203	0.797	0.000	0.559
12	0.189	0.811	0.000	0.598
14	0.180	0.820	0.000	0.629
20	0.160	0.840	0.000	0.655
30	0.144	0.856	0.000	0.655
40	0.135	0.865	0.000	0.655
50	0.129	0.871	0.000	0.655
60	0.126	0.874	0.000	0.655
70	0.123	0.877	0.000	0.655
80	0.121	0.879	0.000	0.655
90	0.119	0.881	0.000	0.655
100	0.117	0.883	0.000	0.655
150	0.113	0.887	0.000	0.655
200	0.111	0.889	0.000	0.655
300	0.109	0.891	0.000	0.655

Table 1. Example of capillary pressure and relative permeability drainage and imbibition tables for rock type 6 (RQI=0.35)

The resulting AoR from these refinements of the led to a reduction in area of concentrated CO2, but a more complex distribution of the CO2 plume (**Figure 5**). The areas of higher CO2 saturation are areas of higher porosity and permeability and distribution, based on interpolation using the depth-migrated seismic, is more realistic of the likely distribution of the peritidal flats, suggesting

tidal channel-form features along which ponded hypersaline brine may have led to precipitation of the gypsum that later dissolved as undersaturated waters again occupied the area.

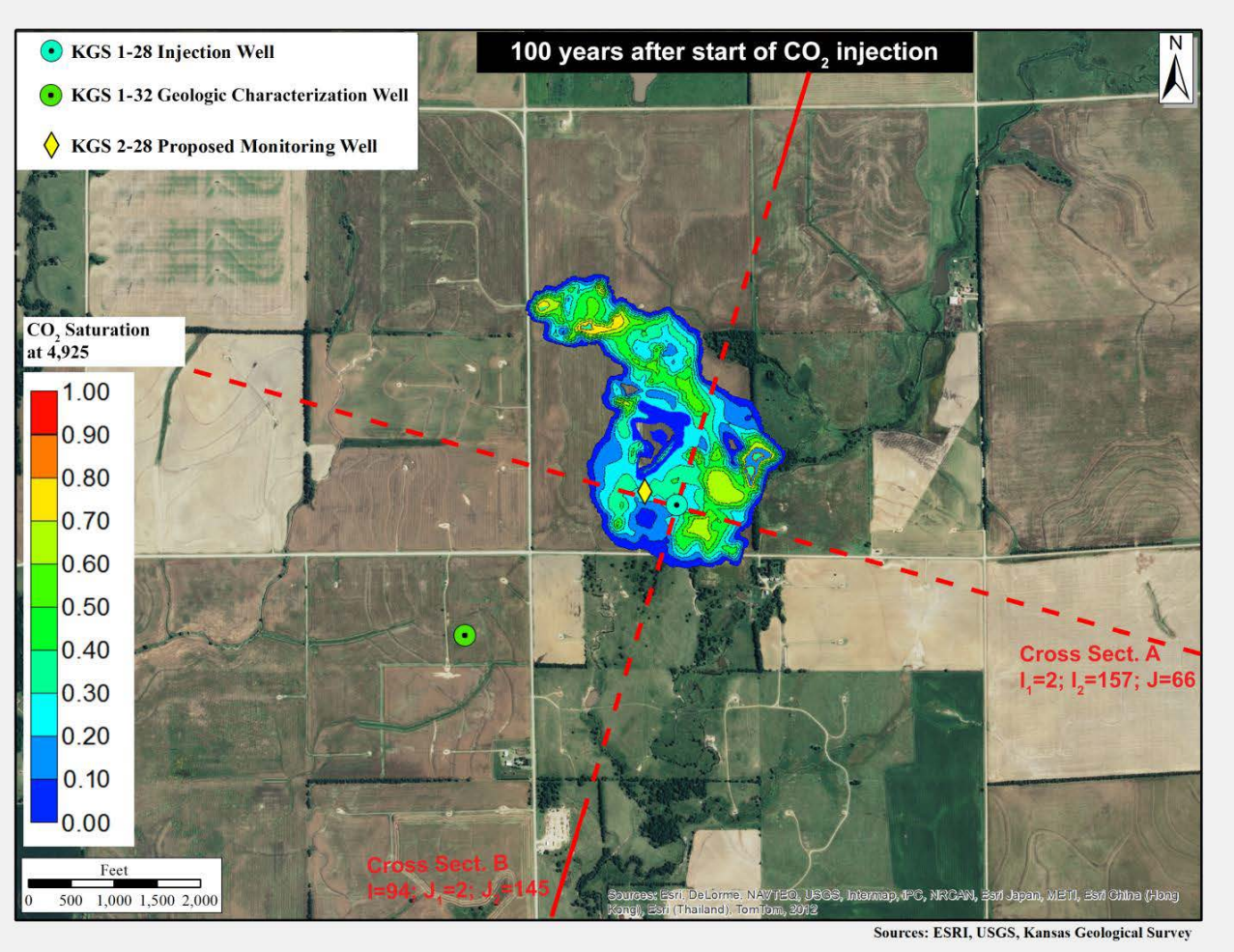

Figure 5. The Area of Review was revised to include the location of CO2 saturation after 100 years.

The CO2 saturation after 100 years post injection is shown in cross section view in **Figure 6**. The thin stratified layers of varying CO2 saturation reflect the meter-scale peritidal cycles of a succession of rock types in the injection zone.

A map of pressure after 9-months of CO2 injection show safe levels of pressure under 30 psi at distances of more than 500 ft from the injection well. This is indicative of the benign nature of the CO2 plume (**Figure 6**).

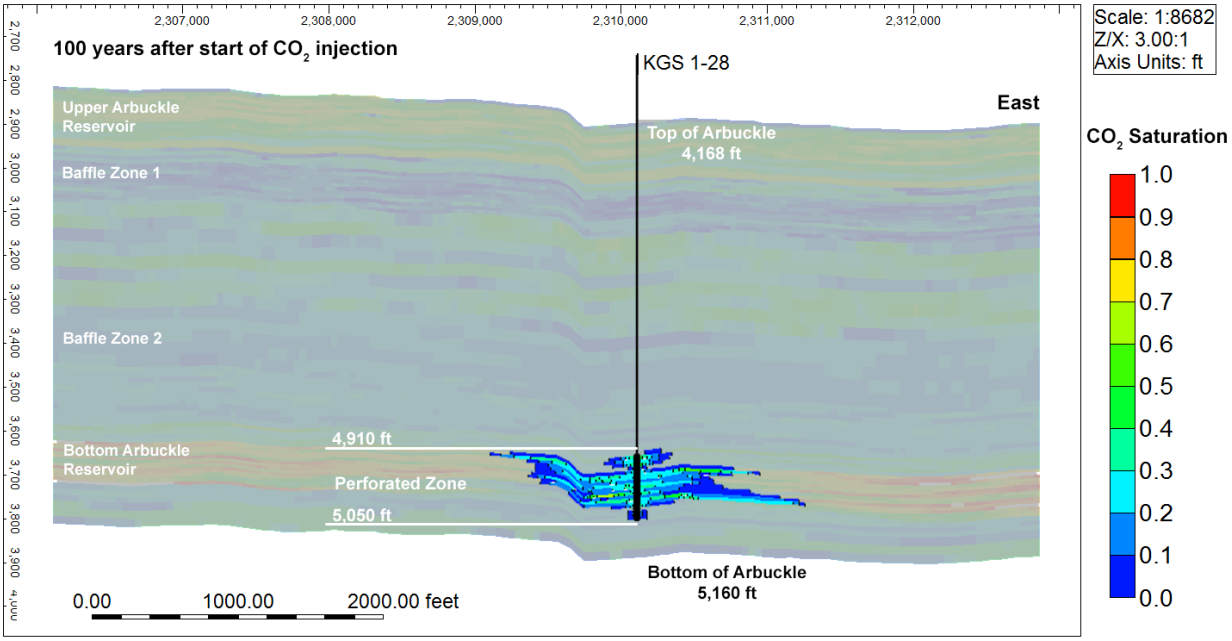

Figure 5. West to east cross section depicts CO2 saturation after 100 years post injection. Cross section index line show on map in Figure 6.

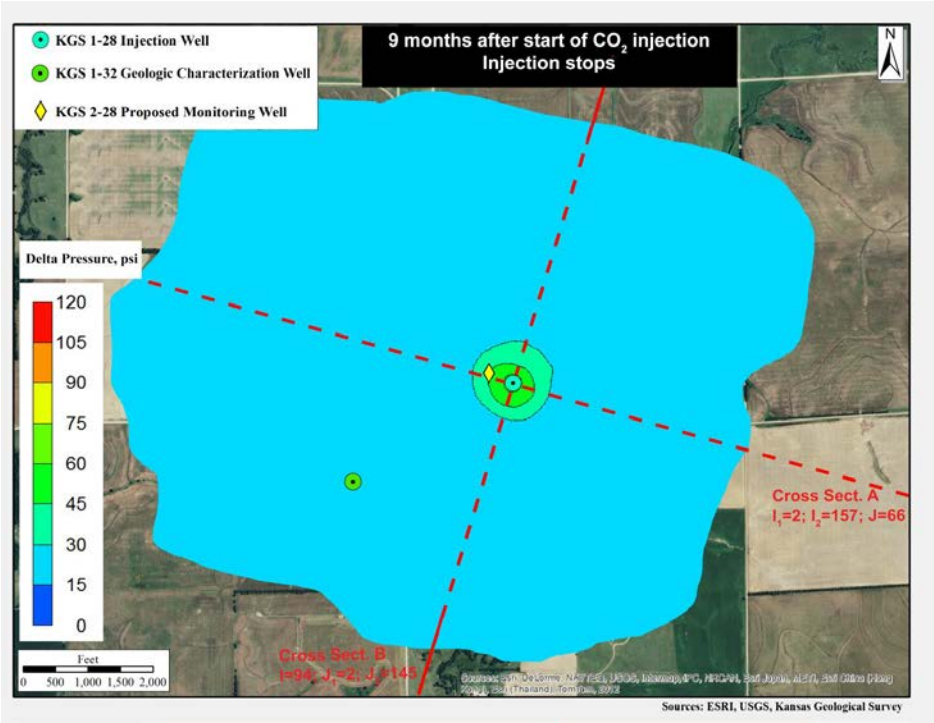

Figure 6. Map of delta pressure in injection zone follow 9 months of CO2 injection.

The delta pressure vs. distance plot for varying times since injection started are shown in **Figure 7**. Pressure drops off rapidly beyond 500 ft from the injection well.

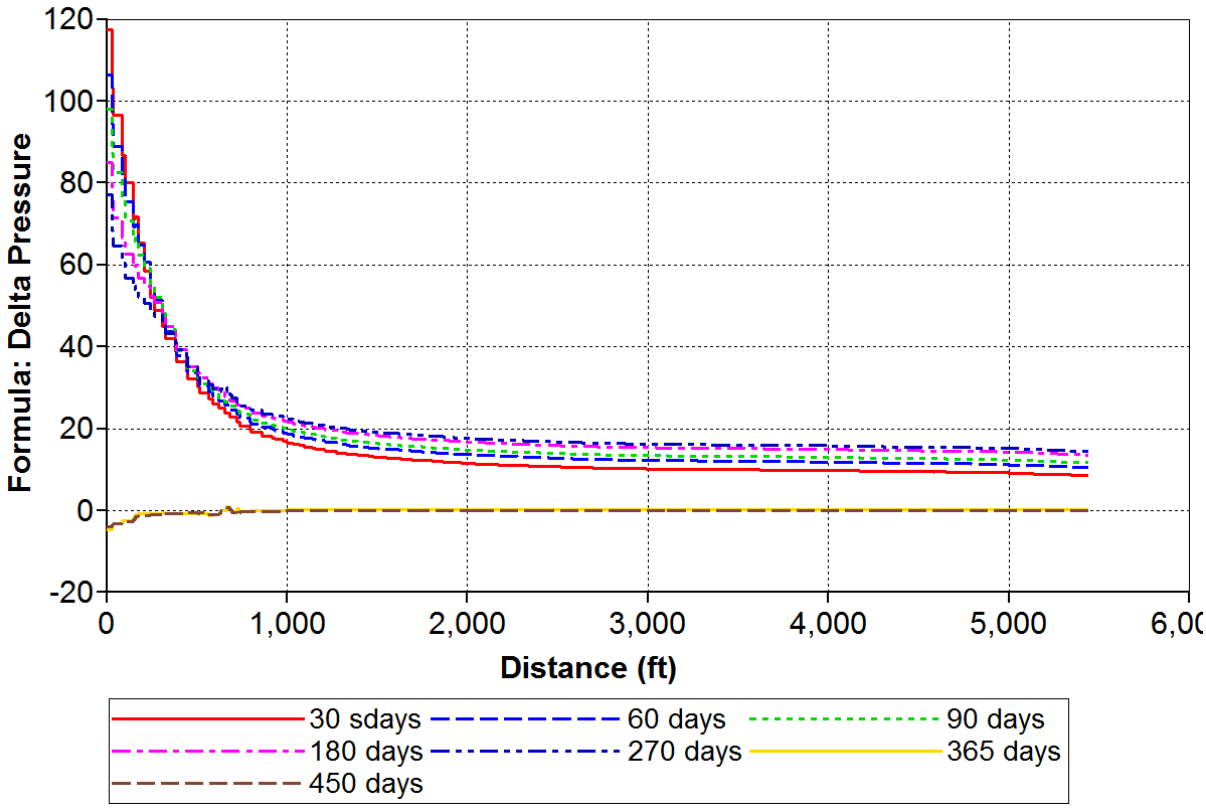

Figure 7. Pore pressure as a function of lateral distance from the injection well (KGS 1-28) at 7 time intervals for the highest induced pressure case (k-0.75/phi-0.75).

Class VI Permit for Arbuckle CO2 Injection

We will complete the work and submit information to EPA including Fault and induced seismicity, the AoR Evaluation of Completeness, and the Financial Responsibility (FR) table. We have sought and have been receiving official quotes from contractors to meet EPA requirements for the financial responsibility. We will use this cost estimates to update budget projections for the PISC period for our upcoming Continuation Application to extend the project period and continue into BP3. We are using this opportunity to refine monitoring activities to reflect new findings that have been learned since the original plans were developed, e.g., cost-effective utilization of the AVO for CO2 detection with the repeat 3D and 2D surveys. Revised estimates for seismic acquisition and processing are low and advantageous to the project.

Task 3. Site Characterization of Mississippian Reservoir for CO2-EOR – Wellington Field

The Mississippian reservoir model continues to be refined with the new data and is being used to estimate behavior of the CO2-EOR.

Task 10. Pre-Injection MVA- establish background (baseline) readings.

EPA has determine that the Wellington site does not have a viable USDW based on the reporting provided to date. The brine analyses have moved on o evaluating the progress of the CO2 flood in the Mississippian oil reservoir.

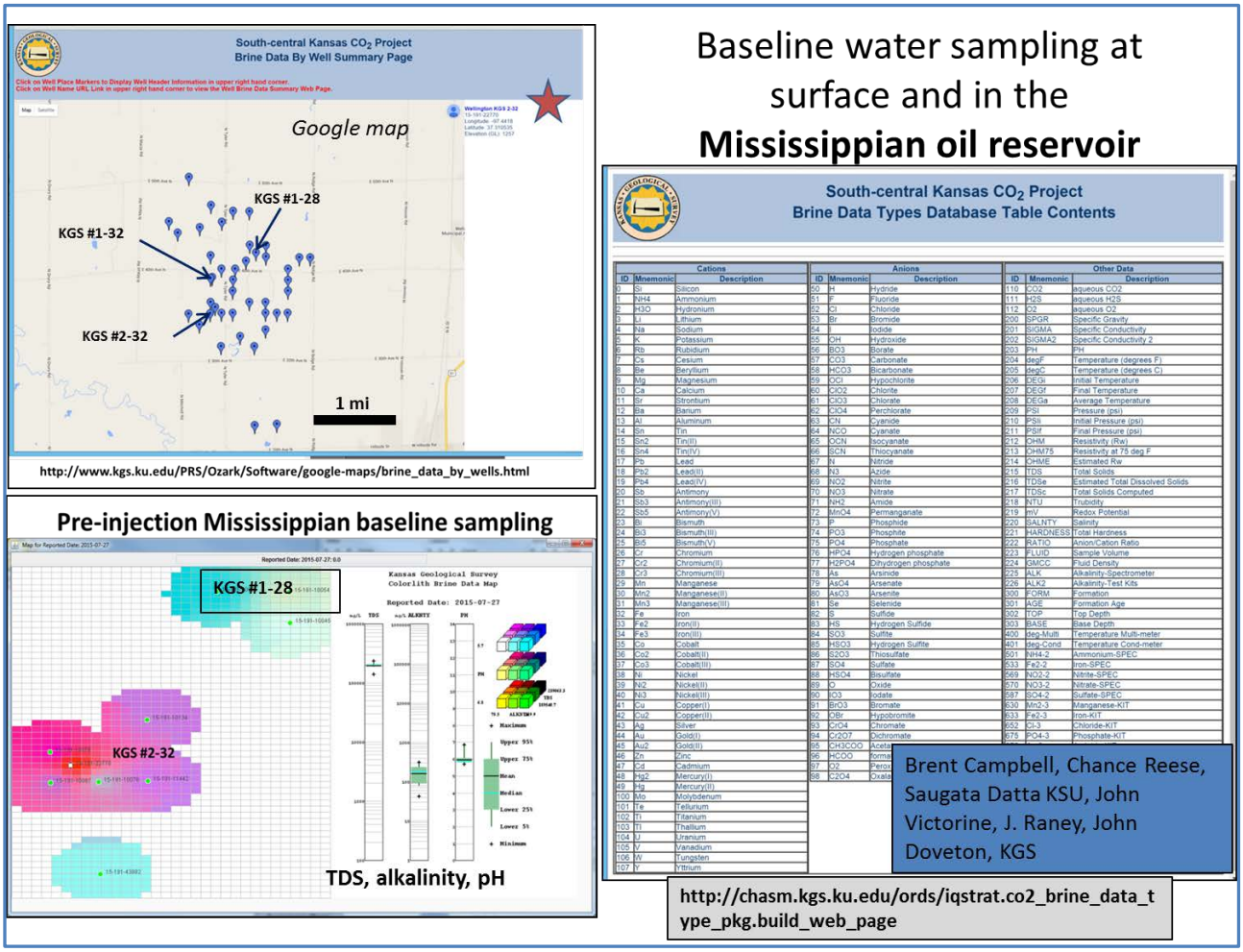

Figure 8. Web applications used access and analyze the brine chemistry.

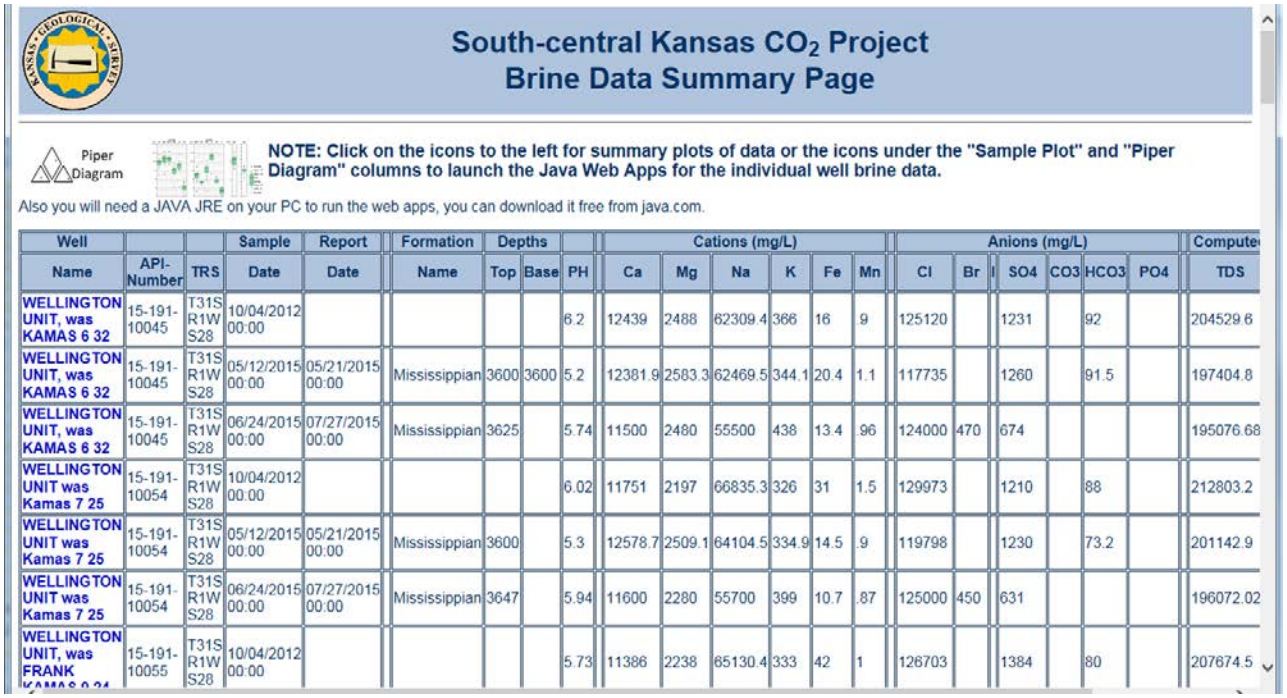

South-central Kansas CO_2 Project
Brine Data Summary Page

Piper Diagram

NOTE: Click on the icons to the left for summary plots of data or the icons under the "Sample Plot" and "Piper Diagram" columns to launch the Java Web Apps for the individual well brine data.

Also you will need a JAVA JRE on your PC to run the web apps, you can download it free from java.com.

Well			Sample	Report	Formation	Depths			Cations (mg/L)						Anions (mg/L)						Compute
Name	API-Number	TRS	Date	Date	Name	Top	Base	PH	Ca	Mg	Na	K	Fe	Mn	Cl	Br	SO4	CO3	HCO3	PO4	TDS
WELLINGTON UNIT, was KAMAS 6 32	15-191-10045	T31S R1W S28	10/04/2012 00:00					6.2	12439	2488	62309.4	366	16	9	125120		1231		92		204529.6
WELLINGTON UNIT, was KAMAS 6 32	15-191-10045	T31S R1W S28	05/12/2015 00:00	05/21/2015 00:00	Mississippian	3600	3600	5.2	12381.9	2583.3	62469.5	344.1	20.4	1.1	117735		1260		91.5		197404.8
WELLINGTON UNIT, was KAMAS 6 32	15-191-10045	T31S R1W S28	06/24/2015 00:00	07/27/2015 00:00	Mississippian	3625		5.74	11500	2480	55500	438	13.4	96	124000	470	674				195076.68
WELLINGTON UNIT was Kamas 7 25	15-191-10054	T31S R1W S28	10/04/2012 00:00					6.02	11751	2197	66835.3	326	31	1.5	129973		1210		88		212803.2
WELLINGTON UNIT was Kamas 7 25	15-191-10054	T31S R1W S28	05/12/2015 00:00	05/21/2015 00:00	Mississippian	3600		5.3	12578.7	2509.1	64104.5	334.9	14.5	9	119798		1230		73.2		201142.9
WELLINGTON UNIT was Kamas 7 25	15-191-10054	T31S R1W S28	06/24/2015 00:00	07/27/2015 00:00	Mississippian	3647		5.94	11600	2280	55700	399	10.7	87	125000	450	631				196072.02
WELLINGTON UNIT, was FRANK	15-191-10055	T31S R1W S28	10/04/2012 00:00					5.73	11386	2238	65130.4	333	42	1	126703		1384		80		207674.5

Figure 9. The brine data summary page from the web application provides a means to examine analyses from a succession of sampling dates and to download the data for use in other applications.

The delineation of the USDW continued in October with another round of sampling of the three monitoring wells at Wellington and two domestic wells and Slate Creek off south of the Wellington field (**Figure 10**). Water was analyzed and compared to each other and what had been previously determined. The three monitoring wells show in pattern of increasing TDS with depth toward the Hutchinson Salt layer that lies ~30 ft below the last deepest (200 ft) well (**Figure 11**). The comparison of water from the freshwater samples and the briney monitoring wells at Wellington (**Figures 12 and 13**) show that the shallow Pleistocene terrace sample is proably a mixture of meteoric and natural brine. The natural brines above the Hutchinson Salt in the Wellington Shale look very similar to the Mississippian brine that are compared in **Figure 13**.

A color map based on the pH, alkalinity, and TDS values in from the shallow sampling show the contrast between the fresh and briney wells (**Figure 14**). The tabular summary of this data is shown in **Figure 15**.

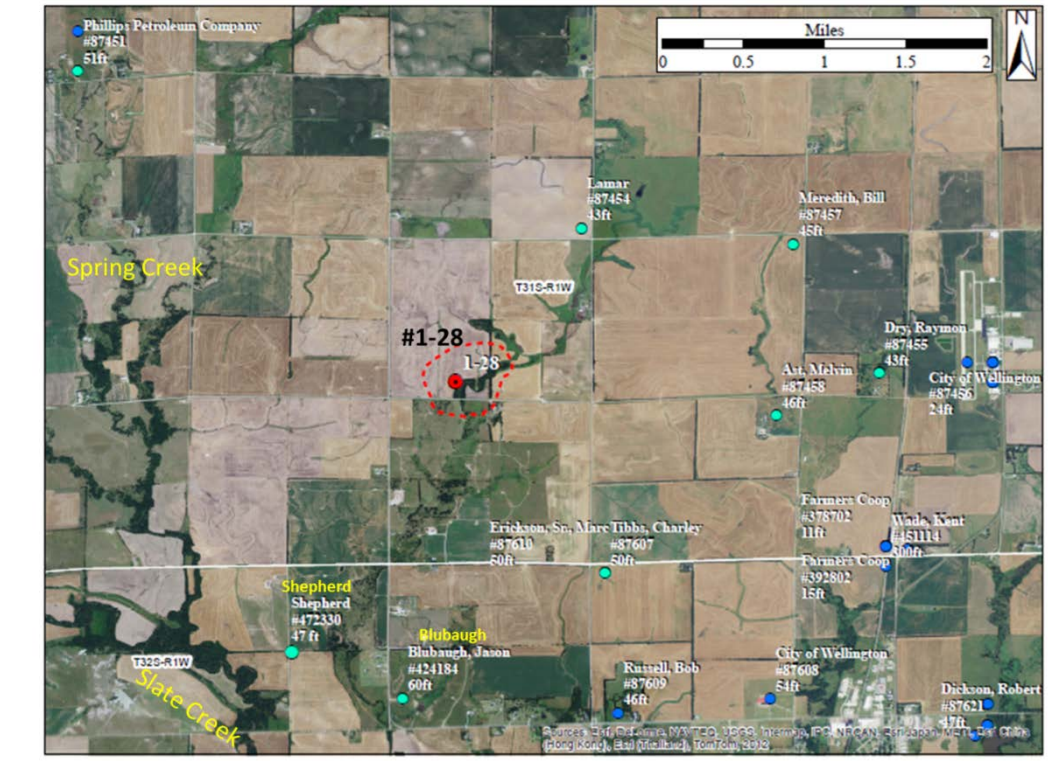

Figure 10. Location of injection well #1-28 and CO2 plume (red dashed line) compared to freshwater wells and Slate Creek to the south and southwest.

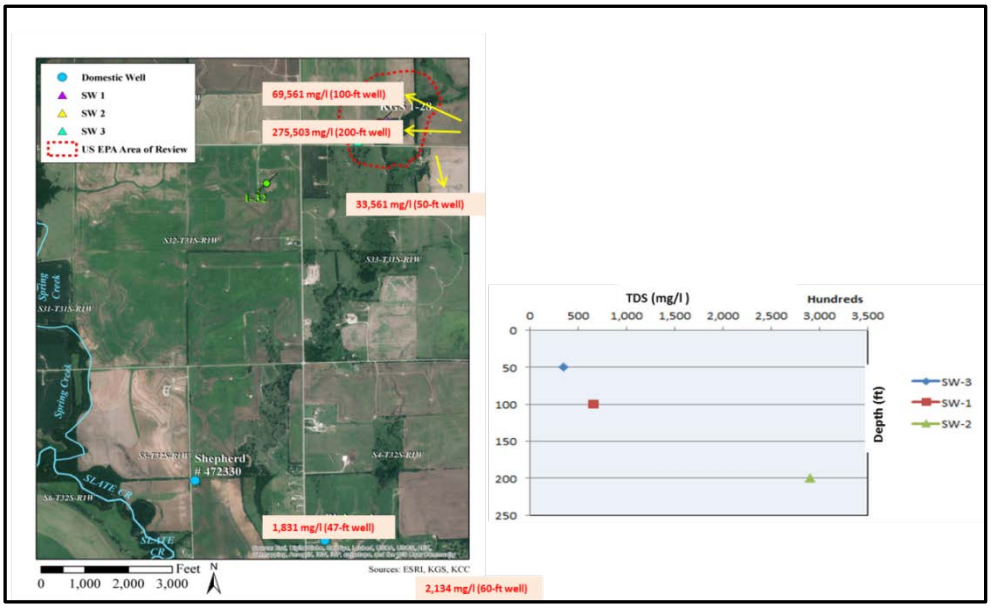

Figure 11. Total dissolved solids (TDS) in mg/l from early October sampling of freshwater wells and test wells at Wellington Field. The plot shows the TDS vs. depth (ft) for the three Wellington wells

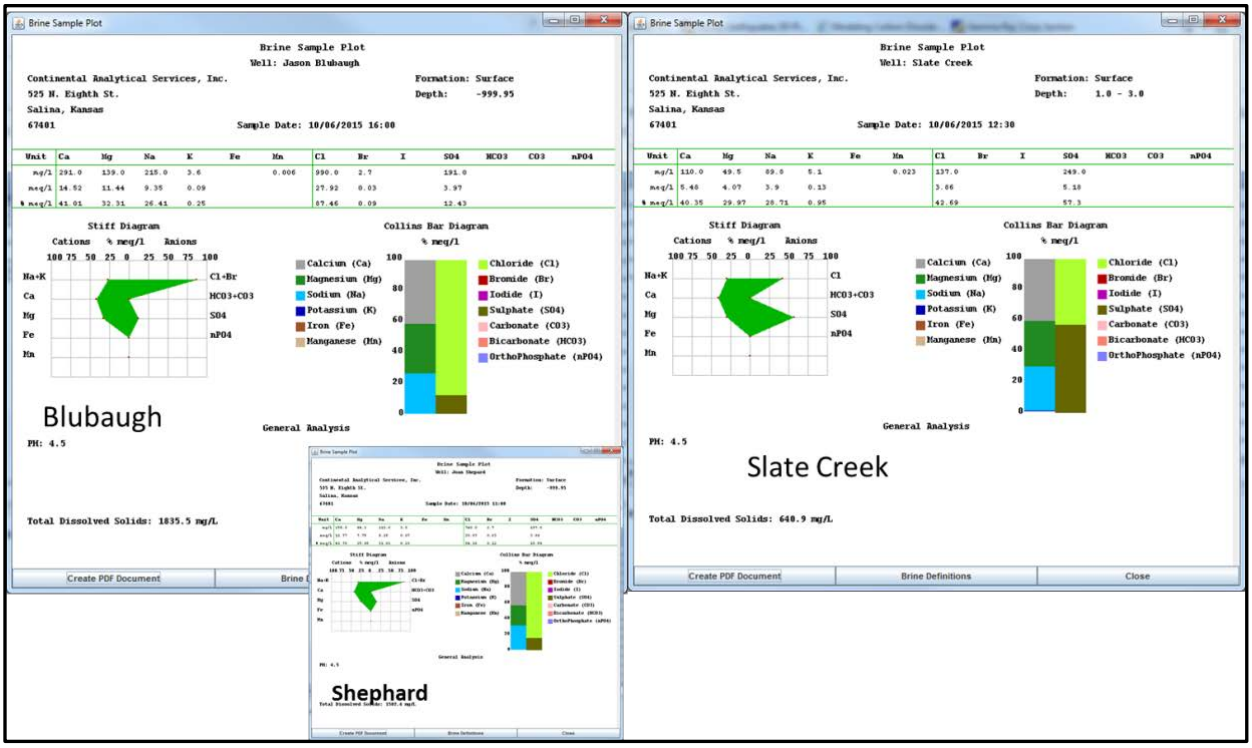

Figure 12. Stiff and Collins Bar Diagrams for domestic water wells and Slate Creek that are yielding water from along the incised valley that cuts the Wellington Shale. The charts have similar patterns to each other.

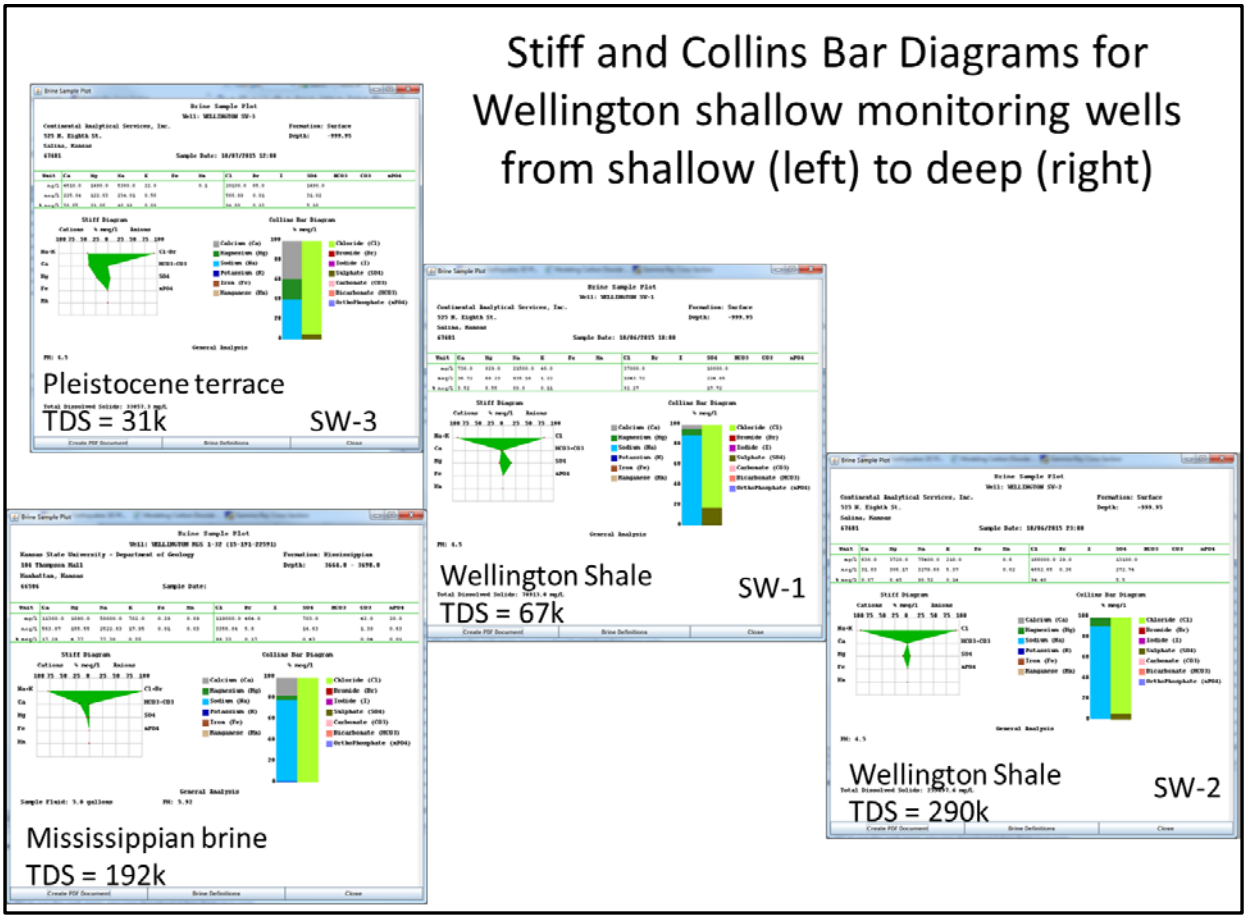

Figure 13. Stiff and Collins bar diagrams for Wellington shallow monitoring wells from shallow to deep (left to right). These are compared to the Mississippian brine on the lower left.

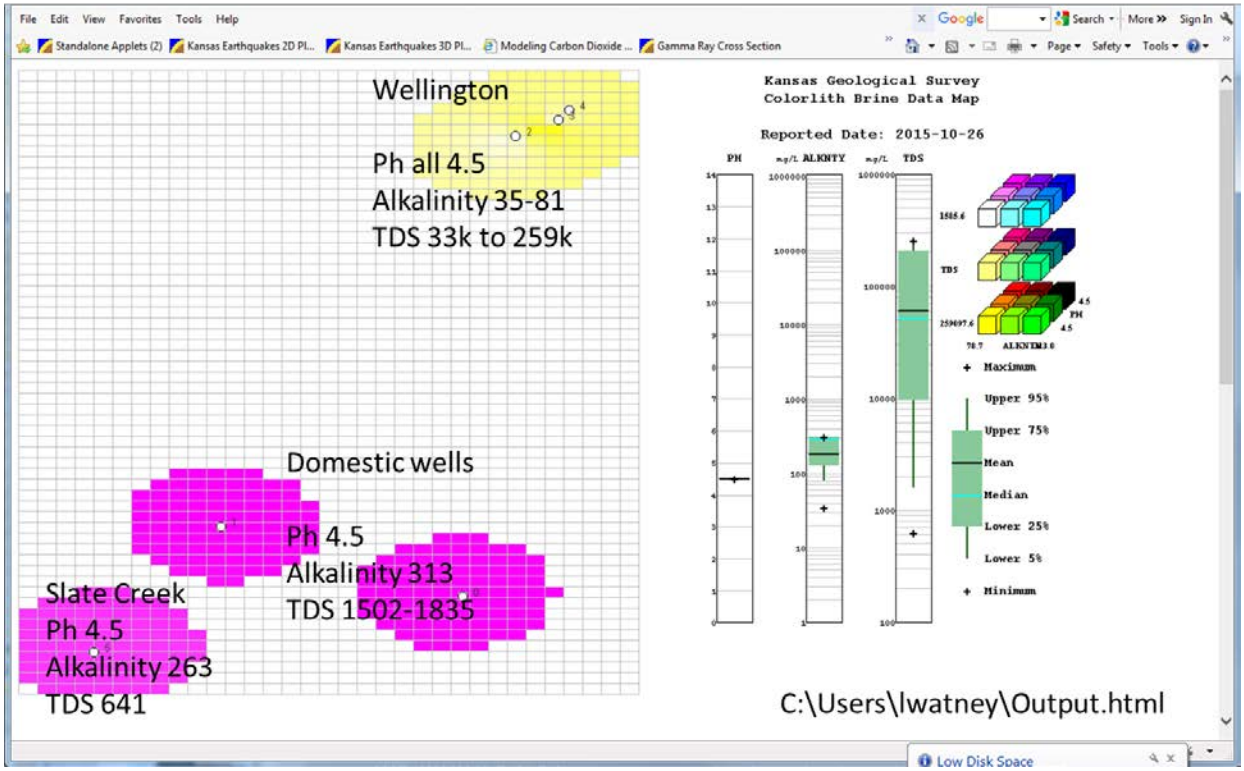

Figure 14. A "colorlith" map showing distribution of three components (pH, alkalinity, and TDS) from the brine analyses for the sets of freshwater wells and Slate Creek in the south and the monitoring wells at Wellington Field on the north.

Oil & Gas Well Data

API Number	Well Name	Latitude	Longitude	PH	ALKNTY	TDS
0	Jason Blubaugh	37.291148	-97.438162	4.5	313.0	1835.5
1	Joan Shepard	37.2953918	-97.447967	4.5	313.0	1502.4
2	WELLINGTON SW-3	37.318081	-97.43542	4.5	81.0	33057.3
3	WELLINGTON SW-2	37.319006	-97.433636	4.5	35.0	259097.6
4	WELLINGTON SW-1	37.319583	-97.4332	4.5	78.0	70913.0
5	Slate Creek	37.288111	-97.453333	4.5	263.0	640.9

Data Statistics

MNEM	Description	Minimum	5%	25%	Mean	Median	75%	95%	Maximum
PH	PH	4.5	4.5	4.5	4.5	4.5	4.5	4.5	4.5
ALKNTY	Alkalinity	35.0	78.75	126.5	288.0	180.5	313.0	313.0	313.0
TDS	Total Solids Computed	640.9	1585.67	9640.95	51985.15	61174.45	212051.45	259097.6	259097.6

Gridding Parameter & Calculated Data

Grid Area Parameters

Minimum X in feet: 509442.0
Maximum X in feet: 516966.0
Number of Columns: 34
Minimum Grid Spacing: 228.0
Minimum Y in feet: -912.0
Maximum Y in feet: 12532.0
Number of Rows: 59

Search Parameter Selection

Inverse Distance Weighting Exponent: 2.0
Number of Nearest Neighbors: 6
Maximum Distance to Nearest data point, ft: 1254.0
Maximum Search Radius, ft: 2508.0

Colorlith Plot Limits

			Minimum		Maximum	
MNEM	Description	Color	BrineData	Color Value	Brine Data	Color Value
PH	PH	RED	4.5	255	4.5	0
ALKNTY	Alkalinity	GREEN	78.7	255	313.0	0
TDS	Total Solids Computed	BLUE	1585.6	255	259097.6	0

Figure 15. Tabular summary of data shown in map in Figure 14.

Task 27. (Milestone 7) Evaluate CO2 Sequestration Potential of CO2-EOR Pilot

The first truckload of CO2 was injected into the Mississippian oil reservoir on December 23rd. Full-scale injection began on January 12, 2016 (**Table 2**).

12/18/15	Increase injection to 500 bwpd. Move in first CO2 storage tank.
12/23/15	Move in one transport truckload of CO2. Hook up truck to suction side of Berexco CO2 injection pump. Pump 17 US tons of CO2 down the KGS 2-32 CO2 injection well using the CO2 injection pump over 2.5 hours total. Starting pressure 500 psi, final injection pressure 300 psi. Resume water injection. Total CO2 pumped down well 34,135 lbs. Max rate 1750 bbl per day rate at 300 psi, which is approx 310 tons per day. Resume injection at 500 bwpd. Cumulative water injection to date: 21,894 bbl water.
12/24/15	500 bwipd
12/29/15	Begin filling CO2 storage tanks. Four 70 ton storage tanks on location.
1/4/16	Begin test CO2 injection with all equipment on site operational.
1/5-1/11/16	test injection of CO2.
1/12/16	Begin full scale injection of CO2.
1/13/16	Injecting CO2 at 1202 Bbl/day rate, 200 psi wellhead pressure. Plant ran overnight OK. Cumulative CO2 injection to date 1587 bbl CO2.
1/14/16	Injected 1231 BBL CO2 @ 185# TP. Linde's CO2 source was shut down, and as a result, was unable to deliver CO2. Ceased CO2 injection at 5:00 pm and killed well with 13 BBL water through injection pump. Began water injection from Wellington Unit.
1/15/16	Injected 426 BBL CO2 before switching to water. Injected 206 BBL water. Currently injecting 394 BWPD at vacuum.

Table 2. Well report for the CO2-EOR injection well during the time from the initial test CO2 injection on December 23 to full-scale CO2 injection on January 12, 2016.

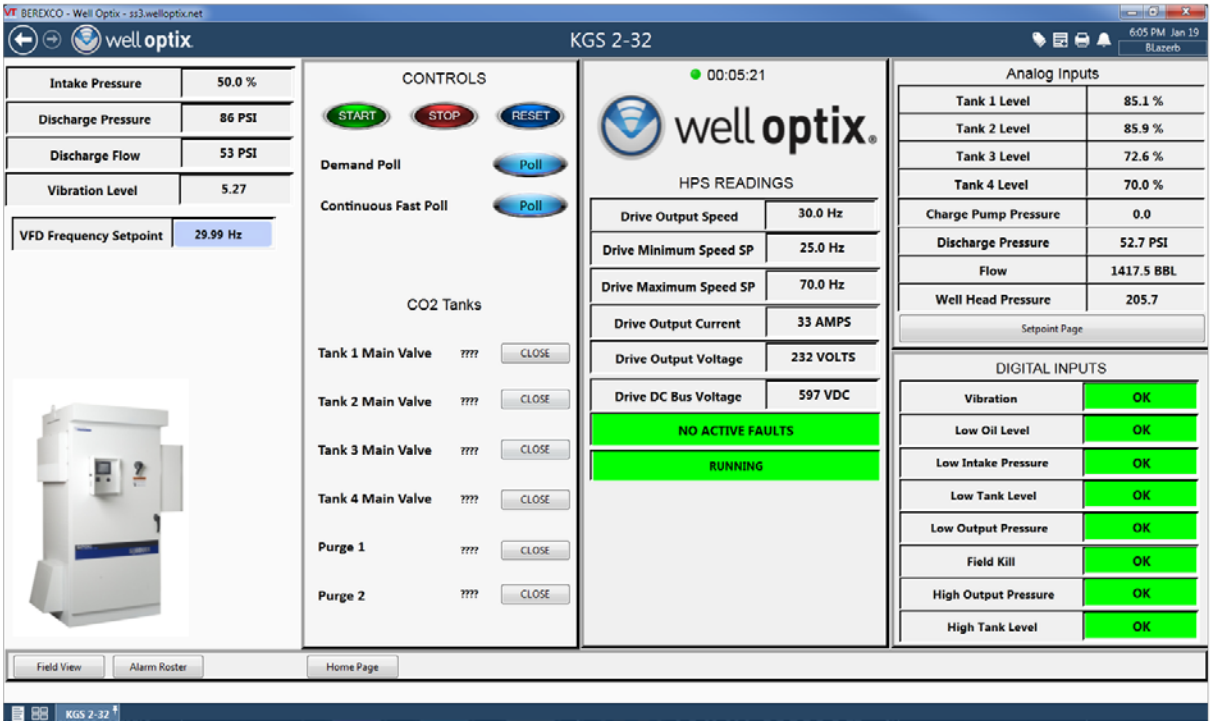

Figure 16. Test display panel for web-based Mississippian CO2 injection at well #2-32 on January 19, 2016.

A total of 3,531 metric tons of CO2 have been injected in the Mississippian oil reservoir for week ending Feb. 5, 2016. The incremental injection has increased to approximately 250 metric tons per day (**Figure 17**). Berexco has developed an operational that that is both efficient and reliable for the injection of the CO2, closely monitoring the volumes of CO2 injected and installing flow meters and CO2 detectors so that the material balance of CO2 and brine injected can be compared with the CO2, oil, brine, and other gases can be established. Linde has indeed proven that they can deliver a steady supply that is being adjusted (increased) as the injectivity of the well is established. Onsite storage is sufficient to handle approximately 700 tonnes to accommodate short interruptions when the source undergoes maintenance (**Figure 18**). CO2 continues to be supplied by fertilizer plants in Enid and Woodward Oklahoma.

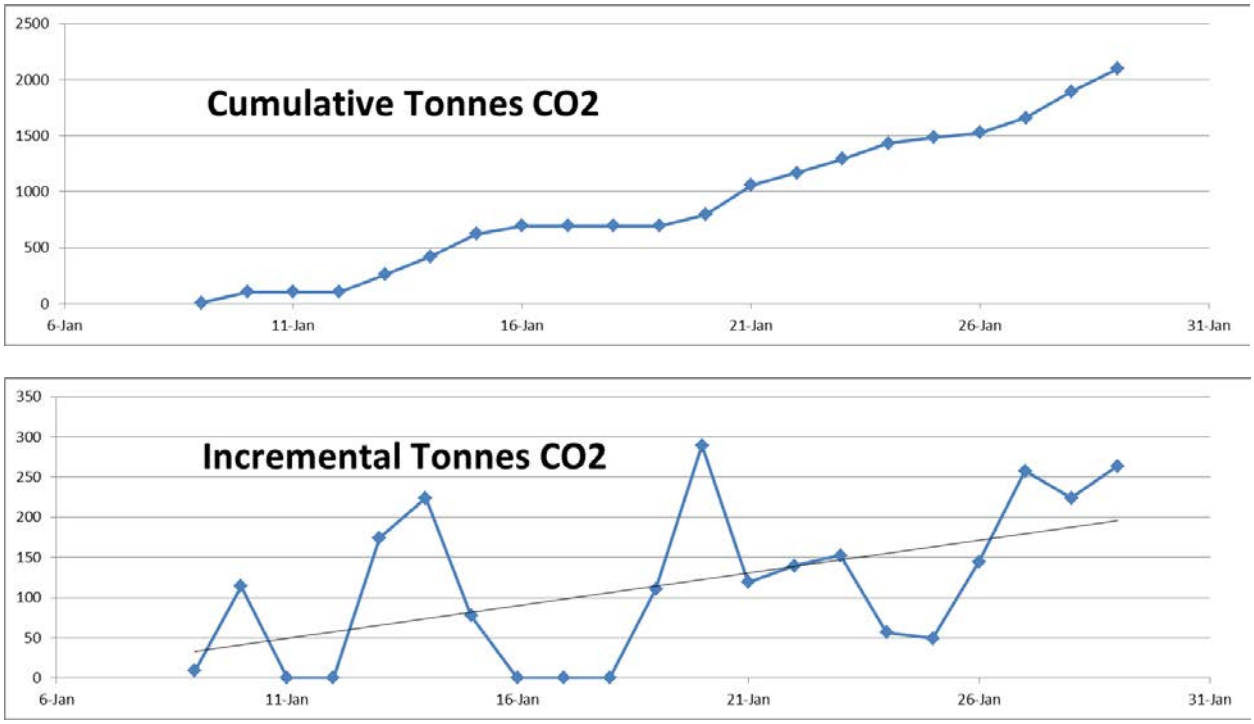

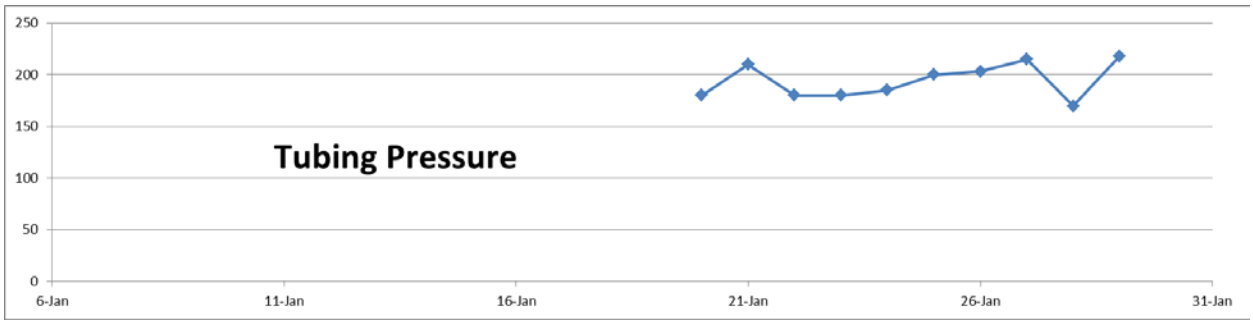

Figure 17. Cumulative and incremental CO2 being injected into the Mississippian oil reservoir at Wellington Field. Tubing pressure at the injection well remains approximately 200 psi.

Monitoring and sampling of gases and brine from producing wells are prioritized through the use of a ring map (**Figure 19**). The wells in the inner ring are currently being monitored twice a week for ph, alkalinity, TDS, casing head gas composition, and a suite of anions and cations. Over the past month the baseline monitoring was expanded to include 15 wells comparable to the wells sampled in summer 2015 before waterflooding and pressurization of the reservoir began in the area of the CO2 injection. A new round of sampling of these wells was made this past week, Feb. 3 and 4.

Figure 18. Flowmeter is now installed on #61 and #62 and soon on wells #53 and #69.

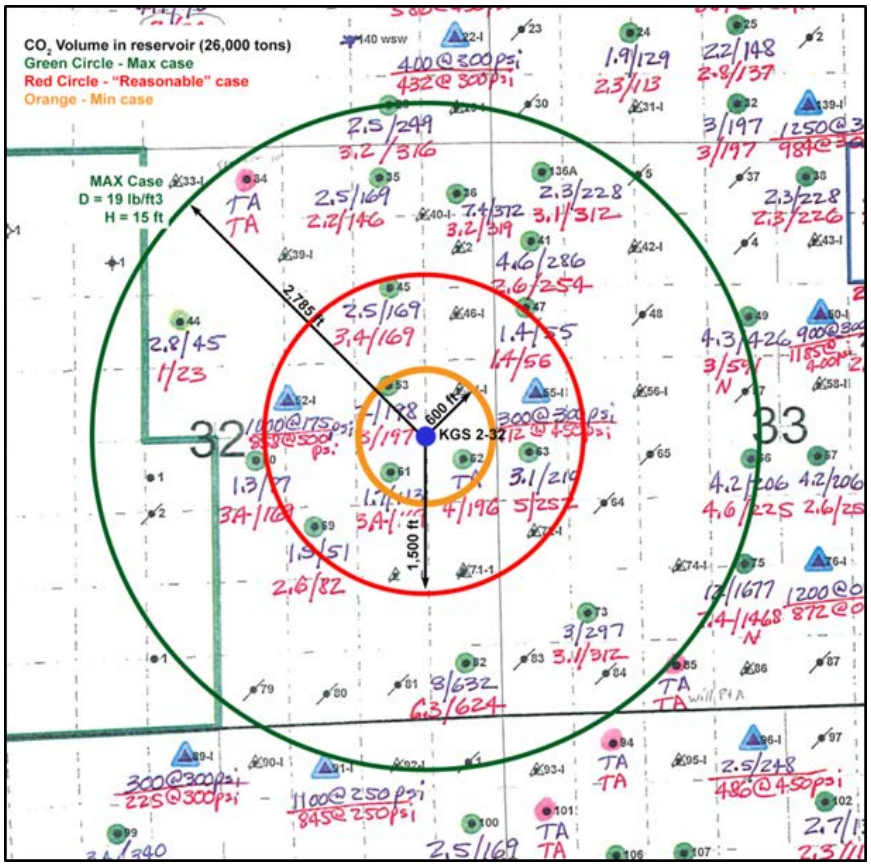

Figure 19. Ring map used for well monitoring. Inner ring monitored twice a week. Wells in the middle and outer rings currently sampled once a week. Sampling being carried out by the KGS, KU, and Baker-Hughes.

A map of the pH, TDS, and bicarbonate show considerable lateral variability between the nine wells sampled on 1-19-16 (**Figure 20**). Southwest of the Injection well, #2-32, the pH and TDS are low while bicarbonate is high relative to wells east of the injection well. The legacy brine analyses sampled over multiple years over the entire field show similar variation in the vicinity of the injection well (**Figure 21**). Thus, the gradient observed thus far in the area of injection is considered normal. The variation in a field that has been waterflooded for decades will undoubtedly show temporal and spatial variations with changes in rates and volumes of brine that is recycled as in the case of this field

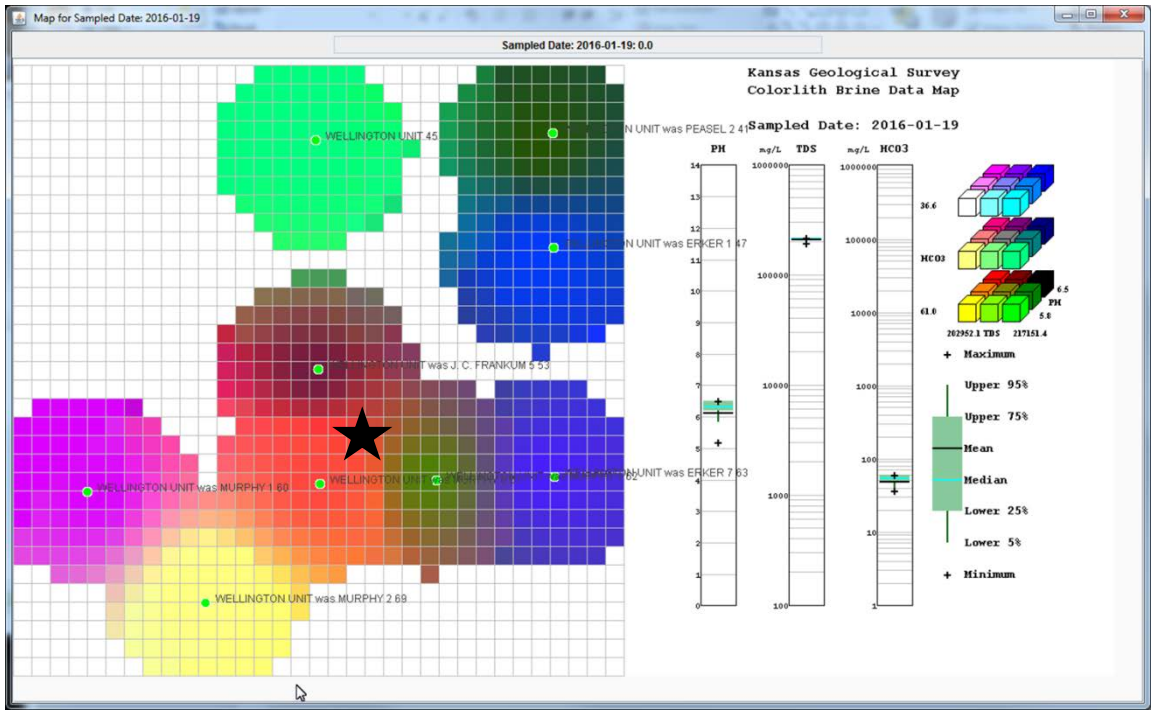

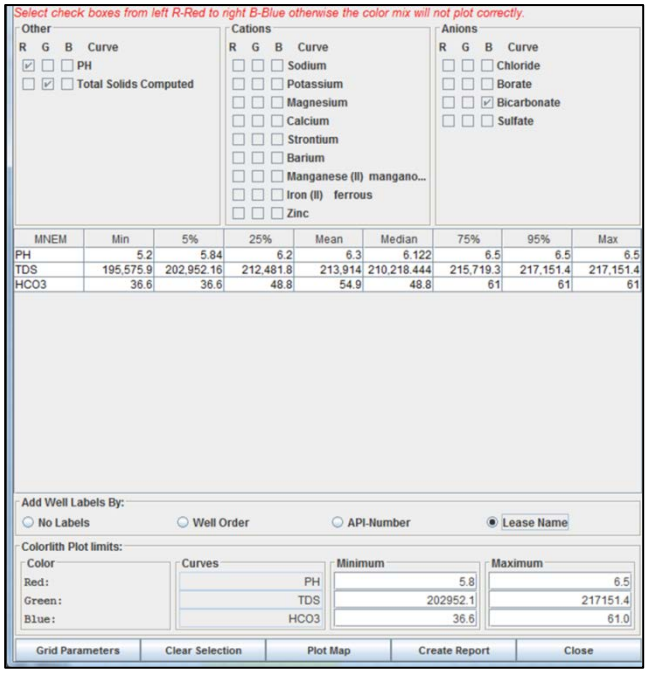

Figure 19. (upper – map) Spatial variation of pH, TDS, and bicarbonate among nine wells sampled on January 19th. The black star is the location of the CO2 injection well, #2-32. (chart to left) The control panel for the map shows the statistics of the variables selected in the mapping above. The user can set the color ranges manually, but default is based on the range of the variable being compared.

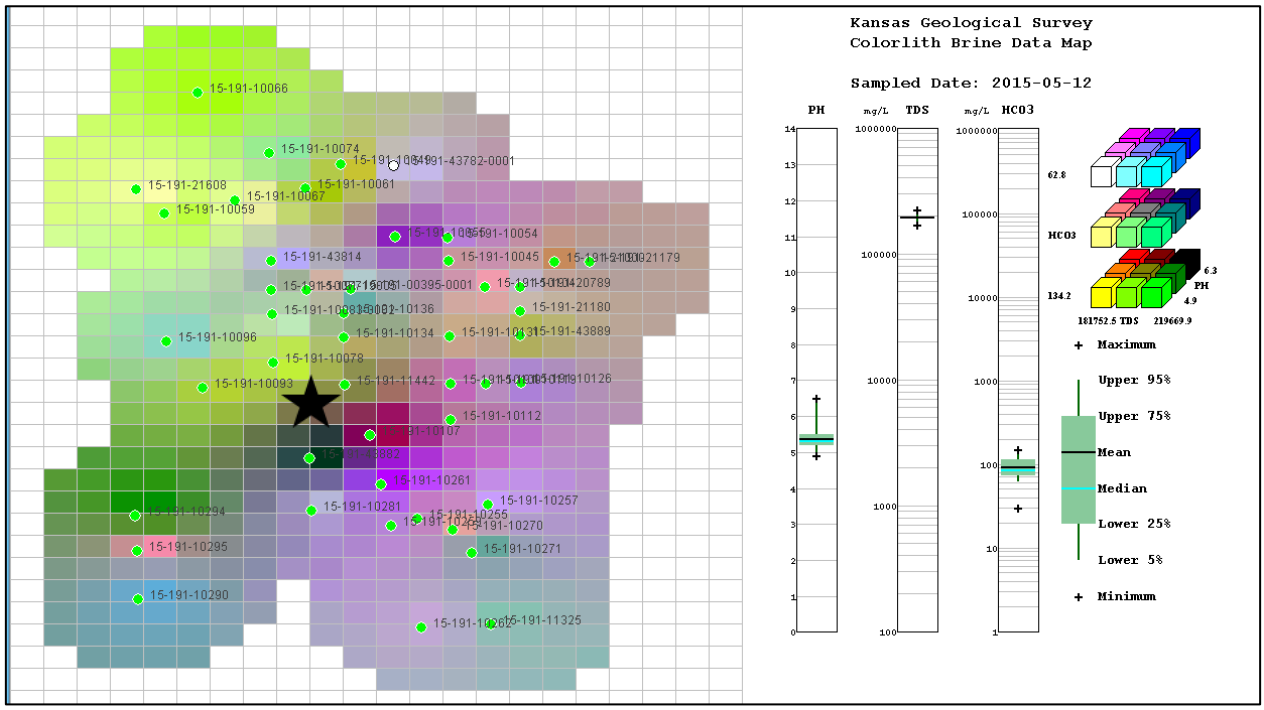

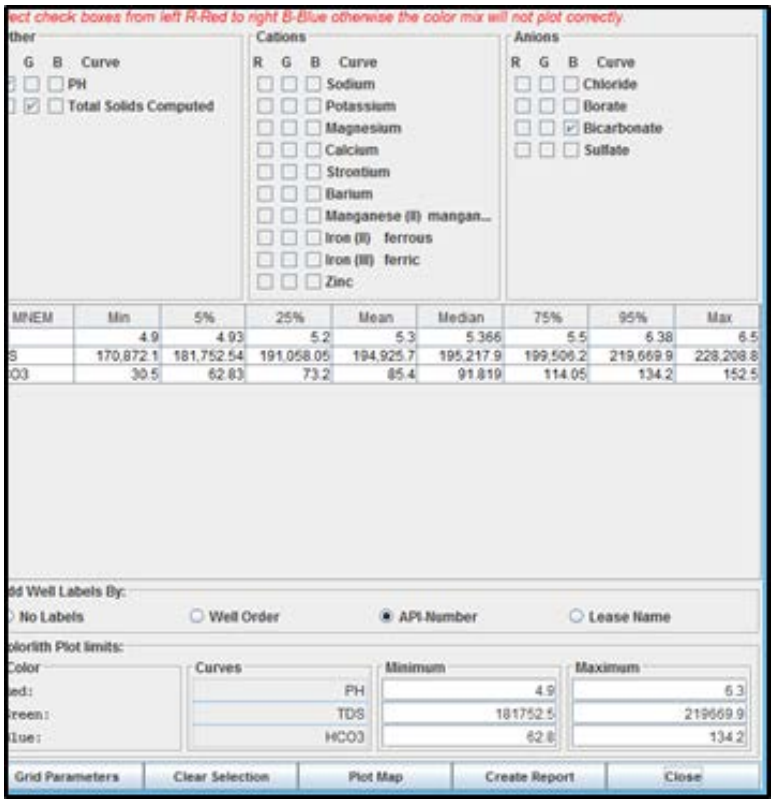

Figure 20. Spatial variation of pH, TDS, and bicarbonate from legacy brine analyses for 47 wells from the entire Wellington Field sampled over multiple years. The black star corresponds with the location of the CO2 injection well, #2-32. The pH, and TDS are generally lower on the west side of the field, while the bicarbonate is higher.

Well List:

(R)-Required (O)-Optional (C)-Select "Compute UTM" Button (S)-Select "Select Well Status" Button

API Number(R)	Well Name(R)	Operator(O)	Field(O)	Status(S)	Latitude(R)	Longitude(R)	Zone(C)	UTM X(C)	UTM Y(C)	TD(O)	GL(O)	KB(O)	DF(O)
15-191-21179	COLE 2	TERRA RESOURC...	WELLINGTON	OIL	37.3186181	-97.4222009	14.0	639806.6	4131181.86	3900.0	1266.0	1277.0	0.0
15-191-10083-...	WELLINGTON UNIT 45		UNKNOWN	OIL	37.3149436	-97.4427392	14.0	637993.33	4130743.98	3696.0	0.0	0.0	0.0
15-051-03453	HALL 'B' 6	CITIES SERVICE OI...	Bemis-Shutts	OIL	39.0717603	-99.1819223	14.0	484262.55	4324547.59	3413.0	0.0	0.0	1954.0
15-191-10132	ERKER 4	SHAWVER E B	WELLINGTON	OIL	37.3113585	-97.4313515	14.0	639009.09	4130362.92	3688.0	0.0	0.0	1255.0
15-191-19005	WELLINGTON UNIT 36	BEREXCO INC	WELLINGTON	OIL	37.316789	-97.4404585	14.0	638192.06	4130952.06	3700.0	1266.0	0.0	0.0
15-191-10077	WELLINGTON UNIT was J. C. FR...	STELBAR OIL CORP	WELLINGTON	OIL	37.3167567	-97.4427281	14.0	637990.99	4130945.15	3711.0	0.0	0.0	1269.0
15-191-43889	WELLINGTON UNIT was F. BARL...	STELBAR OIL CORP	WELLINGTON	OIL	37.3131677	-97.4267918	14.0	639409.85	4130570.36	3699.0	0.0	0.0	1269.0
15-191-00395-...	WELLINGTON UNIT 'A' 136		WELLINGTON	OIL	37.3168299	-97.4376423	14.0	638441.54	4130960.72	3699.0	1259.0	0.0	0.0
15-191-10078	WELLINGTON UNIT was J. C. FR...	STELBAR OIL CORP	WELLINGTON	OIL	37.3113174	-97.4427614	14.0	637997.99	4130341.63	3693.0	0.0	0.0	1255.0
15-051-03420	COLAHAN 'A' 9	CITIES SERVICE OI...	Bemis-Shutts	OIL	39.0827931	-99.1606599	14.0	486104.04	4325768.43	3440.0	0.0	0.0	1964.0
15-191-10113	WELLINGTON UNIT was ERKER ...	STELBAR OIL COR...	WELLINGTON	OIL-P&A	37.3041088	-97.4337049	14.0	638813.86	4129555.11	3699.0	1243.0	0.0	1248.0
15-191-43814	WELLINGTON UNIT was W.H. Ne...	SUNRAY DX OIL CO.	UNKNOWN	OIL	37.3189958	-97.4427138	14.0	637988.17	4131193.61	3707.0	0.0	0.0	1270.0
15-191-10270	Wellington Unit 108	Stelbar Oil Corp., Inc.	WELLINGTON	OIL	37.2985459	-97.4314147	14.0	639027.09	4128941.3	3696.0	0.0	0.0	1240.0
15-191-10295	Wellington Unit 110	Amerada Petroleu...	WELLINGTON	OIL	37.297249	-97.4518072	14.0	637221.89	4128767.61	3657.0	0.0	0.0	1209.0
15-191-10049	WELLINGTON UNIT was CURTIS ...	STELBAR OIL COR...	WELLINGTON	OIL	37.3262015	-97.4380895	14.0	638384.73	4131999.82	3698.0	0.0	0.0	1269.0
15-191-10119	WELLINGTON UNIT was BARLO...	STELBAR OIL CORP	WELLINGTON	OIL	37.3095437	-97.4291032	14.0	639211.69	4130164.88	3701.0	0.0	0.0	1254.0
15-191-43882	WELLINGTON UNIT was MURPH...	SLICK, PRYOR & L...	UNKNOWN	OIL	37.3040974	-97.4405362	14.0	638208.41	4129543.84	3652.0	0.0	0.0	1233.0
15-191-22770	Wellington KGS 2-32	Berexco LLC	WELLINGTON	EOR	37.3105345	-97.4418	14.0	638084.62	4130256.18	3860.0	1257.0	1269.0	1267.0
15-191-10092	WELLINGTON UNIT was MURPH...	BRIDGEPORT OIL	WELLINGTON	OIL	37.3076589	-97.4450532	14.0	637801.56	4129932.38	3696.0	0.0	0.0	1248.0
15-051-19214	Colahan 'A' 32	CITIES SERVICE OI...	Bemis-Shutts	OIL	39.085787	-99.1516701	14.0	486882.15	4326099.33	3450.0	0.0	0.0	1880.0
15-191-10257	Wellington Unit 102	Stelbar Oil Corp. an...	WELLINGTON	OIL	37.3004292	-97.4291577	14.0	639223.67	4129153.57	3695.0	0.0	0.0	1246.0
15-191-10107	WELLINGTON UNIT was ERKER ...	STELBAR OIL CORP	WELLINGTON	OIL	37.3057345	-97.4366087	14.0	638553.5	4129731.23	3671.0	0.0	0.0	1231.0
15-191-20789	Wellington Unit 144	Terra Resources	WELLINGTON	OIL	37.3167935	-97.4267498	14.0	639406.87	4130972.69	4285.0	1276.0	1286.0	1283.0
15-191-10093	WELLINGTON UNIT was MURPH...	KIOWA DRLG CO	WELLINGTON	OIL	37.3094396	-97.4473117	14.0	637598.15	4130126.66	3700.0	0.0	0.0	1238.0
15-051-25895	Hall 'B' 28	Vess Oil Corp.	Bemis-Shutts	OIL	39.065098	-99.1796545	14.0	484457.26	4323807.88	3605.0	2000.0	2005.0	0.0
15-051-24788	RUMSEY 'A' 18	Oxy USA, Inc.	Bemis-Shutts	OIL	39.075727	-99.1684913	14.0	485425.23	4324985.53	3717.0	2105.0	2110.0	0.0
15-051-22106	MCCORD 'A' 17	CITIES SERVICE OI...	Bemis-Shutts	OIL	39.0665882	-99.167972	14.0	485468.28	4323971.31	3647.0	2096.0	2101.0	2098.0
15-191-22591	WELLINGTON KGS 1-32	BEREXCO LLC	WELLINGTON	OTHER	37.315444	-97.442414	14.0	638021.23	4130799.98	5240.0	1259.0	1272.0	1270.0
15-191-10054	WELLINGTON UNIT was Kamas ...	Sinclair Prairie Oil ...	WELLINGTON	OIL	37.3206206	-97.4312801	14.0	638998.36	4131390.63	3681.0	0.0	0.0	1258.0
15-191-10131	WELLINGTON UNIT was ERKER ...	SHAWVER E B	WELLINGTON	OIL	37.3131714	-97.4313305	14.0	639007.62	4130564.08	3689.0	0.0	0.0	1255.0
15-191-10066	WELLINGTON UNIT was LUDWIG 6	COOPERATIVE RE...	WELLINGTON	OIL	37.331713	-97.4471575	14.0	637571.2	4132598.07	3687.0	0.0	0.0	1273.0
15-191-10112	WELLINGTON UNIT was ERKER ...	STELBAR OIL CORP	WELLINGTON	OIL	37.3068262	-97.431404	14.0	639012.78	4129859.99	3684.0	0.0	0.0	1249.0
15-191-10262	Wellington Unit 128	Coop. Refining Ass...	WELLINGTON	OIL	37.291225	-97.433637	14.0	638843.56	4128125.79	3689.0	0.0	0.0	1231.0
15-191-11442	WELLINGTON UNIT was ERKER ...	STELBAR OIL CO.	WELLINGTON	OIL	37.3095512	-97.4381806	14.0	638407.19	4130152.38	3675.0	0.0	0.0	1249.0
15-191-10100	WELLINGTON UNIT was ERKER ...	STELBAR OIL COR...	WELLINGTON	OIL	37.3095456	-97.4313725	14.0	639010.57	4130161.75	3677.0	0.0	0.0	1241.0
15-051-25896	Colahan 'B' 32	Vess Oil Corp.	Bemis-Shutts	OIL	39.0649621	-99.1635135	14.0	485853.67	4323790.16	3580.0	2012.0	2017.0	0.0
15-051-05037-...	DEHOFF 'A' 6	CITIES SERVICE OI...	Bemis-Shutts	SWD	39.0737624	-99.1401915	14.0	487872.87	4324763.36	3329.0	0.0	0.0	1809.0
15-191-10075	MARKLEY 'B' 1	VICKERS PETROL...	WELLINGTON	OIL	37.303968	-97.4496146	14.0	637404.02	4129516.25	3701.0	0.0	0.0	1239.0
15-191-10133	ERKER 5	STELBAR OIL CORP	WELLINGTON	OIL	37.3113613	-97.4347555	14.0	638707.41	4130358.23	3877.0	0.0	0.0	1250.0
15-191-10104	WELLINGTON UNIT was PEASEL ...	SHAWVER E B	WELLINGTON	OIL	37.3167954	-97.4290191	14.0	639205.77	4130969.56	3695.0	0.0	0.0	1271.0
15-191-10281	Wellington Unit 100	Texas Co.	WELLINGTON	OIL	37.3000928	-97.4405128	14.0	638217.82	4129099.58	3683.0	0.0	0.0	1223.0
15-191-10074	WELLINGTON UNIT was LUDWIG...	STELBAR OIL CORP	WELLINGTON	OIL	37.3271537	-97.4426522	14.0	637978.7	4132098.79	3702.0	0.0	0.0	1274.0
15-191-10126	WELLINGTON UNIT was BARLO...	STELBAR OIL CORP	WELLINGTON	OIL	37.3095419	-97.4268338	14.0	639412.82	4130168.02	3708.0	0.0	0.0	1262.0
15-191-11325	Wellington Unit 129	Coop. Refining Ass...	WELLINGTON	OIL	37.2913664	-97.4291	14.0	639245.49	4128148.15	3678.0	0.0	0.0	1231.0
15-191-21608	Wellington Unit 149	Terra Resources	WELLINGTON	OIL	37.3244862	-97.4512991	14.0	637217.41	4131790.24	3800.0	1258.0	1268.0	0.0
15-191-10134	WELLINGTON UNIT was ERKER ...	SHAWVER E B	WELLINGTON	OIL	37.313177	-97.4381385	14.0	638404.27	4130554.71	3694.0	0.0	0.0	1262.0
15-191-10076	WELLINGTON UNIT was MURPH...	SLICK PRYOR AND...	WELLINGTON	OIL	37.3095366	-97.4405029	14.0	638201.4	4130147.36	3686.0	0.0	0.0	1264.0
15-191-22590	WELLINGTON KGS 1-28	BEREXCO LLC	WELLINGTON	OTHER	37.3194833	-97.433378	14.0	638814.56	4131261.36	5250.0	1257.0	1270.0	0.0
15-191-10096	WELLINGTON UNIT was FRANKU...	BRIDGEPORT OIL	WELLINGTON	OIL	37.3130335	-97.4495591	14.0	637392.44	4130522.12	3681.0	0.0	0.0	1246.0
15-191-10261	Wellington Unit 94	Continental Oil Co.	WELLINGTON	OIL	37.3020297	-97.4359747	14.0	638616.5	4129321.11	3681.0	0.0	0.0	1244.0
15-191-10061	WELLINGTON UNIT was W. I. GA...	STELBAR OIL CORP	WELLINGTON	OIL	37.3244208	-97.440403	14.0	638183.0	4131798.87	3704.0	0.0	0.0	1274.0
15-191-21180	Wellington Unit 145	Terra Resources	WELLINGTON	OIL	37.3149806	-97.4267708	14.0	639408.36	4130771.52	3810.0	1269.0	1278.0	0.0
15-191-10087	WELLINGTON UNIT was MURPH...	TRANSWESTERN ...	WELLINGTON	OIL	37.3095043	-97.4427725	14.0	638000.32	4130140.46	3697.0	0.0	0.0	1258.0
15-051-26218-...	McCord 'A' 20-H	Vess Oil Corp.	Bemis-Shutts	OIL	39.069952	-99.1695539	14.0	485332.12	4324344.85	3782.0	2086.0	2100.0	0.0
15-191-10045	WELLINGTON UNIT was KAMAS 6...	Sinclair Prairie Oil ...	WELLINGTON	OIL	37.3188077	-97.4312801	14.0	639001.7	4131189.49	3678.0	0.0	0.0	1246.0
15-191-10294	Wellington Unit 99	Amerada Petroleu...	WELLINGTON	OIL	37.2998989	-97.4518557	14.0	637212.78	4129061.54	3671.0	0.0	0.0	1222.0
15-191-10259	Wellington Unit 106	Continental Oil Co.	WELLINGTON	OIL	37.2988754	-97.4353874	14.0	638674.35	4128972.01	3691.0	0.0	0.0	1243.0
15-191-10255	Wellington Unit 107	Stelbar Oil Corp. an...	WELLINGTON	OIL	37.2993815	-97.4336889	14.0	638823.97	4129030.66	3699.0	0.0	0.0	1241.0
15-191-10271	Wellington Unit 114	Stelbar Oil Corp., Inc.	WELLINGTON	OIL	37.2967687	-97.4302689	14.0	639131.92	4128745.81	3696.0	0.0	0.0	1240.0
15-191-21000	Cole 1	Terra Resources	WELLINGTON	OIL	37.3186655	-97.4244707	14.0	639605.37	4131183.76	4156.0	0.0	1284.0	0.0
15-191-10136	WELLINGTON UNIT was PEASEL ...	SLICK PRYOR AND...	WELLINGTON	OIL	37.3149899	-97.4381175	14.0	638402.81	4130755.88	3689.0	0.0	0.0	1262.0
15-051-21871	HAUSER 'A' 7	CITIES SERVICE OI...	Bemis-Shutts	OIL	39.0553471	-99.2028642	14.0	482446.86	4322730.03	3695.0	2120.0	2125.0	2123.0
15-051-22209	DEHOFF 'A' 7	CITIES SERVICE OI...	Bemis-Shutts	OIL	39.0720723	-99.1477866	14.0	487215.56	4324576.85	3420.0	1847.0	1852.0	1850.0
15-191-10055	WELLINGTON UNIT was FRANK ...	Sinclair Prairie Oil ...	WELLINGTON	OIL	37.3206917	-97.4346848	14.0	638696.53	4131393.51	3709.0	0.0	0.0	1264.0
15-191-10290	Wellington Unit 123	Stelbar Oil Corp., Inc.	WELLINGTON	OIL	37.2935546	-97.4517973	14.0	637229.48	4128357.74	3676.0	0.0	0.0	1204.0
15-191-10059	WELLINGTON UNIT was RIDDEL ...	COOPERATIVE RE...	WELLINGTON	OIL	37.3226624	-97.4494956	14.0	637380.53	4131590.52	3690.0	0.0	0.0	1257.0
15-191-10067	WELLINGTON UNIT was MILLER ...	LAURA JANE OIL CO	WELLINGTON	OIL	37.3235416	-97.4449493	14.0	637781.77	4131694.68	3699.0	0.0	1268.0	0.0
15-191-43782-...	Wellington Unit 143-INJ	Coop. Refining Ass...	WELLINGTON	INJ	37.3261311	-97.4347156	14.0	638683.81	4131996.96	3708.0	0.0	1367.0	0.0

UTM Zone: 14.0 | Set all Wells to a Common UTM Zone | Compute UTM for Selected Well Only

Return

Figure 21. Brine database used in Figure 20 accessed via web application.

The brine data used in the map is listed in **Figure 21** is accessible via the web application (**Figure 22**). Each brine analysis of each well is also accessible via a web application (**Figure 23**) along with tools provided to summarize the particular analysis of the well and standard sample plot to show the variation. **Figure 23** also illustrates the January 19th sample for four wells near the #2-32 CO2 injection well. At this level of comparison the major cations and anions in the brines in the nearby producers are very similar.

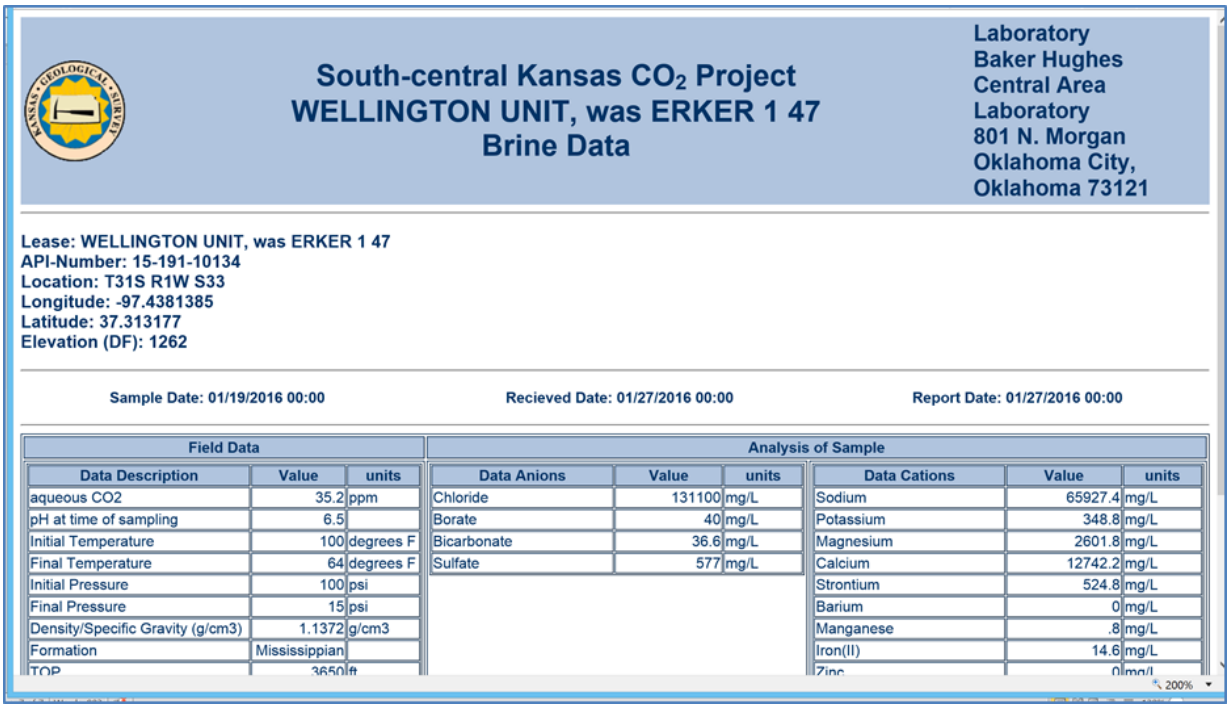

South-central Kansas CO_2 Project
WELLINGTON UNIT, was ERKER 1 47
Brine Data

Laboratory
Baker Hughes
Central Area
Laboratory
801 N. Morgan
Oklahoma City,
Oklahoma 73121

Lease: WELLINGTON UNIT, was ERKER 1 47
API-Number: 15-191-10134
Location: T31S R1W S33
Longitude: -97.4381385
Latitude: 37.313177
Elevation (DF): 1262

Sample Date: 01/19/2016 00:00 Recieved Date: 01/27/2016 00:00 Report Date: 01/27/2016 00:00

Field Data		
Data Description	Value	units
aqueous CO2	35.2	ppm
pH at time of sampling	6.5	
Initial Temperature	100	degrees F
Final Temperature	64	degrees F
Initial Pressure	100	psi
Final Pressure	15	psi
Density/Specific Gravity (g/cm3)	1.1372	g/cm3
Formation	Mississippian	
TOP	3650	ft

Analysis of Sample		
Data Anions	Value	units
Chloride	131100	mg/L
Borate	40	mg/L
Bicarbonate	36.6	mg/L
Sulfate	577	mg/L

Analysis of Sample		
Data Cations	Value	units
Sodium	65927.4	mg/L
Potassium	348.8	mg/L
Magnesium	2601.8	mg/L
Calcium	12742.2	mg/L
Strontium	524.8	mg/L
Barium	0	mg/L
Manganese	.8	mg/L
Iron(II)	14.6	mg/L
Zinc	0	mg/L

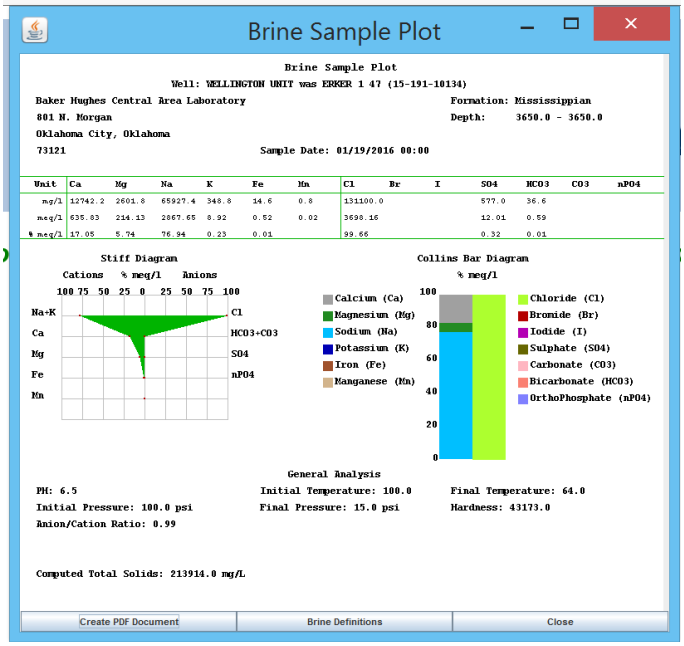

Figure 23. Access to individual brine sample data and standard plots to illustrate the variation.


Brine Sample Plot
Brine Sample Plot
Well: WELLINGTON UNIT was ERSKER 7 63 (15-191-11442)
Baker Hughes Central Area Laboratory
801 N. Morgan
Oklahoma City, Oklahoma
73121
Formation: Mississippian
Depth: 3688.0 - 3688.0
Sample Date: 01/19/2016 08:00
Unit Ca Mg Na K Fe Mn Cl Br I SO4 HCO3 CO3 nPO4
mg/l 13707.1 2791.1 64532.6 333.2 15.9 0.8 132580.0 980.2 36.6
meq/l 687.89 229.72 2806.99 8.52 0.56 0.02 3757.68 20.4 0.59
% meq/l 18.42 6.15 75.17 0.22 0.01 99.44 0.54 0.01
Stiff Diagram
Cations % meq/l Anions
100 75 50 25 0 25 50 75 100
Na+K
Ca
Mg
Fe
Mn
Cl
HCO3+CO3
SO4
nPO4
Collins Bar Diagram
% meq/l
Calcium (Ca)
Magnesium (Mg)
Sodium (Na)
Potassium (K)
Iron (Fe)
Manganese (Mn)
Chloride (Cl)
Bromide (Br)
Iodide (I)
Sulphate (SO4)
Carbonate (CO3)
Bicarbonate (HCO3)
OrthoPhosphate (nPO4)
General Analysis
PH: 6.3
Initial Temperature: 100.0
Final Temperature: 64.0
Initial Pressure: 100.0 psi
Final Pressure: 15.0 psi
Hardness: 46576.0
Anion/Cation Ratio: 1.0
Computed Total Solids: 215536.0 mg/L
Create PDF Document
Brine Definitions
Close


Brine Sample Plot
Brine Sample Plot
Well: WELLINGTON UNIT was MURPHY 2 69 (15-191-10892)
Baker Hughes Central Area Laboratory
801 N. Morgan
Oklahoma City, Oklahoma
73121
Formation: Mississippian
Depth: 3660.0 - 3660.0
Sample Date: 01/19/2016 08:00
Unit Ca Mg Na K Fe Mn Cl Br I SO4 HCO3 CO3 nPO4
mg/l 12411.3 2317.8 59020.8 441.7 7.3 0.6 123900.0 701.2 48.8
meq/l 619.32 190.76 2825.74 11.29 0.26 0.02 3495.06 14.59 0.79
% meq/l 16.54 5.7 75.43 0.33 99.56 0.41 0.02
Stiff Diagram
Cations % meq/l Anions
100 75 50 25 0 25 50 75 100
Na+K
Ca
Mg
Fe
Mn
Cl
HCO3+CO3
SO4
nPO4
Collins Bar Diagram
% meq/l
Calcium (Ca)
Magnesium (Mg)
Sodium (Na)
Potassium (K)
Iron (Fe)
Manganese (Mn)
Chloride (Cl)
Bromide (Br)
Iodide (I)
Sulphate (SO4)
Carbonate (CO3)
Bicarbonate (HCO3)
OrthoPhosphate (nPO4)
General Analysis
PH: 5.8
Initial Temperature: 100.0
Final Temperature: 59.0
Initial Pressure: 100.0 psi
Final Pressure: 15.0 psi
Hardness: 41067.0
Anion/Cation Ratio: 1.05
Computed Total Solids: 198318.0 mg/L
Create PDF Document
Brine Definitions
Close

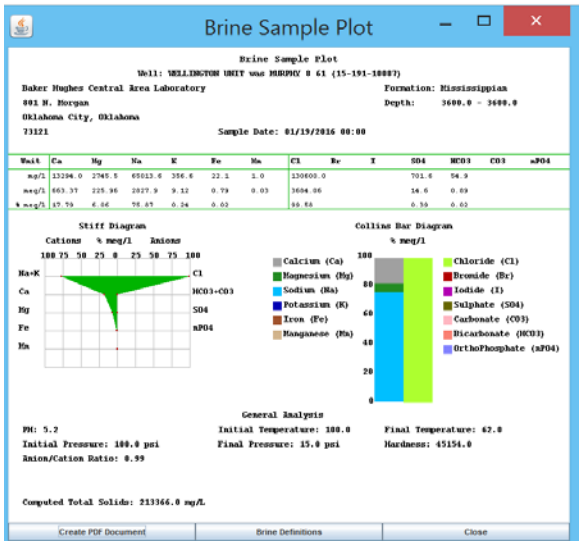
Brine Sample Plot
Brine Sample Plot
Well: WELLINGTON UNIT was MURPHY 8 61 (15-191-10887)
Baker Hughes Central Area Laboratory
801 N. Morgan
Oklahoma City, Oklahoma
73121
Formation: Mississippian
Depth: 3600.0 - 3600.0
Sample Date: 01/19/2016 08:00
Unit Ca Mg Na K Fe Mn Cl Br I SO4 HCO3 CO3 nPO4
mg/l 13294.0 2745.5 65013.6 356.6 22.1 1.0 130600.0 701.6 54.9
meq/l 663.37 225.96 2827.9 9.12 0.79 0.03 3684.06 14.6 0.89
% meq/l 17.79 6.06 75.85 0.24 0.02 99.86 0.39 0.02
Stiff Diagram
Cations % meq/l Anions
100 75 50 25 0 25 50 75 100
Na+K
Ca
Mg
Fe
Mn
Cl
HCO3+CO3
SO4
nPO4
Collins Bar Diagram
% meq/l
Calcium (Ca)
Magnesium (Mg)
Sodium (Na)
Potassium (K)
Iron (Fe)
Manganese (Mn)
Chloride (Cl)
Bromide (Br)
Iodide (I)
Sulphate (SO4)
Carbonate (CO3)
Bicarbonate (HCO3)
OrthoPhosphate (nPO4)
General Analysis
PH: 5.2
Initial Temperature: 100.0
Final Temperature: 62.0
Initial Pressure: 100.0 psi
Final Pressure: 15.0 psi
Hardness: 45154.0
Anion/Cation Ratio: 0.99
Computed Total Solids: 213366.0 mg/L
Create PDF Document
Brine Definitions
Close

Static fluid levels in producing wells offsetting the CO2 injection well have continued to rise since the CO2 injection began in early January (**Figure 24**). Prior to CO2 injection wells were shut in while brine was injected into well #2-32. Pressures taken in the producing wells still reflect the near well pressure drop associated with producing them. Thus, the reservoir pressure away from the producers is higher.

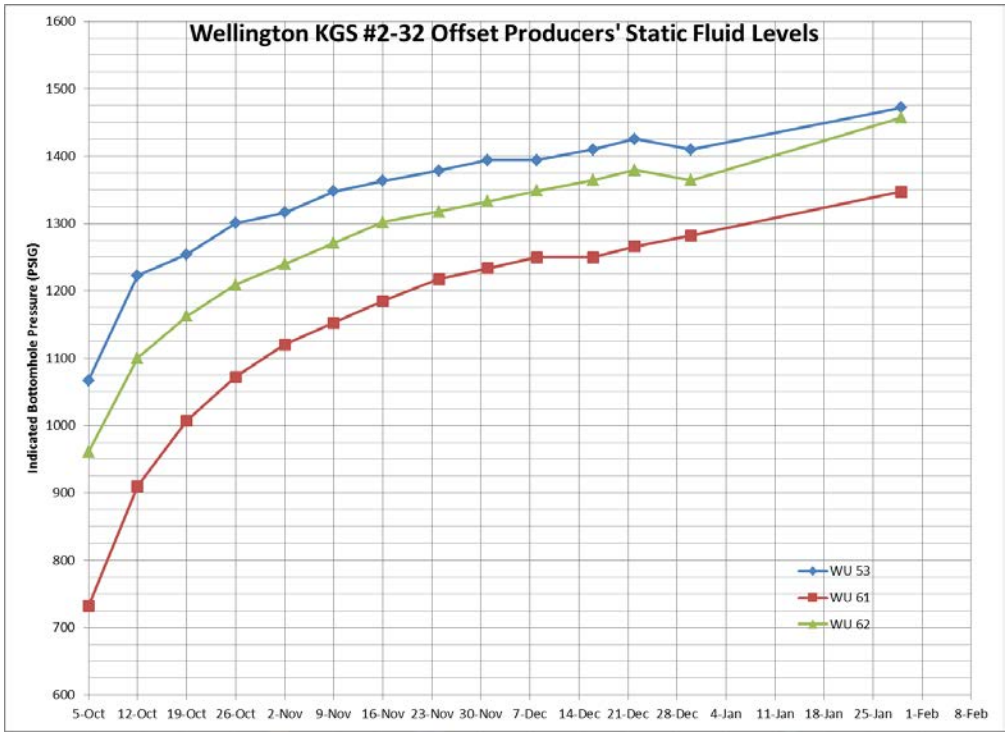

Figure 24. Static fluid levels in offset producing wells from CO2 injector.

Reservoir modeling, oil recovery, and CO2 storage capacity – The reservoir simulation is being refined and will be used to establish a new OOIP based on a revised Soi that is related to revised capillary pressure curves for the various rock types, and sweep efficiency related to the relative permeability tied to rock types and the current pressure data. As yet we have not breakthrough so the CO2 storage is 100%. We are hoping that CO2 breakthrough will be not begin for a least another month. Effort is being taken to manage the pressure/backpressure to contain the CO2.

KEY FINDINGS

1. We continue to increase CO2 injection rate into the Mississippian oil reservoir, now 250 tonnes per day, as it's clear that we have the reservoir capacity and injectivity.

2. There is a clear path toward using the CO2-EOR injection as a field experiement to test lab experiments and validate reservoir simulations. We are closely managing the pressure of the reservoir in the vicinity of the CO2 well to contain the CO2, to maximize the benefit, and improve the sweep efficiency. Monitoring of CO2 volume and equipping wells to meter the CO2 after breakthrough will permit a material balance to be carried out to evaluate carbon sequestration. Sampling of brines and casing head gas extends to 15 wells that surround the injection well to ensure that changes in the brines and gases are detected to herald the approach of an oil bank and the CO2 plume including detection of light end hydrocarbons and non hydrocarbon gases being analyzed with a GC.
3. Progress on the Class VI saline aquifer CO2 test injection advanced significantly with a meeting with EPA whereby no USDW was determined at the Wellington site and a one year PISC and achievable financial assurance were conveyed.
4. The magnitude of induced seismicity has turned the corner and begun to decrease as limitations on large scale brine disposal went into effect along with the decline in drilling due to the unfavorable economics.
5. The operation of the 18-seismometer array is robust and dependable. The results have been verified and the magnitudes and locations of earthquakes detected continue to be refined.

Plans for First Quarter 2016

1. Continue to inject ~250 tonnes/day of CO2 in the Mississippian reservoir through May or June to reach the 26,000 tonne level.
2. Meter volumes of CO2 being injected and eventually that released to the atmosphere. Measure changes to brine chemistry and hydrocarbons produced as an indication to reactions of CO2 with the brine and the reservoir rock. Use information to develop volumetrics and to understand processes related to the sequestration of the CO2.
3. Obtain the draft permit from EPA and file a Continuation Application to allow the project to move to BP3. Provide a budget and detailed justification of updated costs, historical accounting of the project, schedule to complete the project and submit deliverables.

PRODUCTS

Publications, conference papers, and presentations

Watney et al., 2015, Update on Induced Seismicity in Kansas: Kansas Geological Society, December 9th, Wichita, KS.

PARTICIPANTS & OTHER COLLABORATING ORGANIZATIONS

A project organization chart follows (**Figure 25**). The work authorized in this budget period includes office tasks related to preparation of reports and application for a Class VI permit to inject CO_2 into the Arbuckle saline aquifer.

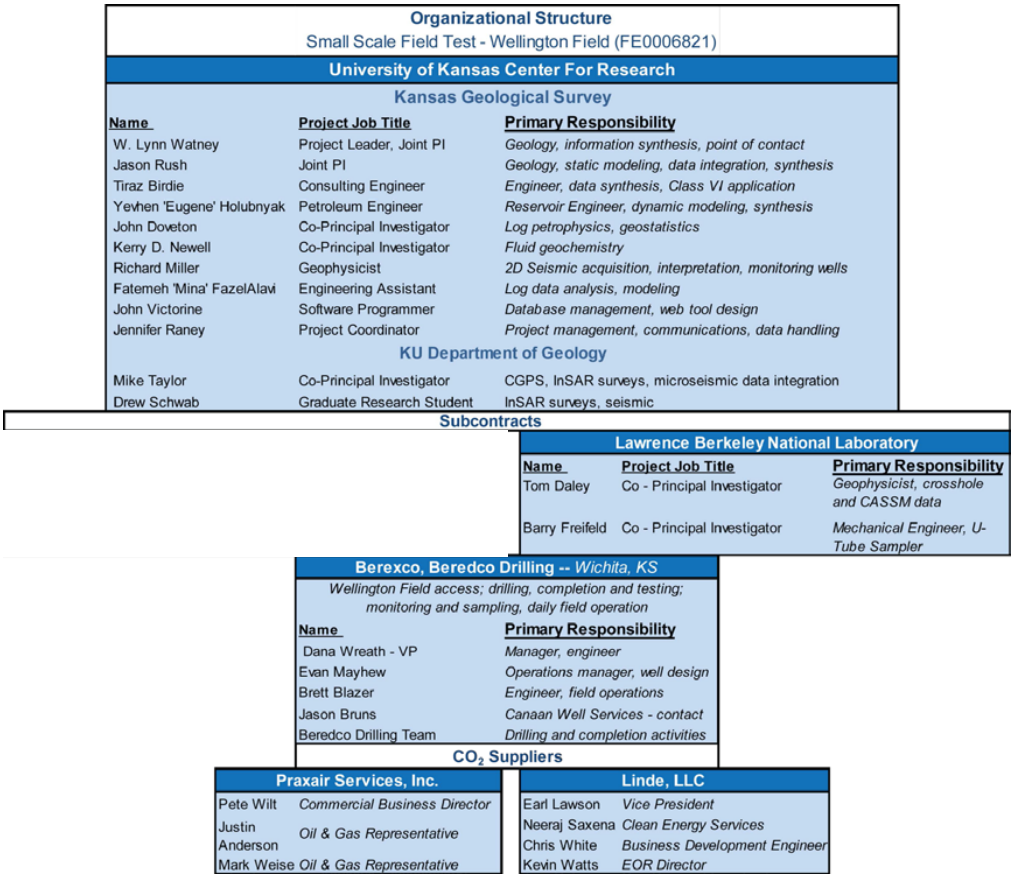

Figure 25. Organizational Chart.

IMPACT

Continuing interaction to provide information on the Class VI permit has slowed progress.

CHANGES/PROBLEMS

Funds are very tight due to the no cost time extensions necessary to permit review and response to for the Class VI permit.

BUDGETARY INFORMATION

Cost Status Report

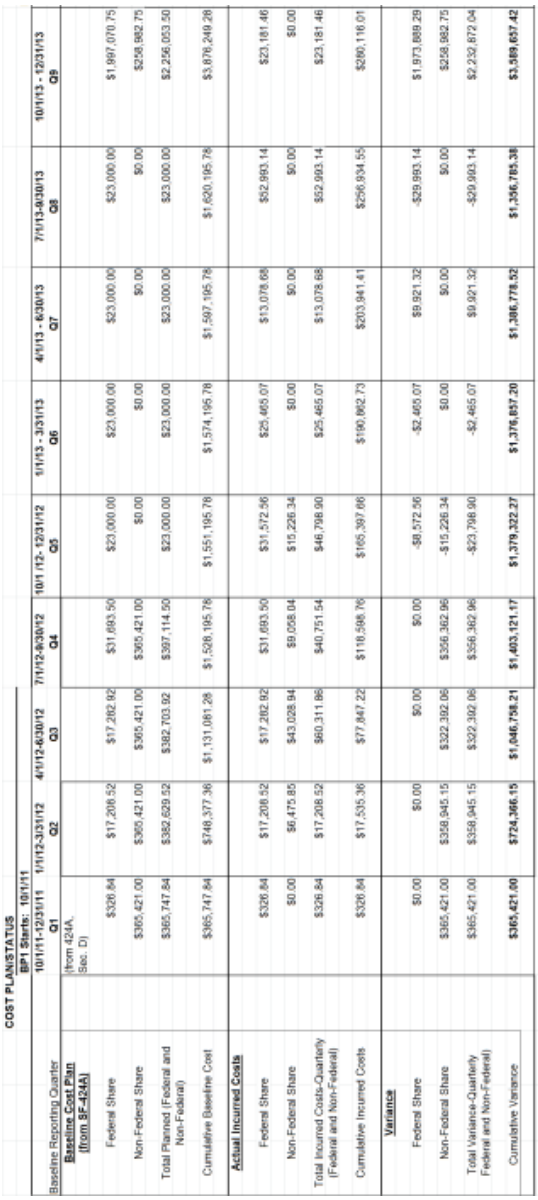

COST PLAN/STATUS

Baseline Reporting Quarter	BP1 Starts: 10/1/11 10/1/11-12/31/11 Q1	1/1/12-3/31/12 Q2	4/1/12-6/30/12 Q3	7/1/12-9/30/12 Q4	10/1/12- 12/31/12 Q5	1/1/13 - 3/31/13 Q6	4/1/13 - 6/30/13 Q7	7/1/13-9/30/13 Q8	10/1/13 - 12/31/13 Q9
Baseline Cost Plan (from SF-424A)	(from 424A, Sec. D)								
Federal Share	$326.84	$17,208.52	$17,282.82	$31,693.50	$23,000.00	$23,000.00	$23,000.00	$23,000.00	$1,997,070.75
Non-Federal Share	$365,421.00	$365,421.00	$365,421.00	$365,421.00	$0.00	$0.00	$0.00	$0.00	$258,982.75
Total Planned (Federal and Non-Federal)	$365,747.84	$382,629.52	$382,703.92	$397,114.50	$23,000.00	$23,000.00	$23,000.00	$23,000.00	$2,256,053.50
Cumulative Baseline Cost	$365,747.84	$748,377.36	$1,131,081.28	$1,528,195.78	$1,551,195.78	$1,574,195.78	$1,597,195.78	$1,620,195.78	$3,876,249.28
Actual Incurred Costs									
Federal Share	$326.84	$17,208.52	$17,282.82	$31,693.50	$31,572.56	$25,465.07	$13,078.68	$52,993.14	$23,181.46
Non-Federal Share	$0.00	$6,475.85	$43,028.84	$9,058.04	$15,226.34	$0.00	$0.00	$0.00	$0.00
Total Incurred Costs-Quarterly (Federal and Non-Federal)	$326.84	$17,208.52	$60,311.86	$40,751.54	$46,798.90	$25,465.07	$13,078.68	$52,993.14	$23,181.46
Cumulative Incurred Costs	$326.84	$17,535.36	$77,847.22	$118,598.76	$165,397.66	$190,862.73	$203,941.41	$256,934.55	$280,116.01
Variance									
Federal Share	$0.00	$0.00	$0.00	$0.00	-$8,572.56	-$2,465.07	$9,921.32	-$29,993.14	$1,973,889.29
Non-Federal Share	$365,421.00	$358,945.15	$322,392.08	$356,362.96	-$15,226.34	$0.00	$0.00	$0.00	$258,982.75
Total Variance-Quarterly Federal and Non-Federal)	$365,421.00	$358,945.15	$322,392.08	$356,362.96	-$23,798.90	-$2,465.07	$9,921.32	-$29,993.14	$2,232,872.04
Cumulative Variance	**$365,421.00**	**$724,366.15**	**$1,046,758.21**	**$1,403,121.17**	**$1,379,322.27**	**$1,376,857.20**	**$1,386,778.52**	**$1,356,785.38**	**$3,589,657.42**

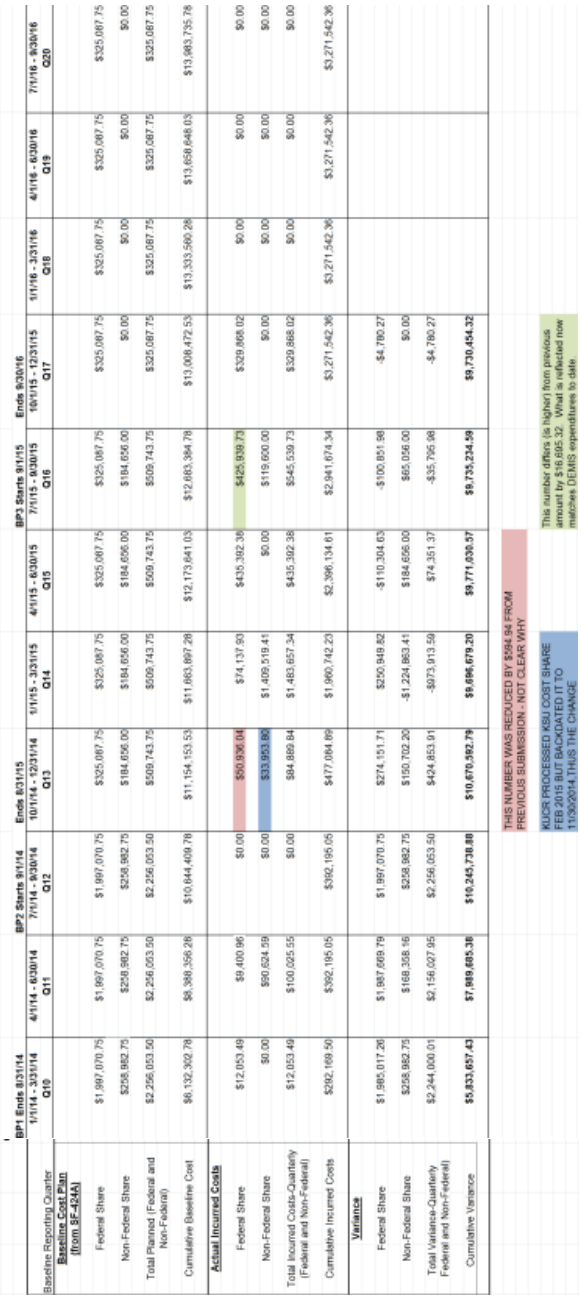

Baseline Reporting Quarter	BP1 Ends 8/31/14 1/1/14 - 3/31/14 Q10	4/1/14 - 6/30/14 Q11	BP2 Starts 9/1/14 7/1/14 - 9/30/14 Q12	Ends 8/31/15 10/1/14 - 12/31/14 Q13	1/1/15 - 3/31/15 Q14	4/1/15 - 6/30/15 Q15	BP3 Starts 9/1/15 7/1/15 - 9/30/15 Q16	Ends 9/30/16 10/1/15 - 12/31/15 Q17	1/1/16 - 3/31/16 Q18	4/1/16 - 6/30/16 Q19	7/1/16 - 9/30/16 Q20
Baseline Cost Plan (from SF-424A)											
Federal Share	$1,997,070.75	$1,997,070.75	$1,997,070.75	$325,087.75	$325,087.75	$325,087.75	$325,087.75	$325,087.75	$325,087.75	$325,087.75	$325,087.75
Non-Federal Share	$258,982.75	$258,982.75	$258,982.75	$184,656.00	$184,656.00	$184,656.00	$184,656.00	$0.00	$0.00	$0.00	$0.00
Total Planned (Federal and Non-Federal)	$2,256,053.50	$2,256,053.50	$2,256,053.50	$509,743.75	$509,743.75	$509,743.75	$509,743.75	$325,087.75	$325,087.75	$325,087.75	$325,087.75
Cumulative Baseline Cost	$6,132,302.78	$8,388,356.28	$10,644,409.78	$11,154,153.53	$11,663,897.28	$12,173,641.03	$12,683,384.78	$13,008,472.53	$13,333,560.28	$13,658,648.03	$13,983,735.78
Actual Incurred Costs											
Federal Share	$12,053.49	$9,400.96	$0.00	$60,936.04	$74,137.93	$435,392.38	$425,839.73	$329,868.02	$0.00	$0.00	$0.00
Non-Federal Share	$0.00	$80,624.59	$0.00	$33,953.80	$1,409,518.41	$0.00	$119,600.00	$0.00	$0.00	$0.00	$0.00
Total Incurred Costs-Quarterly (Federal and Non-Federal)	$12,053.49	$100,025.55	$0.00	$94,889.84	$1,483,657.34	$435,392.38	$545,539.73	$329,868.02	$0.00	$0.00	$0.00
Cumulative Incurred Costs	$292,169.50	$392,195.05	$392,195.05	$477,084.89	$1,960,742.23	$2,396,134.61	$2,941,674.34	$3,271,542.36	$3,271,542.36	$3,271,542.36	$3,271,542.36
Variance											
Federal Share	$1,985,017.26	$1,987,669.79	$1,997,070.75	$274,151.71	$250,949.82	-$110,304.63	-$100,851.98	-$4,780.27			
Non-Federal Share	$258,982.75	$178,358.16	$258,982.75	$150,702.20	-$1,224,863.41	$184,656.00	$65,056.00	$0.00			
Total Variance-Quarterly Federal and Non-Federal)	$2,244,000.01	$2,166,027.95	$2,256,053.50	$424,853.91	-$973,913.59	$74,351.37	-$35,795.98	-$4,780.27			
Cumulative Variance	**$5,833,657.43**	**$7,999,685.38**	**$10,245,738.88**	**$10,670,592.79**	**$9,696,679.20**	**$9,771,030.57**	**$9,735,234.59**	**$9,730,454.32**			

THIS NUMBER WAS REDUCED BY $584.84 FROM PREVIOUS SUBMISSION - NOT CLEAR WHY

KUCR PROCESSED KSU COST SHARE FEB 2015 BUT BACKDATED IT TO 11/30/2014 THUS THE CHANGE

This number differs (is higher) from previous amount by $16,695.32. What is reflected now matches DEMIS expenditures to date

APPENDIX A.

REVISED SECTION 5 RESERVOIR MODELING

Section 5 Reservoir Modeling

5.1 Introduction

This section presents details of the Arbuckle reservoir simulation model that was constructed to project the results of the Wellington Field short-term Arbuckle CO2 pilot injection project and delineate the EPA Area of Review (AoR) documented in Section 9. As required under §146.84(c), the AoR must be delineated using a computational model than can accurately predict the projected lateral and vertical migration of the CO2 plume and formation fluids in the subsurface from the commencement of injection activities until the plume movement ceases and until pressure differentials sufficient to cause the movement of injected fluids or formation fluids into a USDW are no longer present. The model must:

i. Be based on detailed geologic data collected to characterize the injection zone(s), confining zone(s), and any additional zones; and anticipated operating data, including injection pressures, rates, and total volumes over the proposed life of the geologic sequestration project;
ii. Take into account any geologic heterogeneities, other discontinuities, data quality, and their possible impact on model predictions; and
iii. Consider potential migration through faults, fractures, and artificial penetrations.

This section presents the reservoir simulations conducted to fulfill §146.84 requirements stated above. The simulations were conducted assuming a maximum injection of 40,000 metric tons of CO2 over a period of nine months. Based on market conditions, KGS/Berexco now plans to inject a total of only 26,000 tons at the rate of 150 tons/day for a total period of approximately 175 days. The simulation results, therefore, represent impacts of the maximum quantity of CO2 that was originally planned for the Wellington project. The modeling results indicate that the induced pore pressures in the Arbuckle aquifer away from the injection well are of insufficient magnitude to cause the Arbuckle brines to migrate up into the USDW even if there were any artificial or natural penetration in the Arbuckle Group or the overlying confining units.

The simulation results also indicate that the free-phase CO2 plume is contained within the total CO2 plume (i.e., in the free plus dissolved phases) and that it extends to a maximum

lateral distance of 2,150 ft from the injection well. The EPA Area of Review (AoR) is defined by the 1% saturation isoline of the stabilized free-phase plume.

5.2 Conceptual Model and Arbuckle Hydrogeologic State Information

5.2.1 Modeled Formation

The simulation model spans the entire thickness of the Arbuckle aquifer (Figure 5.1a-c). The CO_2 is to be injected in the lower portion of the Arbuckle in the interval 4,910–5,050 feet which has relatively high permeability based on the core data collected at the site. Preliminary simulations indicated that the bulk of the CO_2 will remain confined in the lower portions of the Arbuckle because of the low permeability intervals in the baffle zones as discussed in Section 4.6.6 and also shown in analysis of geologic logs at wells KGS 1-28 and KGS 1-32 (Figure 4.32 a-b). Therefore, no-flow boundary conditions were specified along the top of the Arbuckle. The specification of a no-flow boundary at the top is also in agreement with hydrogeologic analyses presented in Section 4.7, which indicates that the upper confining zone—comprising the Simpson Group, the Chattanooga Shale, and the Pierson formation—has very low permeability, which should impede any vertical movement of groundwater from the Arbuckle Group. Evidence for sealing integrity of the confining zone and absence of transmissive faults include:

1) under-pressured Mississippian relative to pressure gradient in the Arbuckle (Section 4.6.3),

2) elevated chlorides in Mississippian relative to brine recovered at the top of the Arbuckle (Section 4.6.7),

3) Geochemical evidence for stratification of Arbuckle aquifer system and presence of a competent upper confining zone (Appendix E).

Additionally, entry pressure analyses (documented in Section 4.7.4) indicate that an increase in pore pressure of more than 956 psi within the confining zone at the injection well site

is required for the CO_2-brine to penetrate through the confining zone. As discussed in the model simulation results section below, the maximum increase in pore pressure at the top of the Arbuckle is less than 1.5 psi under the worst-case scenario (which corresponds to a low permeability–low porosity alternative model case as discussed in Section 5.4.9). This small pressure rise at the top of the Arbuckle is due to CO_2 injection below the lower vertical-permeability baffle zones present in the middle of the Arbuckle Group, which confines the CO_2 in the injection interval in the lower portions of the Arbuckle Group. The confining zone is also documented to be locally free of transmissive fractures based on fracture analysis conducted at KGS 1-28 (injection well) and documented in Section 4.7.5. There are no known transmissive faults in the area, as documented in Section 6. It should be noted that an Operation Plan For Safe and Efficient Injection has been submitted to the EPA, which has provision for immediate cessation of injection should an anomalous pressure drop be detected owing to development or opening of fractures.

Based on the above evidence, it is technically appropriate to restrict the simulation region within the Arbuckle Group for purposes of numerical efficiency, without compromising predictions of the effects of injection on the plume or pressure fronts. Because of the presence of the Precambrian granitic basement under the Arbuckle Group, which is expected to provide hydraulic confinement, the bottom of the model domain was also specified as a no-flow boundary. Active, real-time pressure and temperature monitoring of the injection zone at the injection and monitoring wells will likely be able to detect any significant movement of CO2 out of the injection zone along fractures. Also, the 18-seismometer array will detect small seismicity and their hypocenters within several hundred feet resolution to provide additional means to monitor the unlikely movement of CO2 above or below the Arbuckle injection zone.

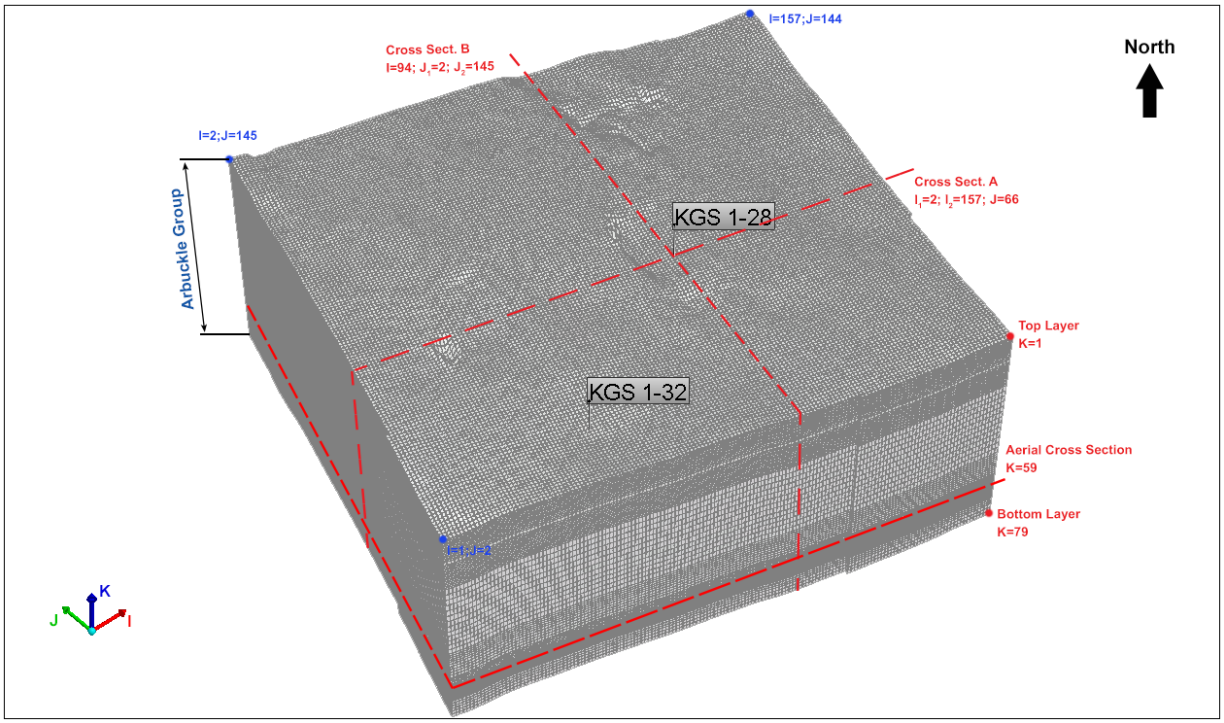

Figure 5.1a Model mesh in 3-D showing location of Arbuckle injection and monitoring wells along with the east-west and north-south cross sections.

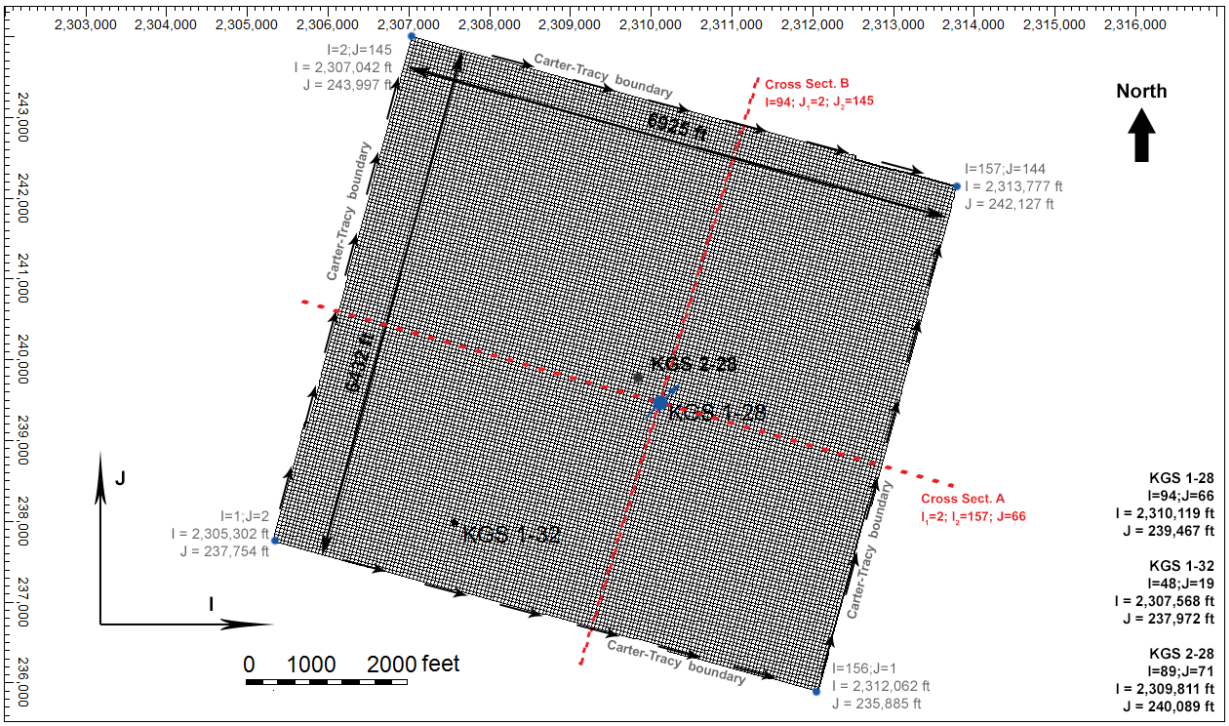

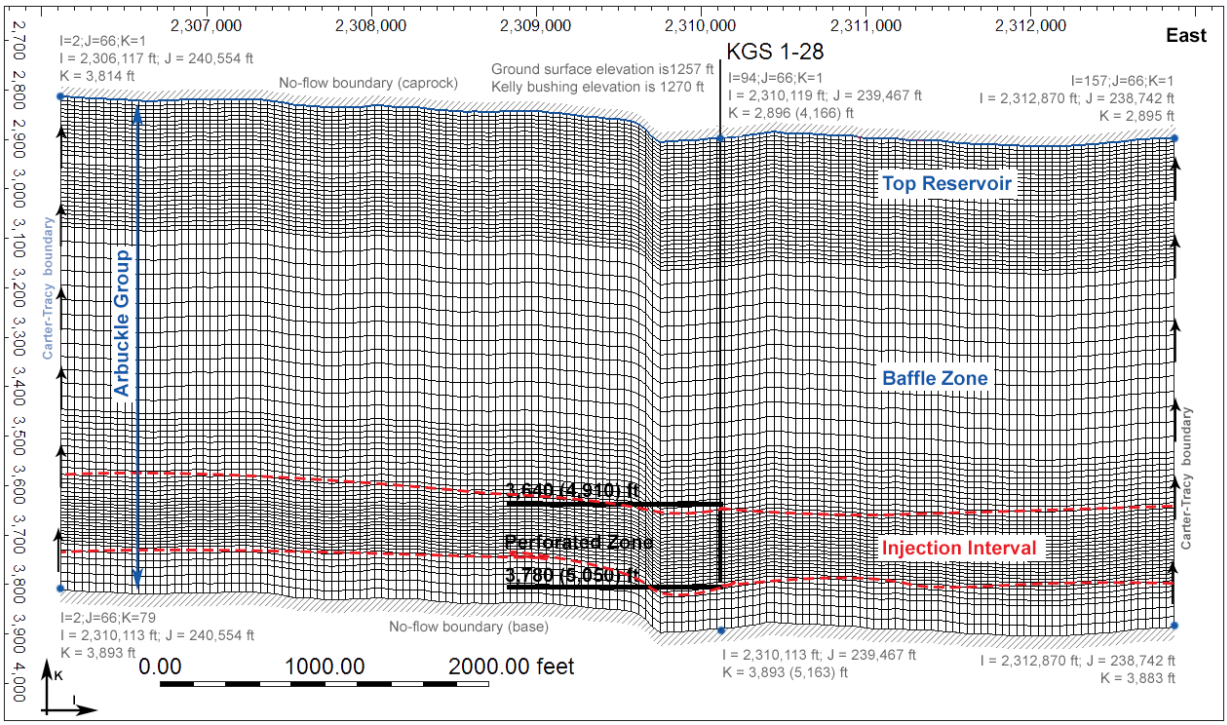

Figure 5.1b—North-South cross section of model grid along column 94 showing boundary conditions.

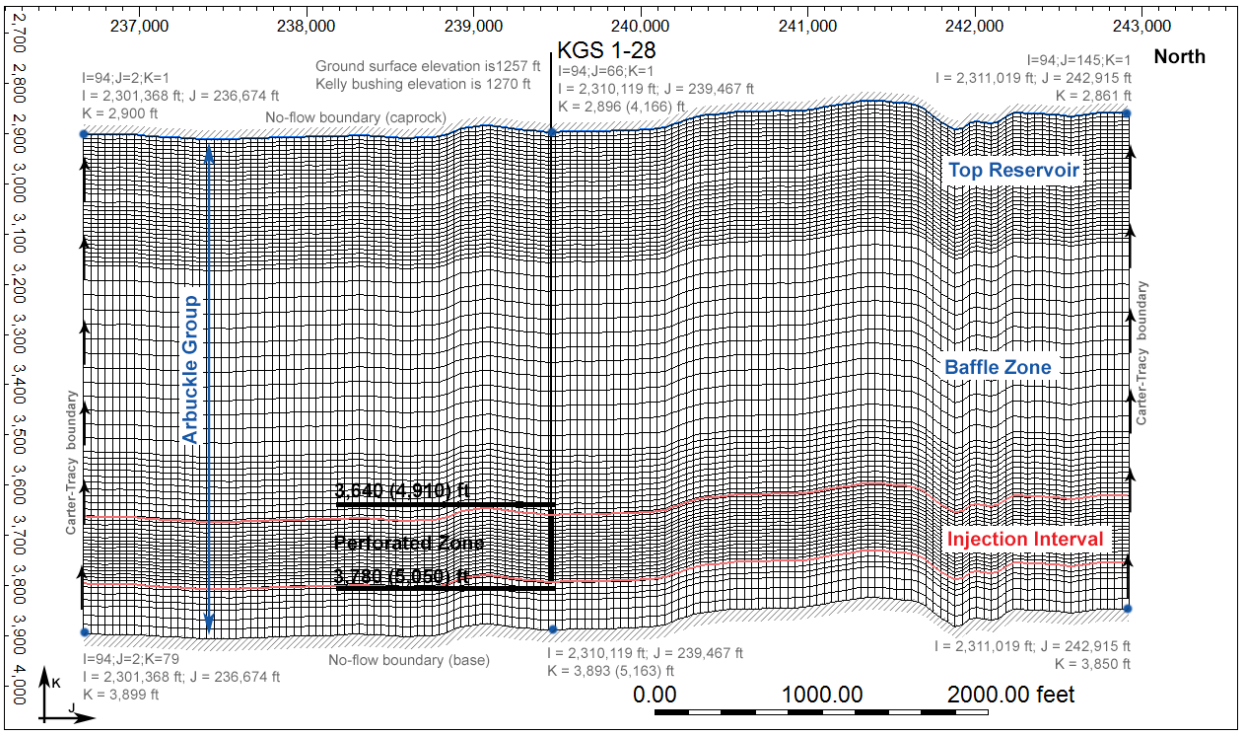

Figure 5.1c—East-west cross section of model grid along row 66 showing boundary conditions.

5.2.2 Modeled Processes

Physical processes modeled in the reservoir simulations included isothermal multi-phase flow and transport of brine and CO2. Isothermal conditions were modeled because the total variation in subsurface temperature in the Arbuckle Group from the top to the base is only slightly more than 10°F (which should not significantly affect the various storage modes away from the injection well), and because it is assumed that the temperature of the injected CO_2 will equilibrate to formation temperatures close to the well. Also, non-isothermal sensitivity simulations were conducted for the EPA in which it was demonstrated that including temperature as a variable impacts the plume extent and the pressure distribution only minimally. Uniform salinity concentration was assumed as the effects of water salinity on the simulated AoR were found to be negligible (less than 0.5%).

Subsurface storage of CO2 occurs via the following four main mechanisms:

- structural trapping,
- aqueous dissolution,
- hydraulic trapping, and
- mineralization.

The first three mechanisms were simulated in the Wellington model. Mineralization was not simulated as geochemical modeling indicated that due to the short-term and small- scale nature of the pilot project, mineral precipitation is not expected to cause any problems with clogging of pore space that may reduce permeability and negatively impact injectivity. Therefore, any mineral storage that may occur will only result in faster stabilization of the CO_2 plume and make projections presented in this model somewhat more conservative with respect to extent of plume migration and CO_2 concentrations.

5.2.3 Geologic Structure

There are no transmissive faults in the Arbuckle Group that breach the overlying confining zone in proximity to the AoR derived from the model results. The closest large mapped fault on top of the Arbuckle and the Mississippian is approximately 12.5 mi southeast of

Wellington, as shown in Figures 6.4 and 6.8. The seismic data at the Wellington site, presented in Section 4.8, also points to the absence of large faults in the immediate vicinity of Wellington Field.

5.2.4 Arbuckle Hydrogeologic State Information

As shown in Figures 4.29, 4.31, and 4.35, the ambient pore pressure, temperature, and salinity vary nearly linearly with depth in the Arbuckle Group. By linear extrapolation, the relationship between depth and these three parameters can be expressed by the following equations using the data in Figures 4.29, 4.31, and 4.35:

Temperature (°F) = (0.011 * Depth + 73.25)

Pressure (psi) = (0.487 * Depth – 324.8)

Chloride (mg/l) = (100.9 * Depth – 394.786)

Where, depth is in feet below Kelly Bushing (KB)

Using the above relationships, the temperature, pressure, and salinity at the top and bottom of the Arbuckle Group at the injection well site (KGS 1-28) are presented in Table 5.1.

Table 5.1—Temperature, pressure, and salinity at the top and bottom of the Arbuckle Group at the injection well site (KGS 1-28).

	Top of Arbuckle (4,168 ft)	Bottom of Arbuckle (5,160 ft)
Temperature (°F)	115	130
Pressure (psi)	1,705	2,188
Chloride (mg/l)	25,765	125,858

5.2.5 Arbuckle Groundwater Velocity

On a regional basis, groundwater flows from east to west in the Arbuckle, as shown in the potentiometric surface map presented in Figure 4.37. Groundwater velocity, however, is estimated to be very slow. The head in Sumner County drops approximately 100 ft over 20 mi (Figure 4.37), resulting in a head gradient of approximately 1.0e-03 ft/ft. Assuming an average large-scale Arbuckle porosity of approximately 6% and a median permeability of 10 mD based on the statistical distribution of this parameter shown in Figure 4.33 , the pore velocity in the Arbuckle is approximately 0.2 ft/year, which is fairly small and can be neglected in

specification of ambient boundary conditions for the purpose of this modeling study.

5.2.6 Model Operational Constraints

The bottom hole injection pressure in the Arbuckle should not exceed 90% of the estimated fracture gradient of 0.75 psi/ft (measured from land surface) as derived in Section 4.6.9. Therefore, the maximum induced pressure at the top and bottom of the Arbuckle Group should be less than 2,813 and 3,483 psi, respectively, as specified in Table 5.2. At the top of the perforations (4,910 ft), pressure will not exceed 2,563 psi.

Table 5.2—Maximum allowable pressure at the top and bottom of the Arbuckle Group based on 90% fracture gradient of 0.675 psi/ft.

Depth (feet, bls)	Maximum Pore Pressure (psi)
4,166 (Top of Arbuckle)	2,813
4,910 (Top of Perforation)	3,314
5,050 (Bottom of Perforation)	3,408
5,163 (Bottom of Arbuckle)	3,483

5.3 Geostatistical Reservoir Characterization of Arbuckle Group

Statistical reservoir geomodeling software packages have been used in the oil and gas industry for decades. The motivation for developing reservoir models was to provide a tool for better reconciliation and use of available hard and soft data (Figure 5.2). Benefits of such numerical models include 1) transfer of data between disciplines, 2) a tool to focus attention on critical unknowns, and 3) a 3-D visualization tool to present spatial variations to optimize reservoir development. Other reasons for creating high-resolution geologic models include the following:

- volumetric estimates

- multiple realizations that allow unbiased evaluation of uncertainties before finalizing a drilling program
- lateral and top seal analyses
- integration (i.e., by gridding) of 3-D seismic surveys and their derived attributes assessments of 3-D connectivity.
- flow-simulation-based production forecasting using different well designs
- optimizing long-term development strategies to maximize return on investment.

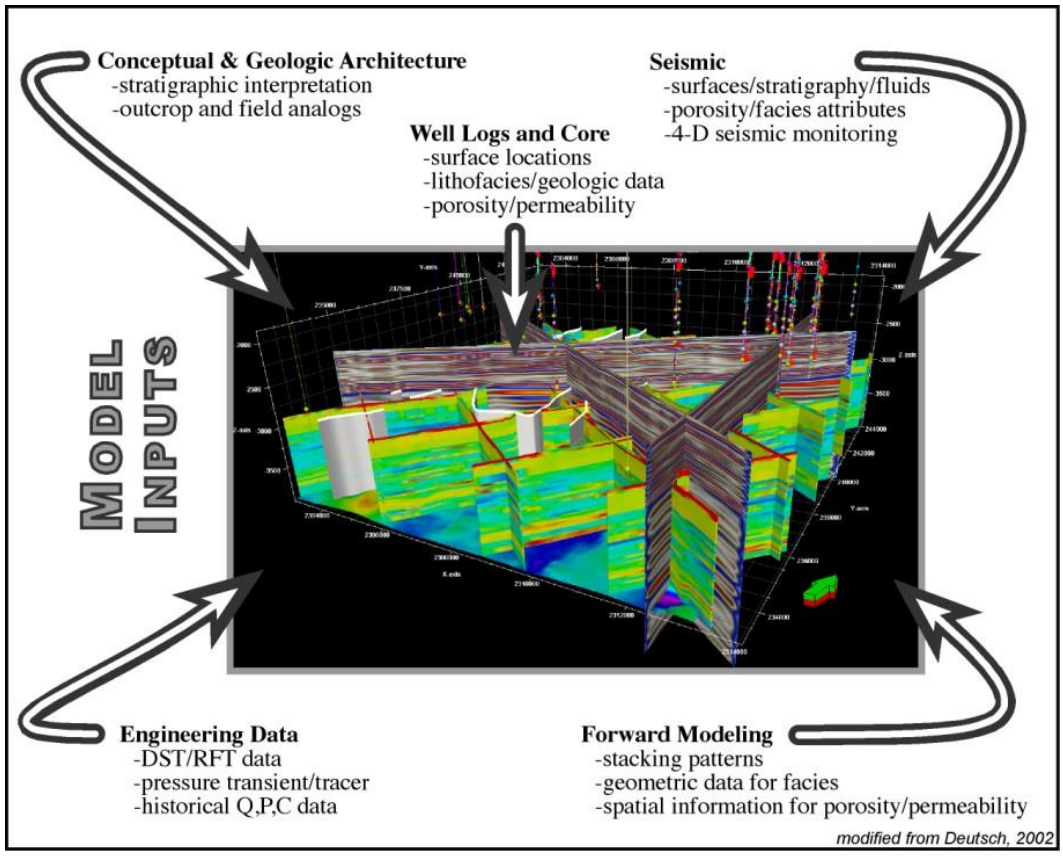

Figure 5.2—A static, geocellular reservoir model showing the categories of data that can be incorporated (source: modified from Deutsch, 2002)

Although geocellular modeling software has largely flourished in the energy industry, its utility can be important for reservoir characterization in CO2 research and geologic storage projects, such as the Wellington Field. The objective in the Wellington project is to integrate various data sets of different scales into a cohesive model of key petrophysical properties, especially porosity and permeability. The general steps for applying this technology are to

model the large-scale features followed by modeling progressively smaller, more uncertain, features. The first step applied at the Wellington Field was to establish a conceptual depositional model and its characteristic stratigraphic layering. The stratigraphic architecture provided a first-order constraint on the spatial continuity of facies, porosity, permeability, saturations, and other attributes within each layer. Next, facies (i.e., rock fabrics) were modeled for each stratigraphic layer using cell-based or object-based techniques. Porosity was modeled by facies and conditioned to "soft" trend data, such as seismic inversion attribute volumes. Likewise, permeability was modeled by facies and collocated, co-kriged to the porosity model.

5.3.1 Conceptual Model

Lower Arbuckle core from Wellington reveals sub-meter-scale, shallowing-upward peritidal cycles. The two common motifs are cycles passing from basal dolo-mudstones/wackestones into algal dololaminites or matrix-poor monomict breccias. Bioclasts are conspicuously absent. Breccias are clast-supported, monomictic, and angular, and their matrix dominantly consists of cement (Figure 5.3). They are best classified as crackle to mosaic breccias (Loucks, 1999) because there is little evidence of transportation. Lithofacies and stacking patterns (i.e., sub-meter scale, peritidal cycles) are consistent with an intertidal to supratidal setting. Breccia morphologies, scale (<0.1 m), mineralogy (e.g., dolomite, anhydrite, length-slow chalcedony), depositional setting, greenhouse climate, and paleo-latitude (~15º S) support mechanical breakdown processes associated with evaporite dissolution. The Arbuckle-Simpson contact (~800 ft above the proposed injection interval) records the super-sequence scale, Sauk-Tippecanoe unconformity, which records subaerial-related karst landforms across the Early Phanerozoic supercontinent Laurentia.

5.3.2 Facies Modeling

The primary depositional lithofacies were documented during core description at KGS 1-32. A key issue was reconciling large variations between permeability measurements derived from wireline logs (i.e., nuclear resonance tool), whole core, and step-rate tests. Poor core recovery from the injection zone resulted from persistent jamming, which is commonly experienced in fractured or vuggy rocks. Image logs acquired over this interval record some

intervals with large pores (cm scale) that are likely solution-enlarged vugs (touching-vugs of Lucia, 1999; Figure 5.4). Touching-vug fabrics commonly form a reservoir-scale, interconnected pore system characterized by Darcy-scale permeability. It is hypothesized that a touching-vug pore system preferentially developed within fracture-dominated crackle and mosaic breccias—*formed in response to evaporite removal*—which functioned as a strataform conduit for undersaturated meteoric fluids (Figure 5.5). As such, this high-permeability, interwell-scale, touching-vug pore system is largely strataform and, therefore, predictable.

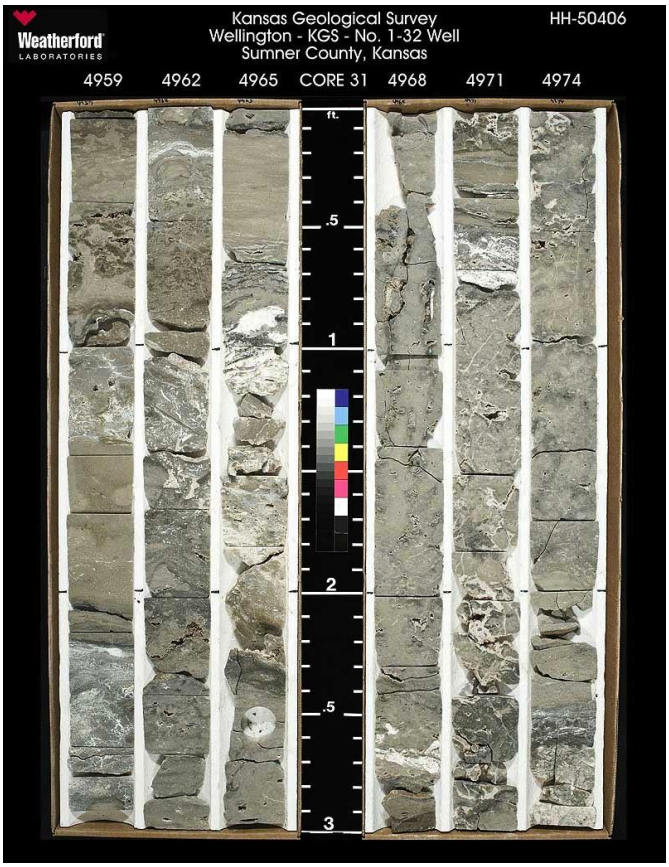

Figure 5.3—Example of the carbonate facies and porosity in the injection zone in the lower Arbuckle (part of the Gasconade Dolomite Formation). Upper half is light olive-gray, medium-grained dolomitic packstone with crackle breccia. Scattered subvertical fractures and limited cross stratification. Lower half of interval shown has occasional large vugs that crosscut the core consisting of a light olive-gray dolopackstone that is medium grained. Variable-sized vugs range from cm-size irregular to subhorizontal.

5.3.2.1 Petrophysical Properties Modeling

The approach taken for modeling a particular reservoir can vary greatly based on available information and often involves a complicated orchestration of well logs, core analysis, seismic surveys, literature, depositional analogs, and statistics. Because well log data were available in only two wells (KGS 1-28 and KGS 1-32) that penetrate the Arbuckle

reservoir at the Wellington site, the geologic model also relied on seismic data, step-rate test, and drill-stem test information. Schlumberger's Petrel™ geologic modeling software package was used to produce the current geologic model of the Arbuckle saline aquifer for the pilot project area. This geomodel extends 1.3 mi by 1.2 mi laterally and is approximately 1,000 ft in thickness, spanning the entire Arbuckle Group as well as a portion of the sealing units (Simpson/Chattanooga shale).

Porosity Modeling

In contrast to well data, seismic data are extensive over the reservoir and are, therefore, of great value for constraining facies and porosity trends within the geomodel. Petrel's volume attribute processing (i.e., genetic inversion) was used to derive a porosity attribute from the prestack depth migration (PSDM) volume to generate the porosity model (Figure 5.6). The seismic volume was created by re-sampling (using the original exact amplitude values) the PSDM 50 ft above the Arbuckle and 500 ft below the Arbuckle (i.e., approximate basement). The cropped PSDM volume and conditioned porosity logs were used as learning inputs during neural network processing.

A correlation threshold of 0.85 was selected and 10,000 iterations were run to provide the best correlation. The resulting porosity attribute was then re-sampled, or upscaled (by averaging), into the corresponding 3-D property grid cell.

The porosity model was constructed using sequential Guassian simulation (SGS). The porosity logs were upscaled using arithmetic averaging. The raw upscaled porosity histogram was used during SGS. The final porosity model was then smoothed. The following parameters were used as inputs:

I. Variogram

a. Type: spherical

b. Nugget: 0.001

c. Anisotropy range and orientation

i. Lateral range (isotropic): 5,000 ft

ii. Vertical range: 10 ft

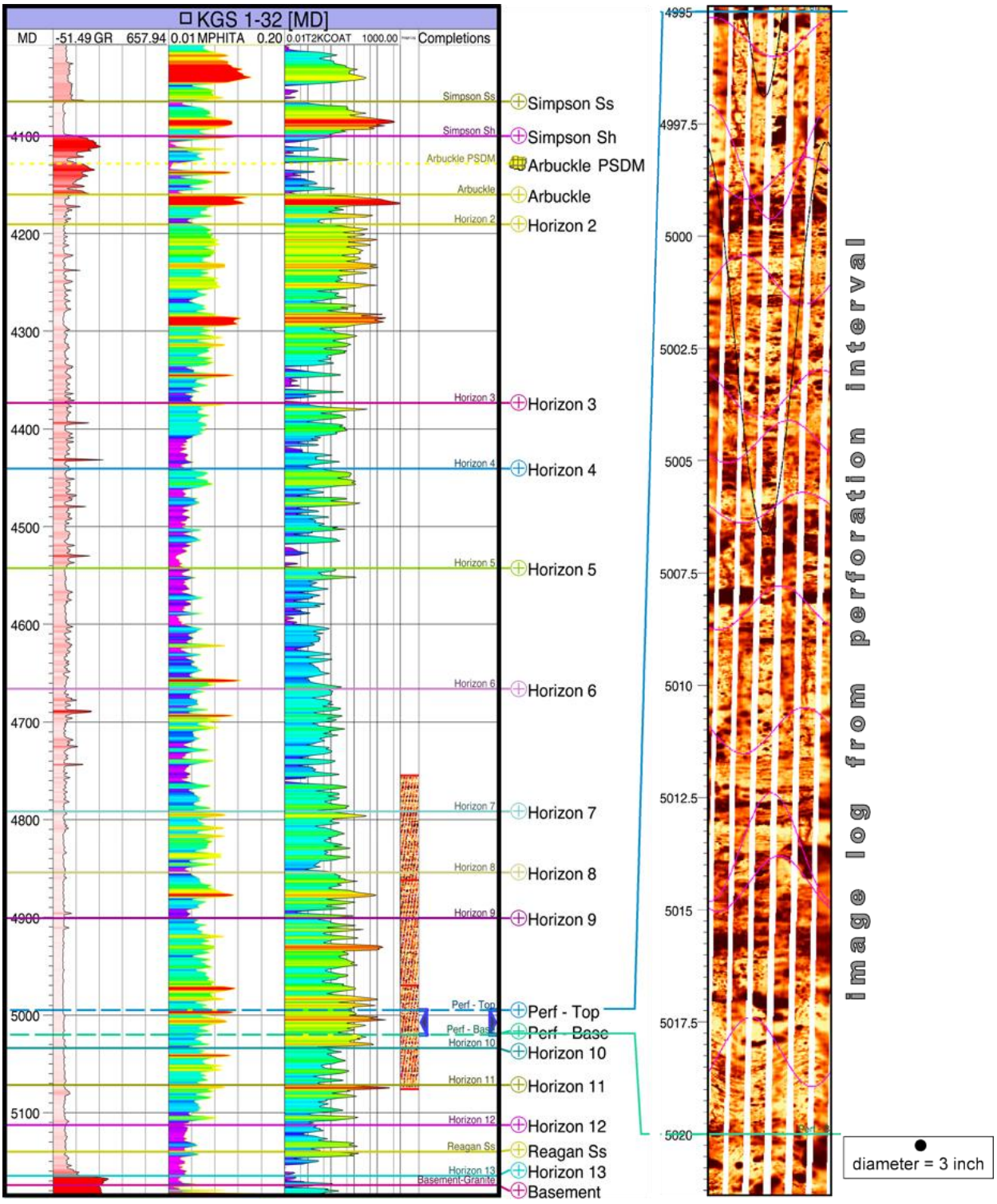

Figure 5.4—Geophysical logs within the Arbuckle Group at KGS 1-32. (Notes: MPHITA represents Haliburton porosity. Horizon markers represent porosity package. Image log on right presented to provide example of vugs; 3-in diameter symbol represents size of vug).

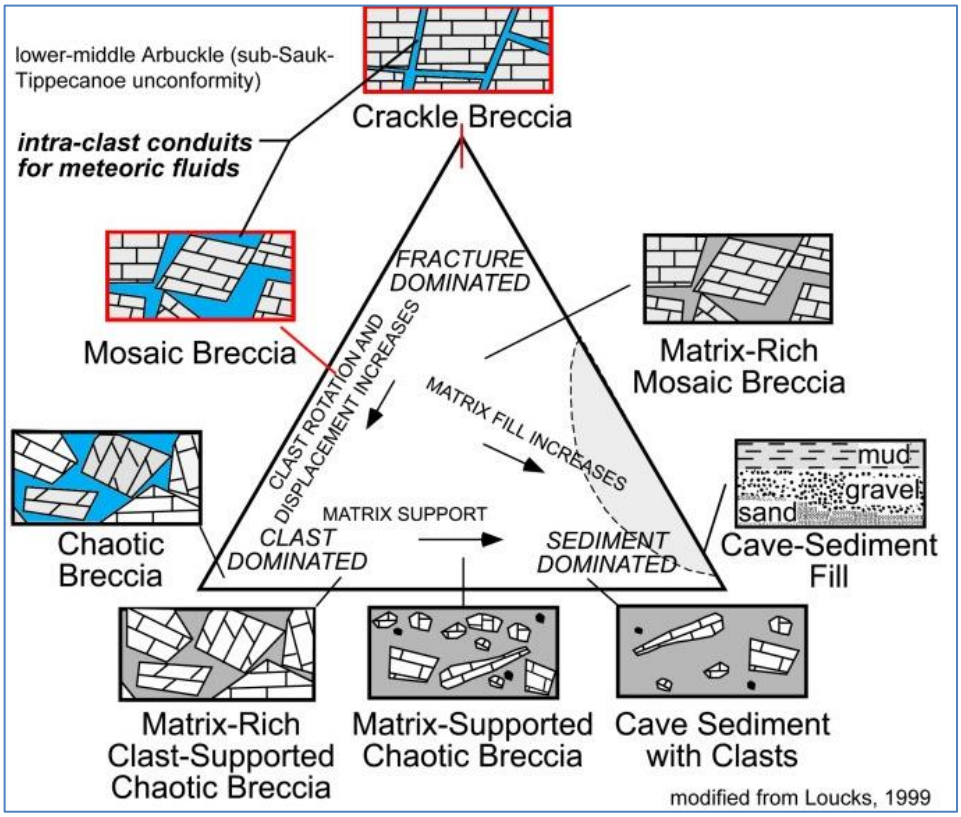

Figure 5.5—Classification of breccias and clastic deposits in cave systems exhibiting relationship between chaotic breccias, crackle breccias, and cave-sediment fill (source: Loucks, 1999).

II. Distribution: actual histogram range (0.06–0.11) from upscaled logs

III. Co-Kriging

a. Secondary 3-D variable: inverted porosity attribute grid

b. Correlation coefficient: 0.75

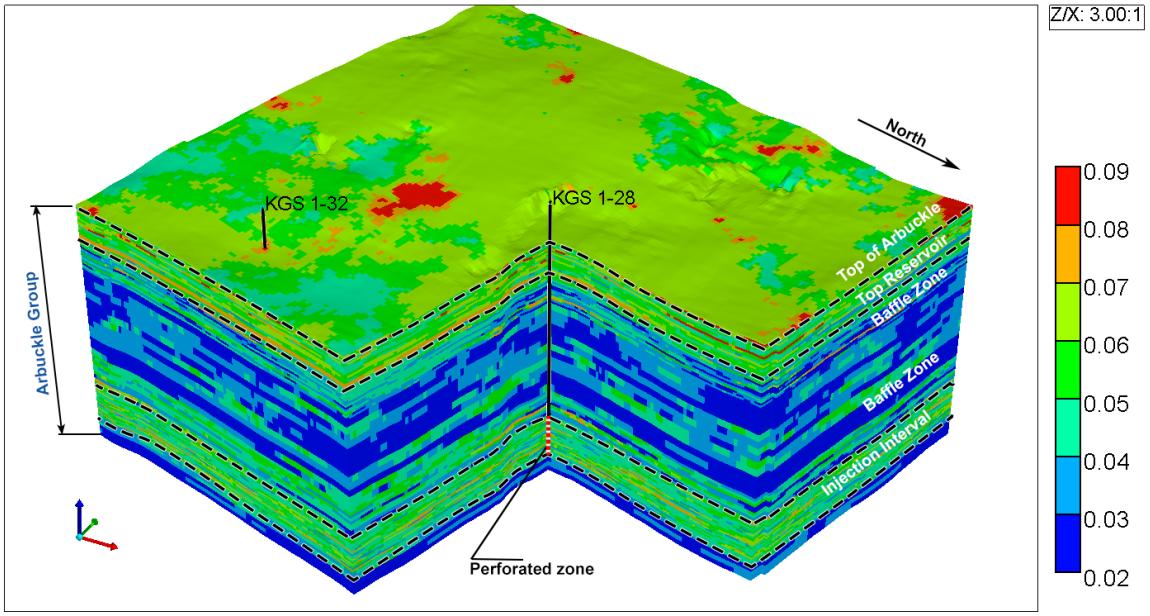

Figure 5.6—Upscaled porosity distribution in the Arbuckle Group based on the Petrel geomodel

Permeability Modeling

The upscaled permeability logs shown in Figure 5.4 were created using the following controls: geometric averaging method; logs were treated as points; and method was set to simple. The permeability model was constructed using SGS. Isotropic semi-variogram ranges were set to 3,000 ft horizontally and 10 ft vertically. The permeability was collocated and co-Kriged to the porosity model using the calculated correlation coefficient (~0.70). The resulting SGS-based horizontal and vertical permeability distributions are presented in Figure 5.7a-f, which shows the relatively high permeability zone selected for completion within the injection interval. Table 5.3 presents the minimum, maximum, and average permeabilities within the Arbuckle Group in the geomodel.

Table 5.3—Hydrogeologic property statistics in hydrogeologic characterization and simulation models.

	Reservoir Characterization Geomodel			Reservoir Simulation Numerical Model		
Property	min	max	avg	min	max	avg
Porosity (%)	3.2	12.9	6.8	3.2	12.9	6.7
Horizontal Permeability (mD)	0.05	23,765	134.2	0.05	23,765	130.7
Vertical Permeability (mD)	.005	1,567	387	0.005	1,567	385

5.4 Arbuckle Reservoir Flow and Transport Model

An extensive set of computer simulations were conducted to estimate the potential impacts of CO2 injection in the Arbuckle injection zone. The key objectives were to determine the resulting rise in pore pressure and the extent of CO2 plume migration. The underlying motivation was to determine whether the injected CO2 could affect the USDW or potentially escape into the atmosphere through existing wells or hypothetical faults/fractures that might be affected by the injected fluid.

As in all reservoirs, there are data gaps that prevent an absolute or unique characterization of the geology and petrophysical properties. This results in conceptual, parametric, and boundary condition uncertainties. To address these uncertainties, a comprehensive set of simulations were conducted to perform a sensitivity analysis using alternative parameter sets. A key objective was to derive model parameter sets that would result in the most negative impacts (the worst-case scenario; i.e., maximum formation pressures and largest extent of plume migration). However, simulations involving alternative parameter and boundary conditions that resulted in more favorable outcomes were also conducted to bracket the range of possible induced system states and outcomes.

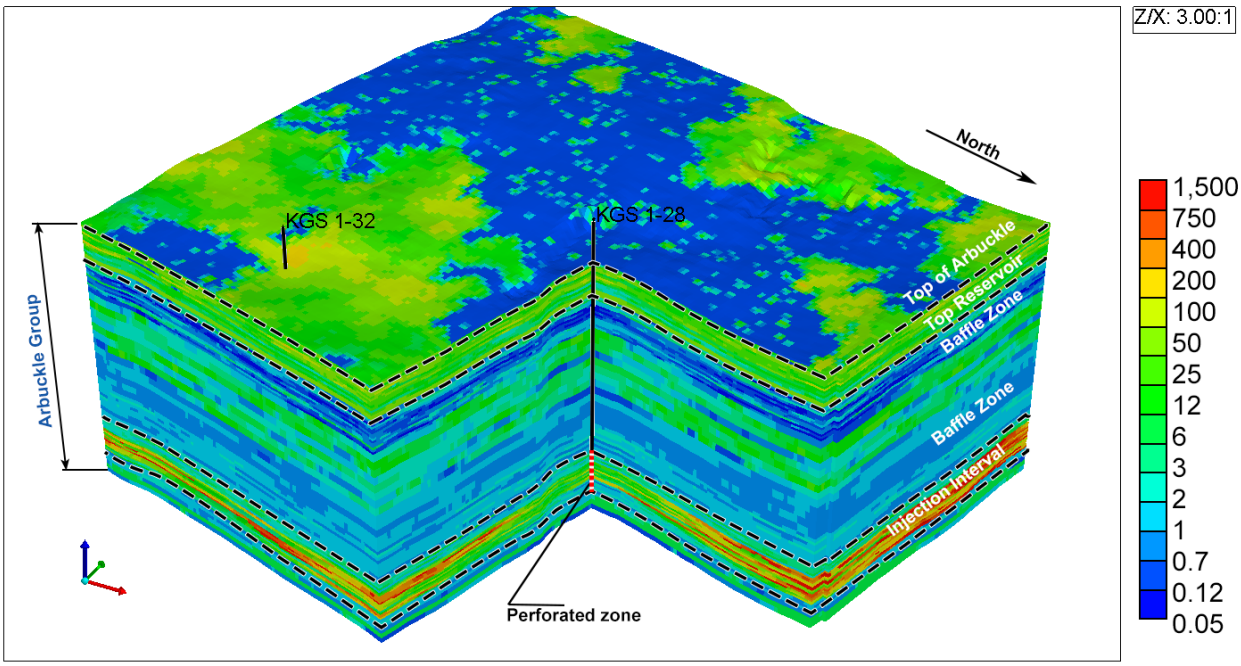

Figure 5.7a—Upscaled horizontal permeability (mD) distributions in the Arbuckle Group derived from Petrel geo-model.

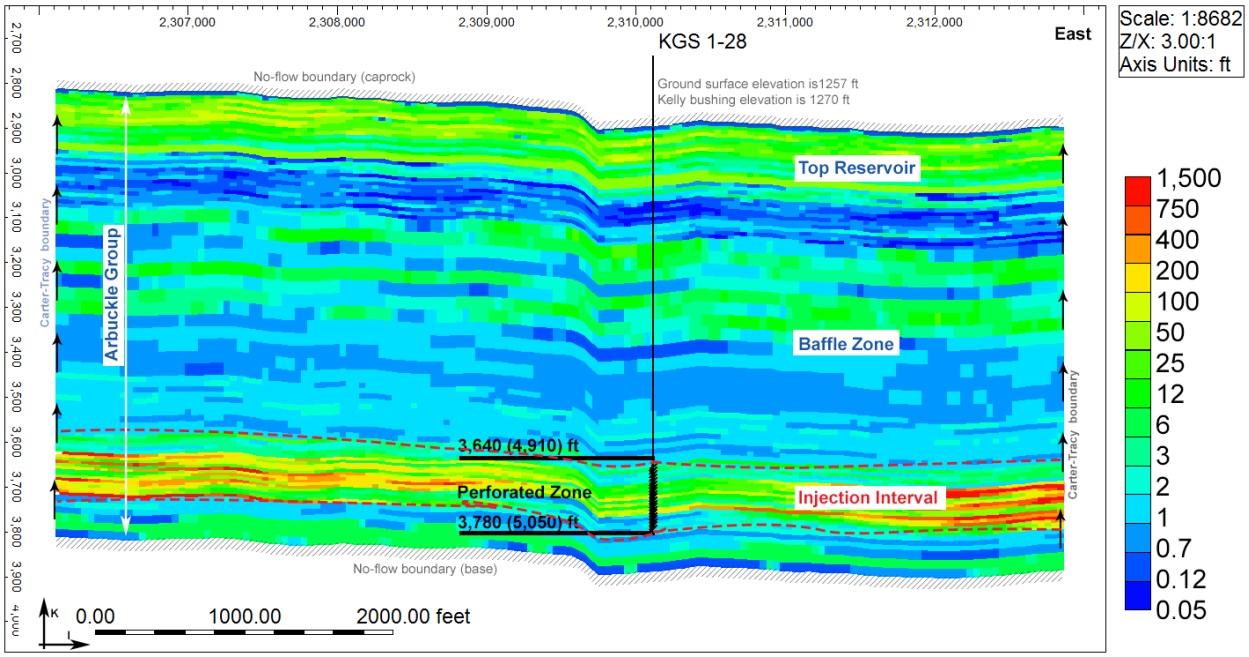

Figure 5.7b— Horizontal permeability (mD) distribution within an east-west cross section through the injection well (KGS 1-28), vertical cross-section A.Location of cross section shown in Figure 5.1a.

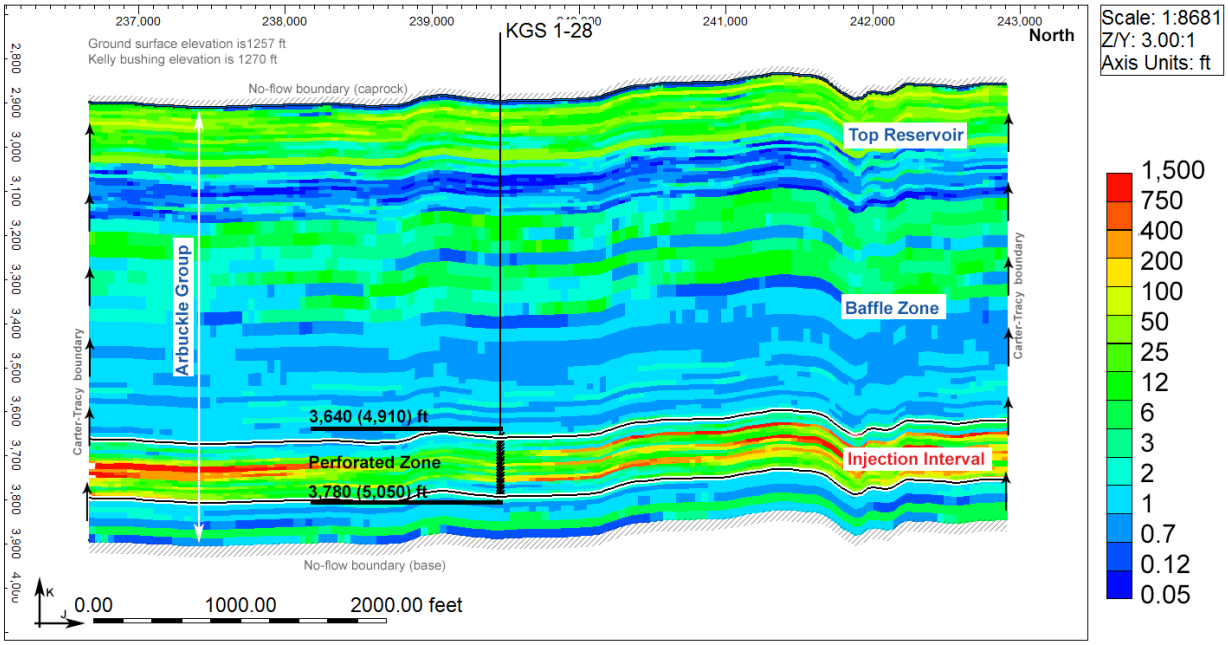

Figure 5.7c— Horizontal permeability (mD) distribution within an north-south cross section through the injection well (KGS 1-28), vertical cross-section B. Location of cross section shown in Figure 5.1a.

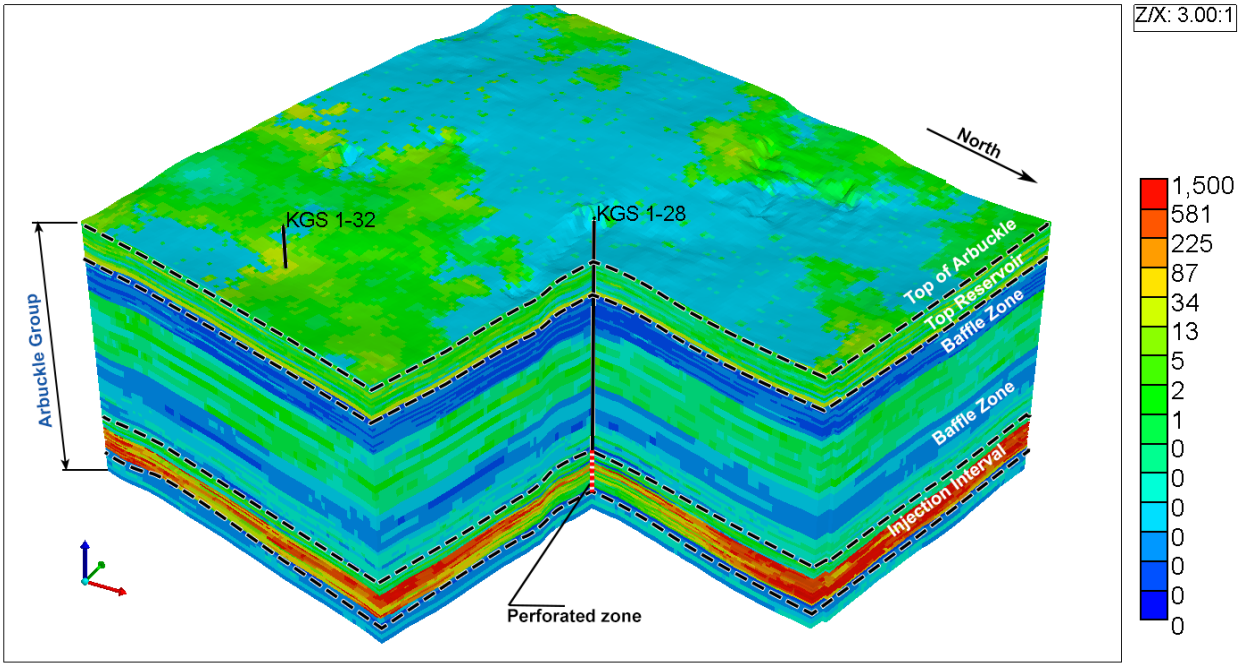

Figure 5.7d—Upscaled vertical permeability (mD) distributions in the Arbuckle Group derived from Petrel geomodel.

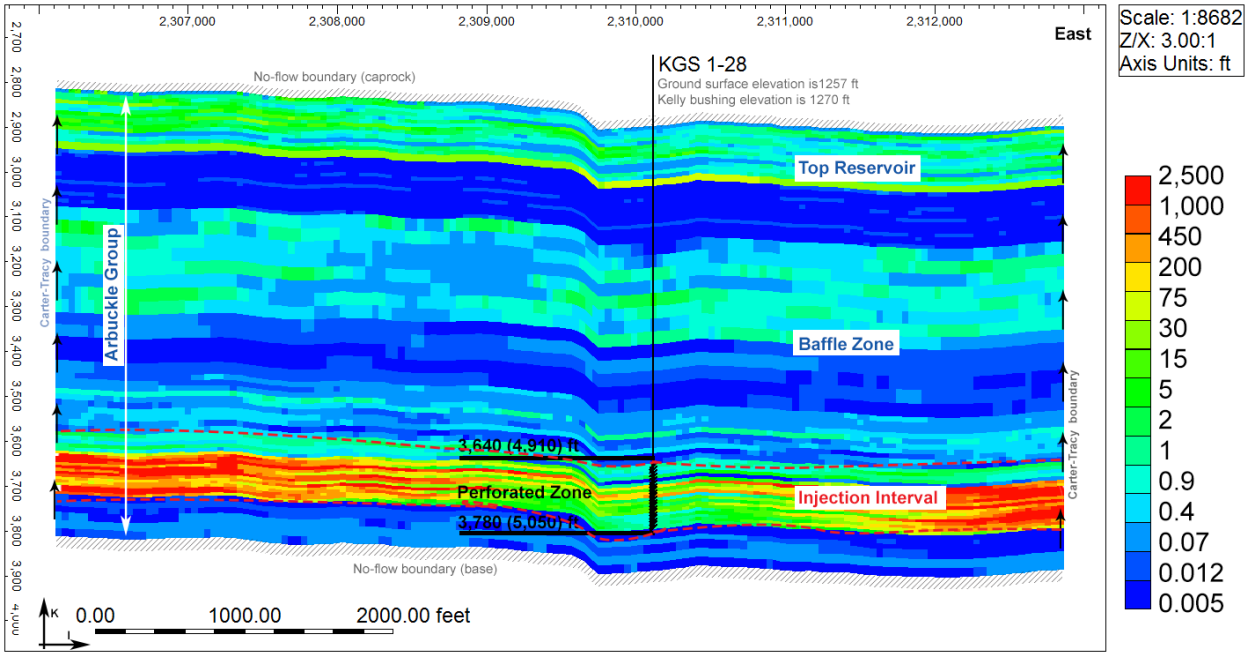

Figure 5.7e—Vertical permeability (mD) distribution within an east-west cross section through the injection well (KGS 1-28), vertical cross-section A. Location of cross section shown in Figure 5.1a.

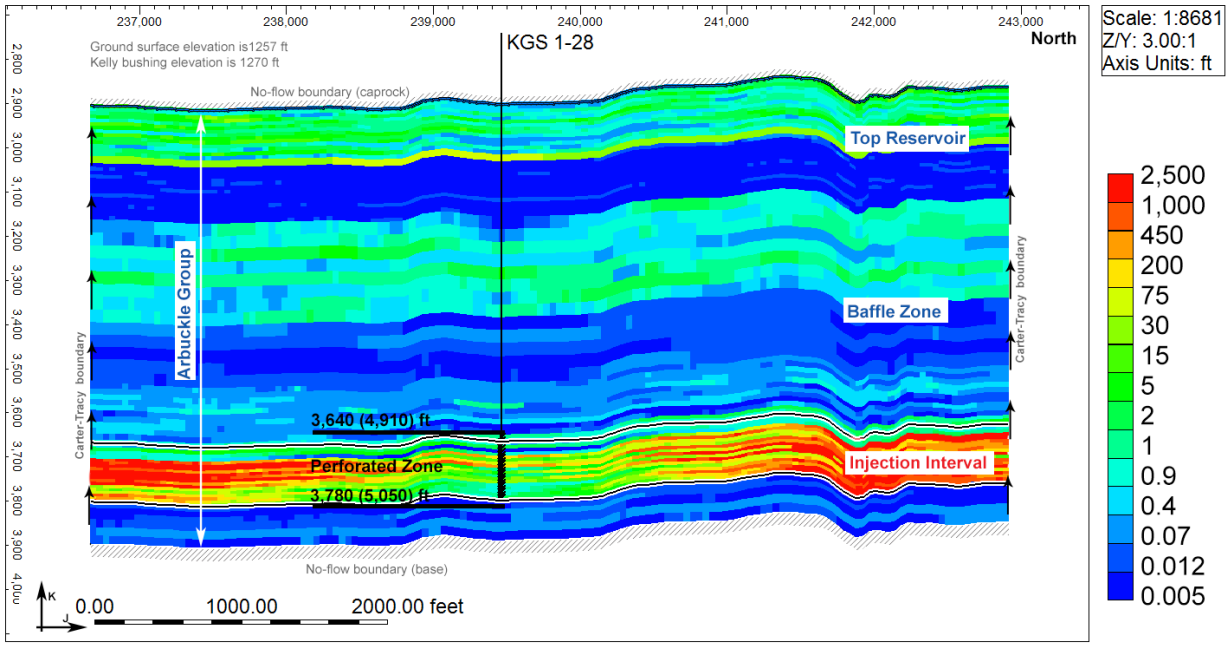

Figure 5.7f—Vertical permeability (mD) distribution within a north-south cross section through the injection well (KGS 1-28), vertical cross-section B. Location of cross section shown in Figure 5.1a.

5.4.1 Simulation Software Description

The reservoir simulations were conducted using the Computer Modeling Group (CMG) GEM simulator. GEM is a full equation of state compositional reservoir simulator with advanced features for modeling the flow of three-phase, multi-component fluids and has been used to conduct numerous CO2 studies (Chang et al., 2009; Bui et al., 2010). It is considered by DOE to be an industry standard for oil/gas and CO_2 geologic storage applications. GEM is an essential engineering tool for modeling complex reservoirs with complicated phase behavior interactions that have the potential to impact CO_2 injection and transport. The code can account for the thermodynamic interactions between three phases: liquid, gas, and solid (for salt precipitates). Mutual solubilities and physical properties can be dynamic variables depending on the phase composition/system state and are subject to well-established constitutive relationships that are a function of the system state (pressures,

saturation, concentrations, temperatures, etc.). In particular, the following assumptions govern the phase interactions:

- Gas solubility obeys Henry's Law (Li and Nghiem, June 1986)
- The fluid phase is calculated using Schmit-Wenzel or Peng-Robinson (SW-PR) equations of state (Soreide-Whitson, 1992)
- Changes in aqueous phase density with CO_2 solubility, mineral precipitations, etc., are accounted for with the standard or Rowe and Chou correlations.
- Aqueous phase viscosity is calculated based on Kestin, Khalifa, and Correia (1981).

5.4.2 Model Mesh and Boundary Conditions

The Petrel-based geomodel mesh discussed above consists of a 706 x 654 horizontal grid and 79 vertical layers for a total of 36,476,196 cells. The model domain spans from the base of the Arbuckle Group to the top of the Pierson Group. To reduce reservoir simulation time, this model was upscaled to a 157 x 145 horizontal mesh with 79 layers for a total of 1,798,435 cells to represent the same rock volume as the Petrel model for use in the CMG simulator. The thickness of the layers varies from 5 to 20 ft based on the geomodel, with an average of 13 feet.

Based on preliminary simulations, it was determined that due to the small scale of injection and the presence of a competent confining zone, the plume would be contained within the Arbuckle system for all alternative realizations of reservoir parameters. Therefore, the reservoir model domain was restricted to the Arbuckle aquifer with no-flow boundaries specified along the top (Simpson Group) and bottom (Precambrian basement) of the Arbuckle group. As discussed in Section 5.2.1, the specification of no-flow boundaries along the top and

bottom of the Arbuckle Group is justified because of the low permeabilities in the overlying and underlying confining zones as discussed in Section 4.7.3. The permeability in the Pierson formation was estimated to be as low as 1.6 nanoDarcy (nD; 1.0-9 Darcy) as documented in Section 4.7.3.

The simulation model, centered approximately on the injection well (KGS 1-28), extends approximately 1.2 mi in the east-west and 1.3 mi in the north-south orientations. Vertically, the model extends approximately 1,000 ft from the top of the Precambrian basement to the bottom of the Simpson Group. As discussed above, the model domain was discretized laterally by 157 x 145 cells in the east-west and north-south directions and vertically in 79 layers. The lateral boundary conditions were set as an infinite-acting Carter-Tracy aquifer (Dake, 1978; Carter and Tracy, 1960) without leakage. This is appropriate since the Arbuckle is an open hydrologic system extending over most of Kansas as discussed in Section 3. Sensitivity simulations indicated that the increase in pore pressures and the plume extent was not meaningfully different by using a closed boundary instead of a Carter-Tracy boundary.

5.4.3 Hydrogeologic Properties

Geologic and hydrologic data pertaining to the Arbuckle Group are detailed in Sections 3 and 4 of the permit application. As discussed in Section 5.3, site-specific hydrogeologic properties were used to construct a geomodel at the Wellington site. The porosity and permeability of the geomodel were upscaled to the coarser grid using a weighted averaging approach so that the total pore space volume in the Petrel geomodel was maintained in the upscaled reservoir simulation model. As shown in Figures 5.8a-b and 5.9, the qualitative representation (i.e., the shape) of the permeability and porosity distribution remained similar in both the geo and reservoir models. The upscaled reservoir grid was imported from Petrel into CMG Builder, where the model was prepared for dynamic simulations assuming an

equivalent porous medium model with flow limited to only the rock matrix. The minimum, maximum, and average porosity and permeabilities in the reservoir model are documented in Table 5.3 alongside the statistics for the geomodel.

5.4.4 Rock Type Assignment

Nine rock types and corresponding tables with capillary pressure hysteresis were developed based on RQI ranges, where RQI is calculated for each grid cell using the formula:

$$RQI = 0.0314\sqrt{Perm/Porosity}$$

Using RQI ranges, rock types are assigned using CMG Builder's Formula Manager. The resulting maps of rock types distribution in the model is outlined in Figure 5.10a-c. The division of the 9 rock-types (RT) was based on dividing the irreducible water saturation into 9 ranges to find their equivalent RQI as shown in the table below. Relative permeability and capillary pressure curves were calculated for each of the 9 RQI.

	RQI		
RT	**RQI from**	**RQI To**	**Ave RQI**
1	40	10	25
2	10	2.5	6.25
3	2.5	1	1.75
4	1	0.5	0.75
5	0.5	0.4	0.45
6	0.4	0.3	0.35
7	0.3	0.2	0.25
8	0.2	0.1	0.15
9	0.1	0.01	0.055

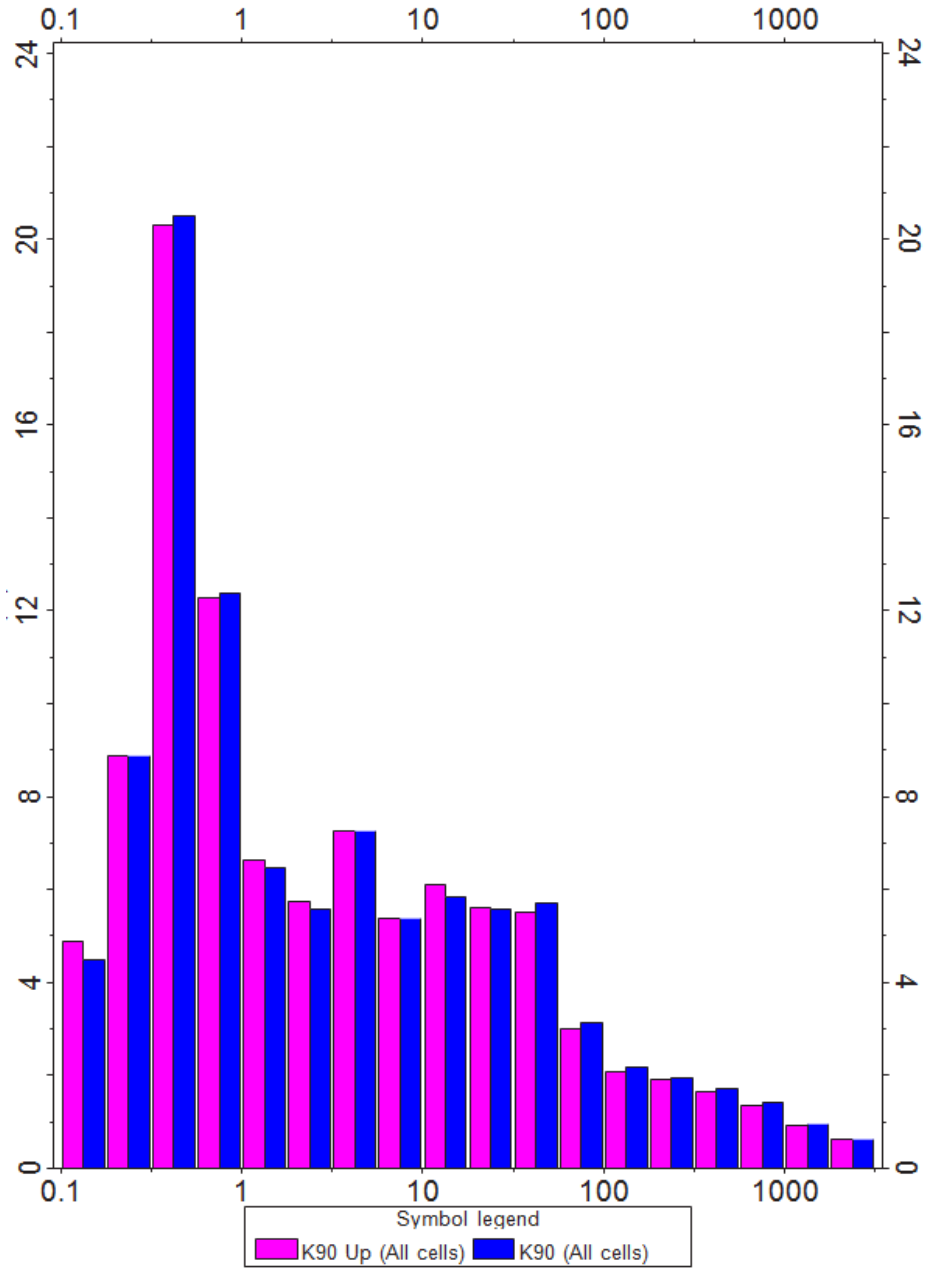

Figure 5.8a—Horizontal permeability distribution histogram comparison for original (blue) and upscaled (pink) model properties.(Note: x-axis represents permeability in milliDarcy, mD.)

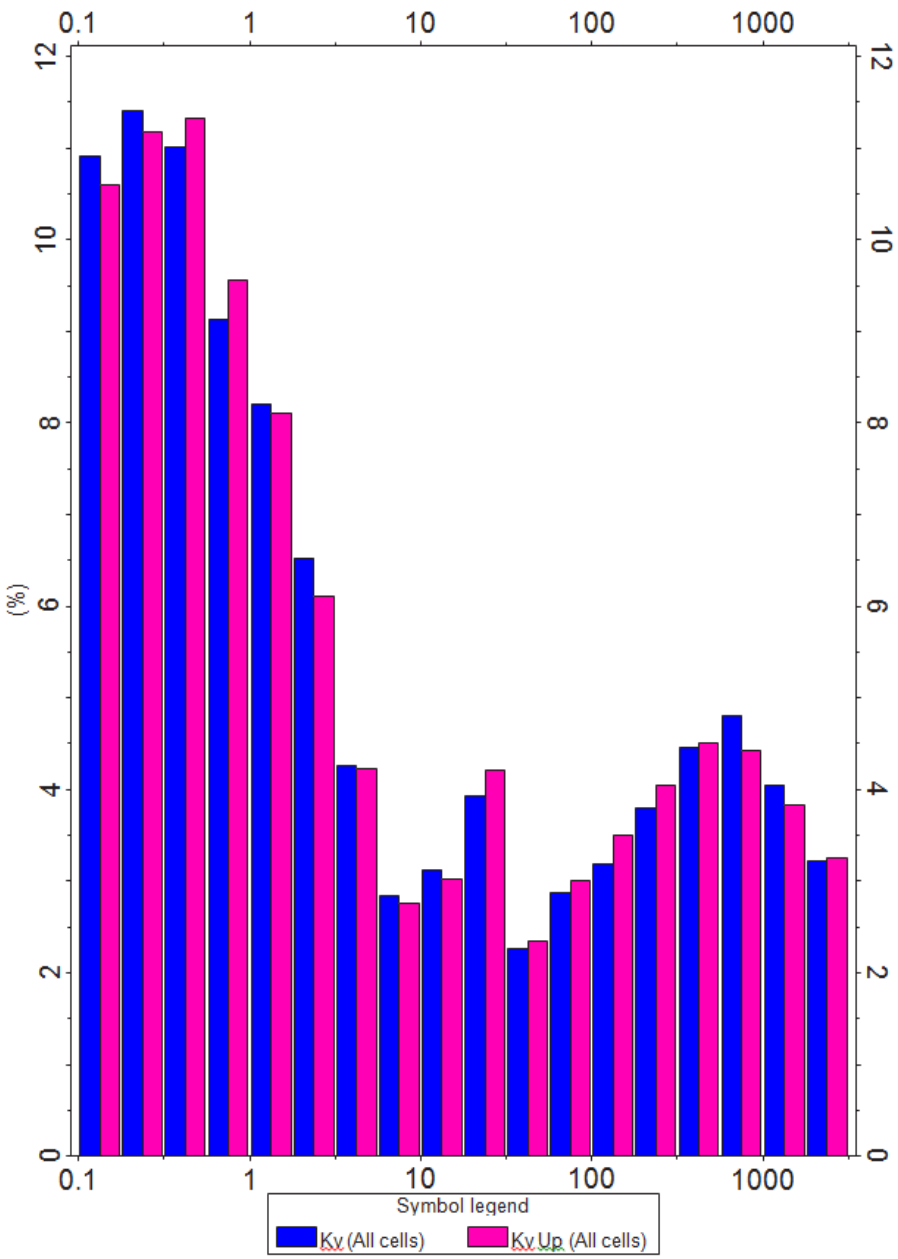

Figure 5.8b—Vertical permeability distribution histogram comparison for original (blue) and upscaled (pink) model properties. (Note: x-axis represents permeability in milliDarcy, mD.)

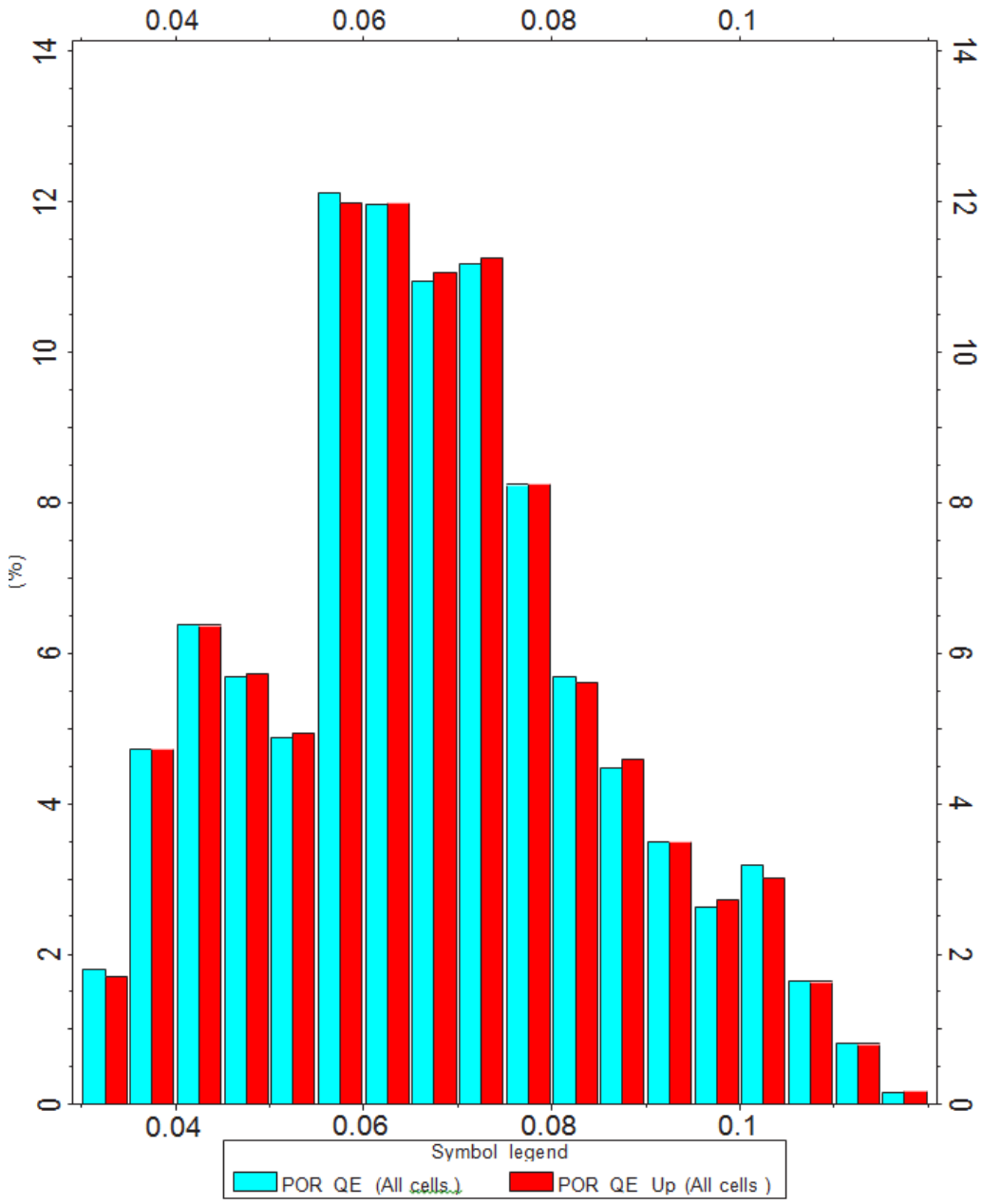

Figure 5.9—Porosity distribution histogram comparison for original and upscaled model properties. (Note: x-axis represents porosity.)

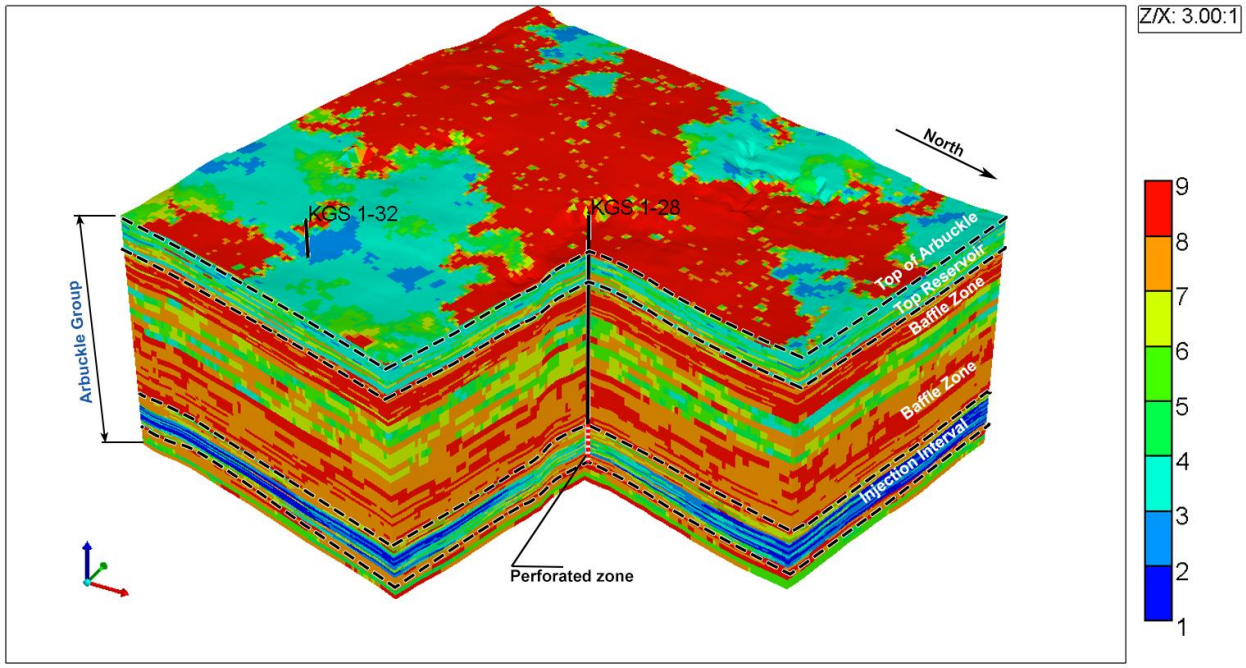

Figure 5.10a—Rock type distribution model

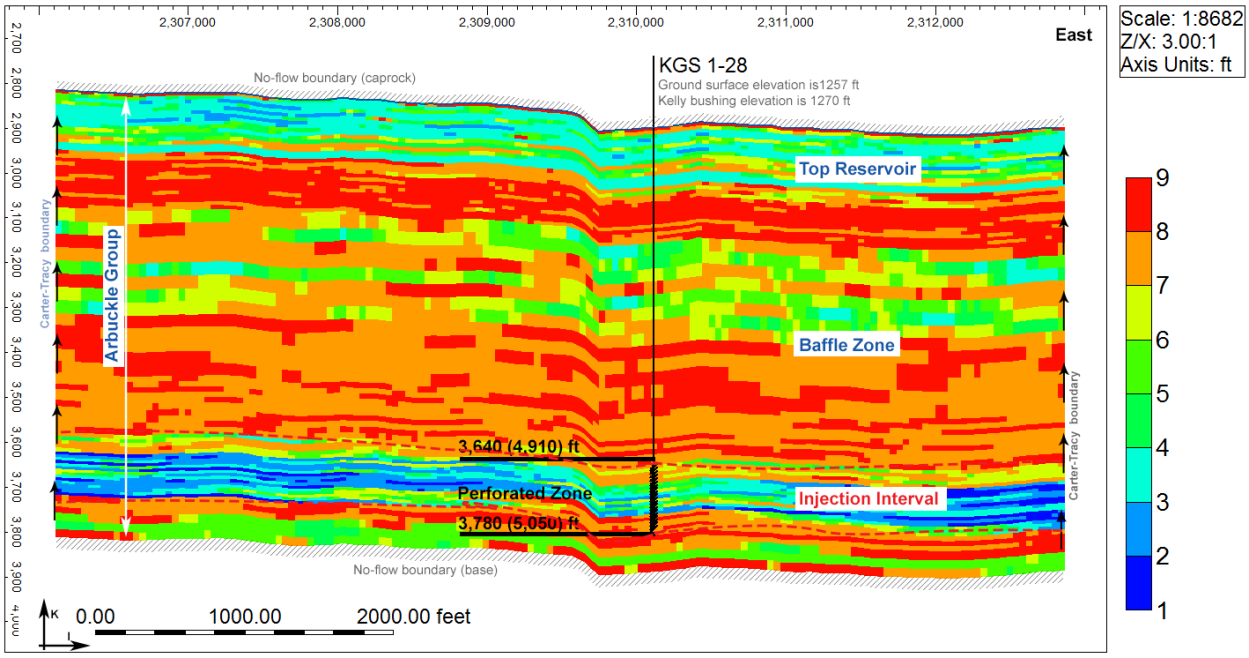

Figure 5.10b—Rock type distribution model, distribution within an east-west cross section through the injection well (KGS 1-28), vertical cross-section A

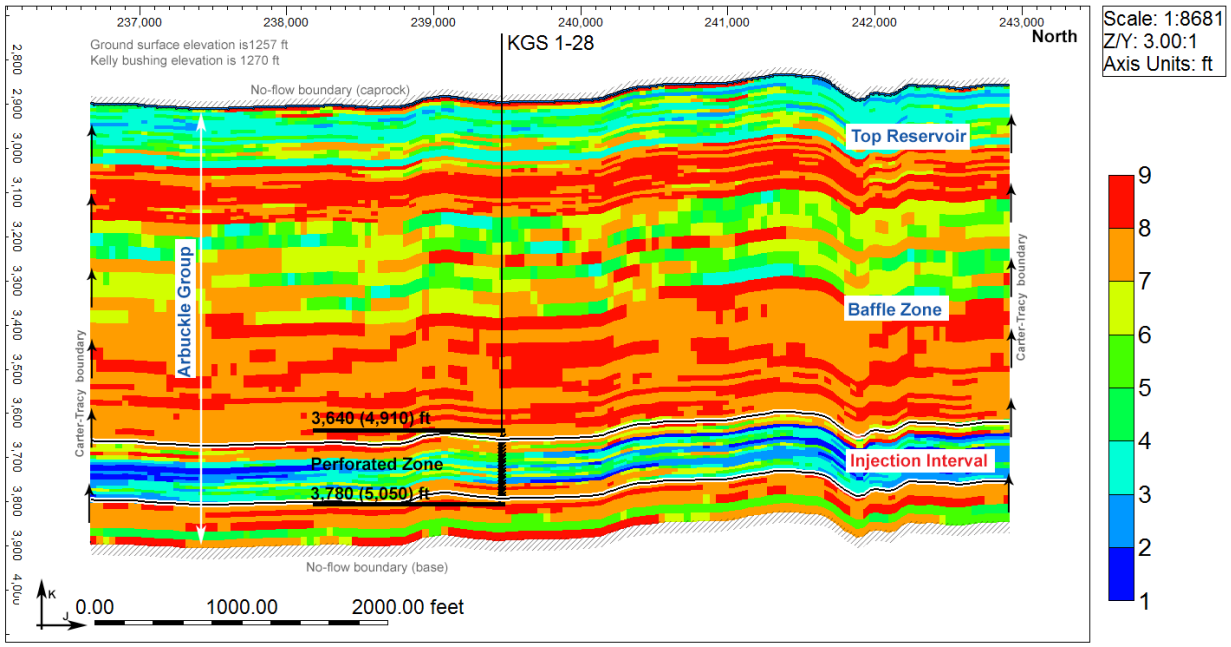

Figure 5.10c—Rock type distribution within a north-south cross section through the injection well (KGS 1-28), vertical cross-section B

5.4.5 Relative Permeability

Nine sets of relative permeability curves for both drainage and imbibition were calculated for the nine rock types. These sets of relative permeability curves were calculated based on a recently patented formula (SMH reference No: 1002061-0002) that relates the end-points to Reservoir Quality Index (RQI), thereby resulting in a realistic relative permeability data set. The validation of the method is presented below under "Validation of the Capillary Pressure and Relative Permeability Methods". Literature experimental studies including Krevor and Benson et al., [2012], Benson et al., [2015], indicate that the maximum experimental CO_2 saturation (S_{CO2max}) and maximum CO_2 relative permeability ($Kr_{CO2\ max}$) in higher permeability samples typically do not reach their actual values and are lower than expected. The authors note that the cause of low experimental endpoints are the unattainable high capillary pressure in the high permeability core samples. Calculations based on the new patented method addresses and resolves this issue. The highest maximum CO_2 relative permeability ($KrCO_{2\ max}$) for drainage curves from literature (Bennion & Bachu, 2005) is 0.54 which is lower than expected; however, the highest maximum CO_2 relative permeability using

the new method is 0.71, which is a more realistic value. As noted above, measured relative permeabilities from literature do not represent the endpoints of relative permeability curves and they need to be adjusted. Using this new method, SCO_{2max} and $KrCO_{2max}$ are scaled up to reasonable values.

Highest and lowest Corey CO_2 exponent values from (Bachu, 2010) were selected and they were assigned to the nine RQIs in a descending order from high to low. The full range of RQI assignments and relative permeability tables can be found in Appendix J. An example of capillary pressure and relative permeability for both drainage and imbibition is presented in Table 5.4. Corey Water exponents for different permeabilities from literature did not show much variability. Therefore, average values were used for both drainage and imbibition curves. Relative permeability curves for RQI of 0.35 is presented in Figure 5.11a for illustrative purposes. The same set of curves for the full range of RQI are presented in Figure 5.11b. Residual CO_2 saturation (SCO_2r) for calculating imbibition curves was needed. SCO_2r was calculated based on a correlation between residual CO_2 saturation (SCO_2r) and initial CO_2 saturation (SCO_2i) [Burnside and Naylor, 2014].

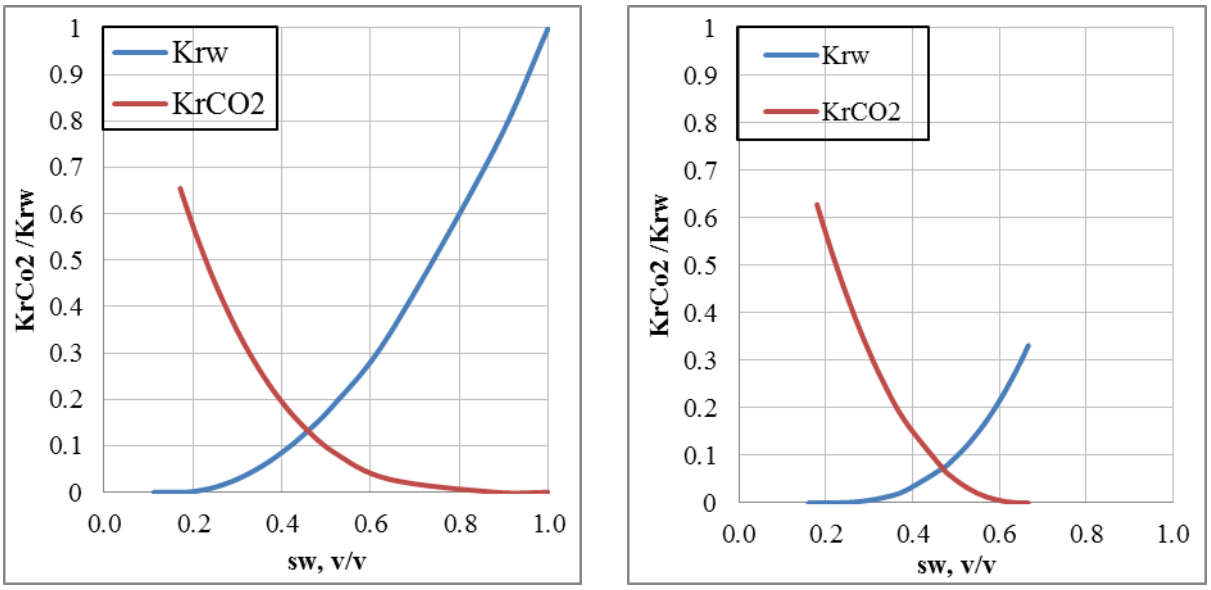

Figure 5.11a Calculated relative permeability for drainage (left) and imbibition (right) for RQI=0.35

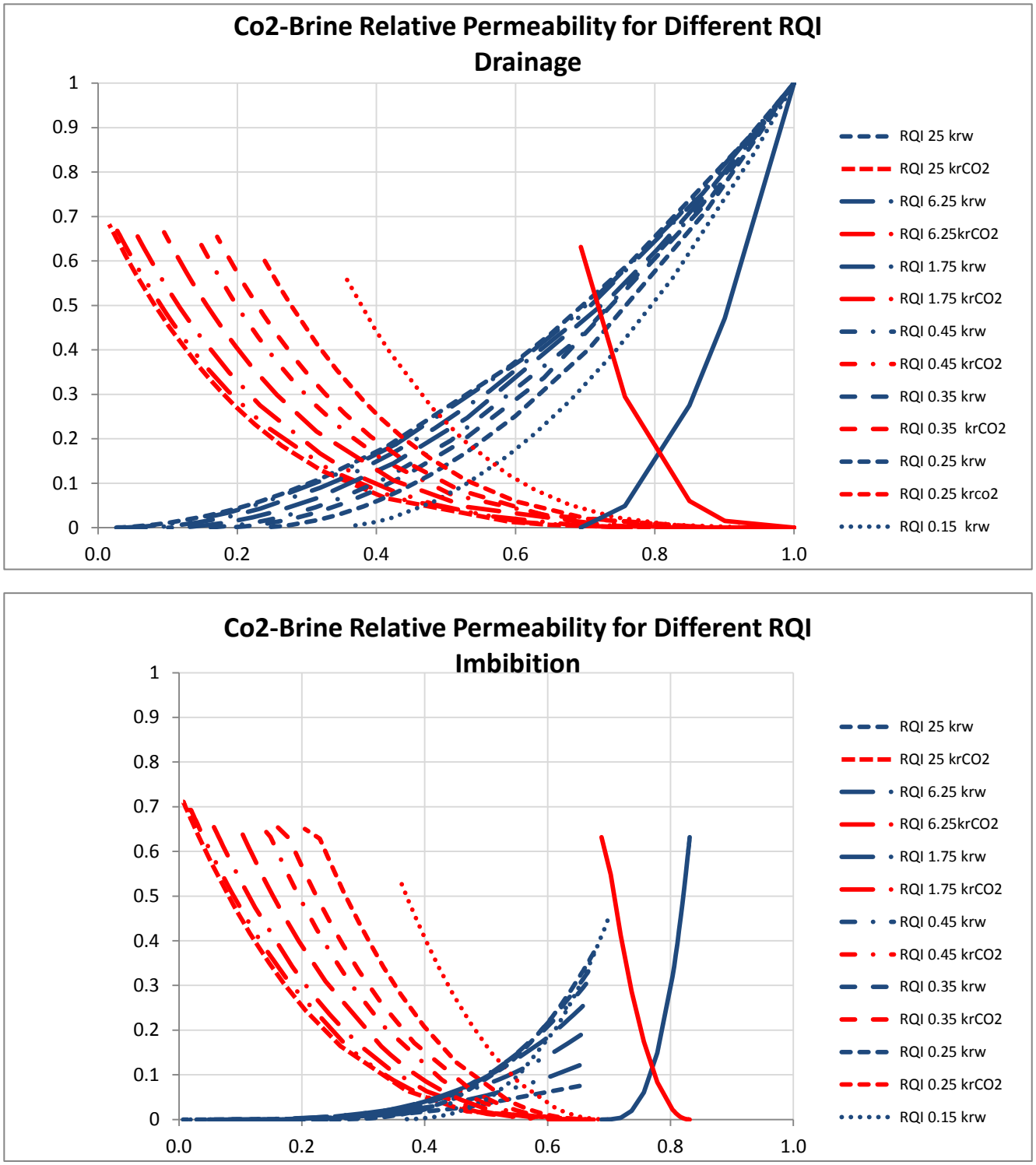

Figure 5.11b Calculated relative permeability for drainage (left) and imbibition (right) for full set of RQI.

Table 5.4—Example of capillary pressure and relative permeability drainage and imbibition tables for rock type 6 (RQI=0.35)

Drainage Curves

RQI range from 0.3-0.4-AveRQI=0.35				
Pc	Sw	sCO_2	Krw	$krCO_2$
1	1.000	0.000	1.000	0.000
2	0.877	0.123	0.735	0.001
3	0.641	0.359	0.338	0.029
4	0.518	0.482	0.190	0.086
5	0.443	0.557	0.119	0.148
6	0.392	0.608	0.080	0.205
7	0.354	0.646	0.056	0.257
8	0.326	0.674	0.041	0.302
9	0.304	0.696	0.030	0.341
10	0.286	0.714	0.023	0.375
12	0.258	0.742	0.013	0.432
14	0.238	0.762	0.008	0.478
18	0.211	0.789	0.003	0.545
20	0.201	0.799	0.002	0.571
25	0.183	0.817	0.000	0.620
30	0.171	0.829	0.000	0.655
40	0.156	0.844	0.000	0.655
50	0.146	0.854	0.000	0.655
60	0.140	0.860	0.000	0.655
70	0.135	0.865	0.000	0.655
80	0.131	0.869	0.000	0.655
90	0.129	0.871	0.000	0.655
100	0.126	0.874	0.000	0.655
150	0.119	0.881	0.000	0.655
200	0.116	0.884	0.000	0.655
300	0.112	0.888	0.000	0.655

Imbibition Curves

RQI range from 0.3-0.4-AveRQI=0.35				
Pc	Sw	sCO_2	Krw	$krCO_2$
0	0.666	0.334	0.331	0.000
0.00	0.665	0.335	0.328	0.000
0.01	0.663	0.337	0.325	0.000
0.02	0.660	0.340	0.319	0.000
0.03	0.657	0.343	0.313	0.000
0.04	0.654	0.346	0.308	0.000
0.05	0.652	0.348	0.302	0.000
0.06	0.649	0.351	0.297	0.000
0.07	0.646	0.354	0.292	0.000
0.08	0.643	0.357	0.287	0.000
0.09	0.640	0.360	0.282	0.001
0.1	0.638	0.362	0.277	0.001
0.2	0.612	0.388	0.234	0.003
0.3	0.589	0.411	0.200	0.008
0.4	0.569	0.431	0.171	0.013
0.5	0.550	0.450	0.148	0.020
0.6	0.532	0.468	0.128	0.029
0.7	0.516	0.484	0.112	0.038
0.8	0.501	0.499	0.098	0.047
0.9	0.487	0.513	0.086	0.057
1	0.474	0.526	0.076	0.067
2	0.383	0.617	0.026	0.172
3	0.329	0.671	0.011	0.261
4	0.293	0.707	0.005	0.333
5	0.267	0.733	0.002	0.390
6	0.248	0.752	0.001	0.437
7	0.233	0.767	0.001	0.476
8	0.221	0.779	0.000	0.508
9	0.211	0.789	0.000	0.536
10	0.203	0.797	0.000	0.559
12	0.189	0.811	0.000	0.598
14	0.180	0.820	0.000	0.629
20	0.160	0.840	0.000	0.655
30	0.144	0.856	0.000	0.655
40	0.135	0.865	0.000	0.655
50	0.129	0.871	0.000	0.655
60	0.126	0.874	0.000	0.655
70	0.123	0.877	0.000	0.655
80	0.121	0.879	0.000	0.655
90	0.119	0.881	0.000	0.655
100	0.117	0.883	0.000	0.655
150	0.113	0.887	0.000	0.655
200	0.111	0.889	0.000	0.655
300	0.109	0.891	0.000	0.655

5.4.6 Capillary Pressure curves

Nine capillary pressure curves were calculated for drainage and imbibition for nine RQI values based on a recently patented formula (SMH reference No: 1002061-0002). The formula constitutes a function for the shape of Pc curves and functions for the end-points that are entry pressure (P_{entry}) and irreducible water saturation (Swir). The end-points are correlated to RQI. P_{entry} was calculated from entry radius (R15) and Winland R35 (R35). There is a relationship between R35 and R15 and a relationship between P_{entry} and R15; therefore, P_{entry} can be calculated from R15 derived from R35. Swir was calculated from the NMR log at a Pc equal to 20 bars (290 psi). For calculating the imbibition curves, another term which is the residual CO_2 saturation (CO_{2r}) was needed. CO_{2r} was calculated from a relationship between initial CO_2 saturation and CO_{2r} that was discussed above. The capillary pressure curves for drainage and imbibition for RQI of 0.35 is presented in Figure 5.12. The capillary pressure data for the full set of RQI is presented in Appendix J.

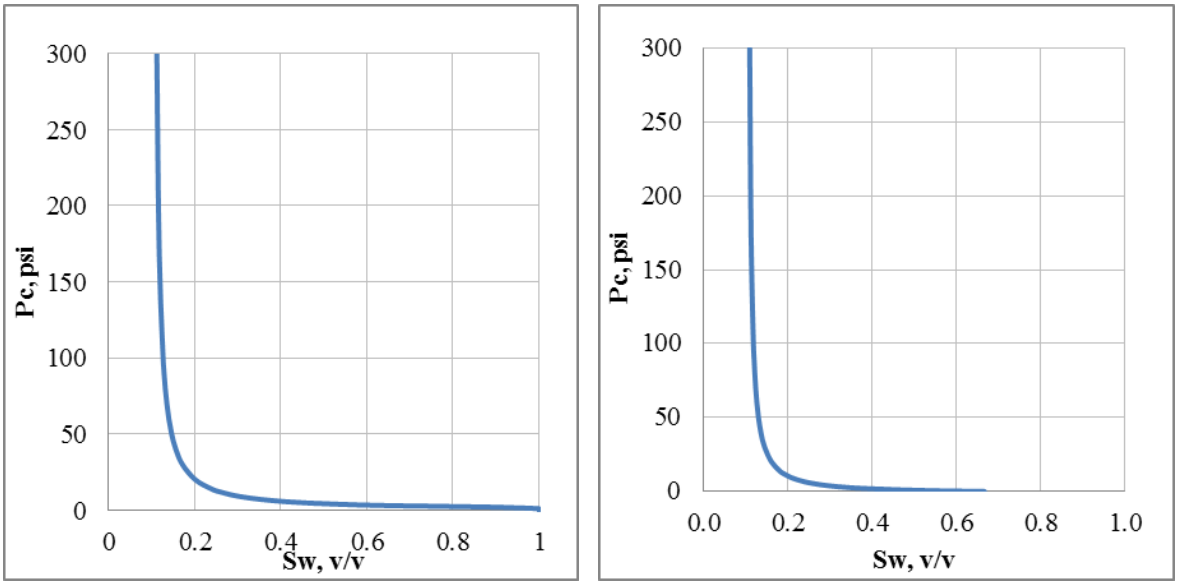

Figure 5.12—Capillary pressure curves for drainage (left) and imbibition (right) for RQI 0.35

5.4.7 Validation of the Capillary Pressure and Relative Permeability Methods

The capillary pressure and relative permeability curves were estimated in the laboratory for the Mississippian Reservoir as part of the Wellington Mississippian Enhanced Oil Recovery (EOR) project located approximately a mile southwest of the Wellington CO_2

storage site. The laboratory derived curves were used to validate the relative permeability and capillary pressure approach for the Arbuckle discussed above and this was deemed reasonable since the same approach that was used in the Mississippian was also used for the Arbuckle.

Two core plug samples with similar RQI were sent to Core Laboratories for capillary pressure and relative permeability measurements. The relative permeability and capillary pressure curves were calculated twice for the Mississippian - prior to and following the core results from the laboratory. The initial estimation of Pc curves was based on the endpoints that were calculated from NMR log. As shown in Figure 5.13a, there is a slight difference between the calculated Pc and measured Pc before calibration. However, there is an excellent match between the calculated Pc and the measured Pc after calibration using the core measured endpoints. Similarly, there is a slight difference between the initial calculated relative permeability and measured relative permeability (Figure 5.13b), but the match is excellent after calibration as shown in Figure 5.13b.

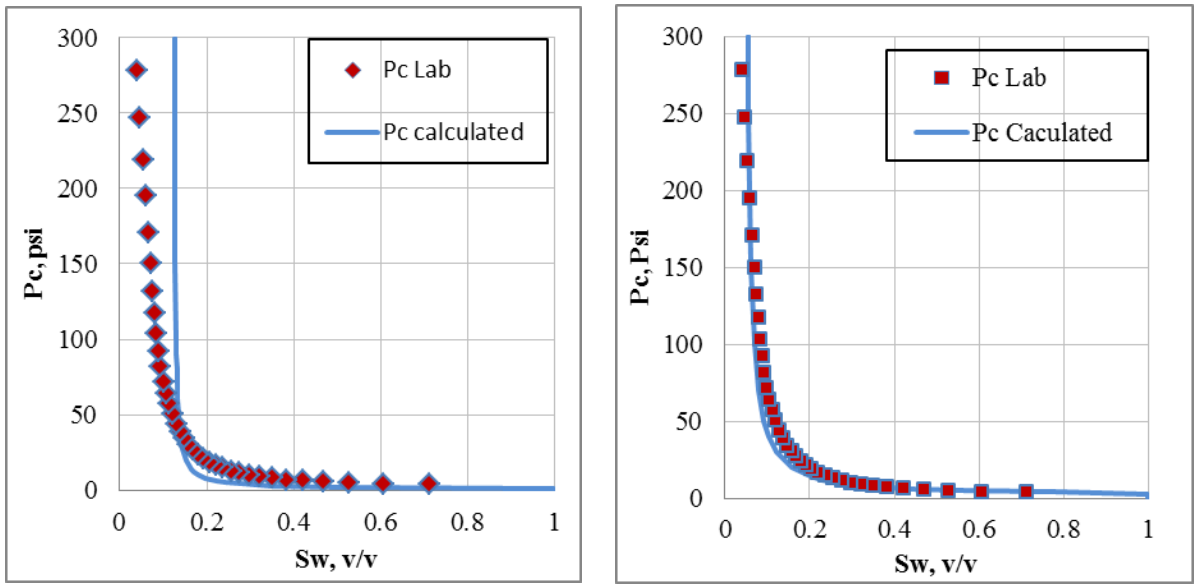

Figure 5.13a Capillary pressure curves for RQI 0.2 before calibration (left) and after calibration (right)

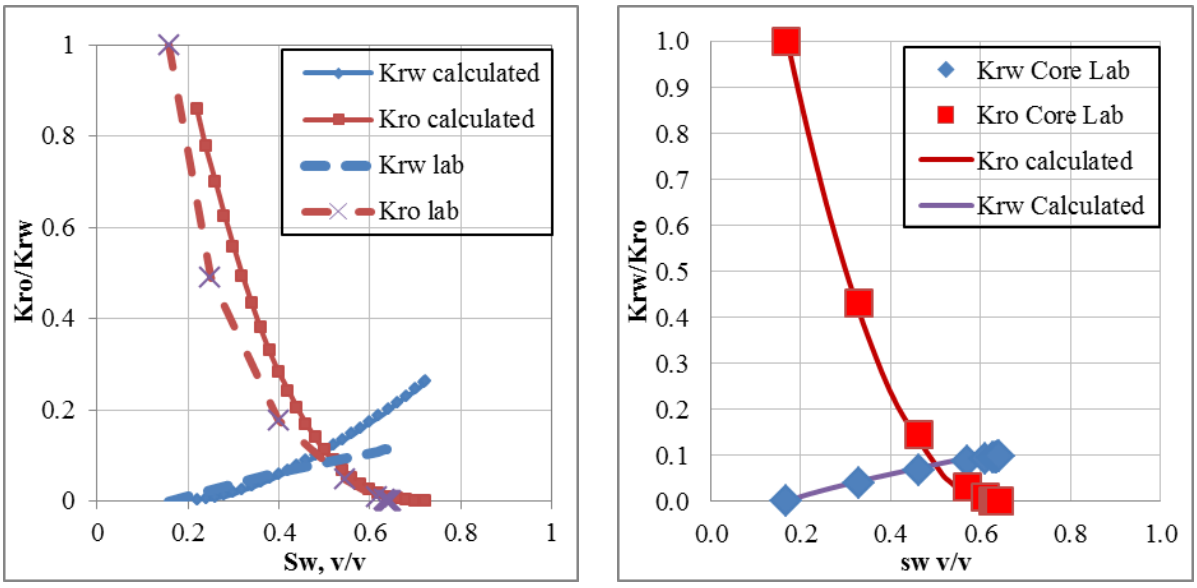

Figure 5.13b Relative permeability curves for RQI 0.16 before calibration (left) and after calibration (right.)

5.4.8 Initial Conditions and Injection Rates

The initial conditions specified in the reservoir model are specified in Table 5.5. The simulations were conducted assuming isothermal conditions. Although isothermal conditions were assumed, a thermal gradient of 0.008 °C/ft was considered for specifying petrophysical properties that vary with layer depth and temperature such as CO_2 relative permeability, CO_2 dissolution in formation water, etc. The original static pressure in the injection zone (at a reference depth of 4,960 ft) was set to 2,093 psi and the Arbuckle pressure gradient of 0.48 psi/ft (discussed in Section 4) was assumed for specifying petrophysical properties. A 140-ft thick perforation zone in well KGS-28 was specified between 4,910 and 5,050 ft. A constant brine density of 68.64 lbs/ft3 (specific gravity of 1.1) was assumed. A total of 40,000 metric tons of CO_2 was injected in the Arbuckle formation over a period of nine months at an average injection rate of 150 tons/day

Table 5.5—Model input specification and CO_2 injection rates

Temperature		60 °C (140 °F)
	Temperature Gradient	0.008 °C/ft
Pressure		2,093 psi (14.43 MPa) @ 4,960 ft RKB
Perforation Zone		4,910-5,050 ft
	Perforation Length	140 ft (model layers 54 to 73)
Injection Period		9 months
Injection Rate		150 tons/day
	Total CO_2 injected	40,000 MT

5.4.9 Permeability and Porosity Alternative Models

The base-case reservoir model has been carefully constructed using a sophisticated geomodel as discussed in Section 5.3, which honors site-specific hydrogeologic information obtained from laboratory tests and log-based analyses. However, to account and test for sensitivity of hydrogeologic uncertainties, a set of alternate parametric models were developed by varying the porosity and horizontal hydraulic permeability. Specifically, the porosity and permeability were increased and decreased by 25% following general industry practice (FutureGen Industrial Alliance, 2013). This resulted in nine alternative models, listed in Table 5.6. Simulation results based on all nine models were evaluated to derive the worst-case impacts on pressure and migration of the plume front for purposes of establishing the AoR and ensuring that operational constraints are not exceeded

Table 5.6—Nine alternative permeability-porosity combination models. (Showing multiplier of base-case permeability and porosity distribution assigned to all model cells.)

Alternative Models	Base Porosity x 0.75	Base Porosity	Base Porosity x 1.25
Base Permeability x 0.75	K-0.75/Phi-0.75	K-0.75/Phi-1.0	K-0.75/Phi-1.25
Base Permeability	K-1.0/Phi-0.75	K-1.0/Phi-1.0	K-1.0/Phi-1.25
Base Permeability x 1.25	K-1.25/Phi-0.75	K-1.25/Phi-1.0	K-1.25/Phi-1.25

5.4.10 Reservoir Simulation Results

For the simulations, 40,000 metric tons (MT) of CO_2 were injected into the KGS 1-28 well at a constant rate of approximately 150 tons per day for a period of nine months. A total of nine models representing three sets of alternate permeability-porosity combinations as specified in Table 5.6 were simulated with the objective of bracketing the range of expected pressures and extent of CO_2 plume migration.

The extent of lateral plume migration depends on the particular combination of permeability-porosity in each of the nine alternative models. These two parameters are independently specified in CMG as they are assumed to be decoupled. A high-permeability value results in farther travel of the plume due to gravity override, bouyancy, and updip migration. Similarly, a low effective porosity for the same value of permeability results in farther travel for the plume as compared to high porosity as the less-connected pore volume results in faster pore velocity. The high-permeability/low-porosity combination (k-1.25/phi-0.75) resulted in the largest horizontal plume dimension. In contrast, the highest induced pressures were obtained for the alternative model with the lowest permeability and the lowest porosity (k-0.75/phi-0.75).

5.4.10.1 CO_2 Plume Migration

Figure 5.14a–f shows the maximum lateral migration of the CO2 plume in the injection interval (elevation 5,010 ft) for the largest areal migration case (k-1.25/phi-0.75). The plume grows rapidly during the injection phase (Figure 5.14a–c) and is largely stabilized by the end of the second year (Figure 5.14d). The plume at the end of 100 years (Figure 5.14f) has spread only minimally since cessation of injection and has a maximum lateral spread of approximately 2,150 ft from the injection well. It does not intercept any well other than the proposed Arbuckle monitoring well KGS 2-28, which as documented in Section 10, will be constructed in compliance with Class VI injection well guidelines.

The evolution of the maximum lateral extent of the free phase plume is shown in

Figure 5.15 for the maximum plume spread case (k-1.25/phi-0.75) The plume grows rapidly during the injection period and up to the second year from commencement of injection. Thereafter, the plume has stabilized to a maximum lateral extent of approximately 2,150 ft. The plume only intercepts the proposed Arbuckle monitoring well KGS 2-28, which will be built to be in compliance with Class VI design and construction requirements. There are no additional natural or artificial penetrations that will allow CO2 to escape upward from the Arbuckle injection zone.

The extent of vertical plume migration for the fast vertical migration case (k-1.25/phi-0.75), the base case (k-1.00/phi-1.00), and the high pressure case (k-0.75/phi-0.75) is shown in Figures 5.16. The free-phase plume remains confined in the injection interval (lower Arbuckle) because of the presence of the low-permeability baffle zones above the injection interval. This same information is shown in Figure 5.14, which shows the maximum extent of vertical migration. For all three cases, the plume remains confined in the injection interval in the lower Arbuckle.

To account for uncertainties of CO_2 movement in the vertical direction an alternate vertical permeability model was also developed in which vertical permeability parameter was increased by 50% along with a porosity of 75% (k-1.50/phi-0.75). The extent of vertical migration of the free phase plume for this case along with base case (k-1.00/phi-1.00) and the k-1.25/phi-0.75 and k-0.75/phi-0.75 cases is presented in Figure 5.16. It can be noted from the figure that the CO2 migrates approximately 30 ft higher for the altered vertical permeability case, but , it does not penetrate the low permeability baffle zone in the middle of the Arbuckle and stays contained within lower Arbuckle injection zone.

In closing, it is worth remarking that the simulation results discussed above are expected to represent conservative estimates of plume migration. This is because the present CMG simulations neglects mineral sequestration trapping Additionally, the modeling results presented in this document do not simulate convection cells, which as demonstrated recently

by Pau et al. (2010) can greatly accelerate the dissolution rate. Because of time and computational constraints, these mechanisms were ignored, and therefore the storage rates and quantities are likely to be underestimated, thus ensuring that the projections presented in this application provide a "worst-case" scenario.

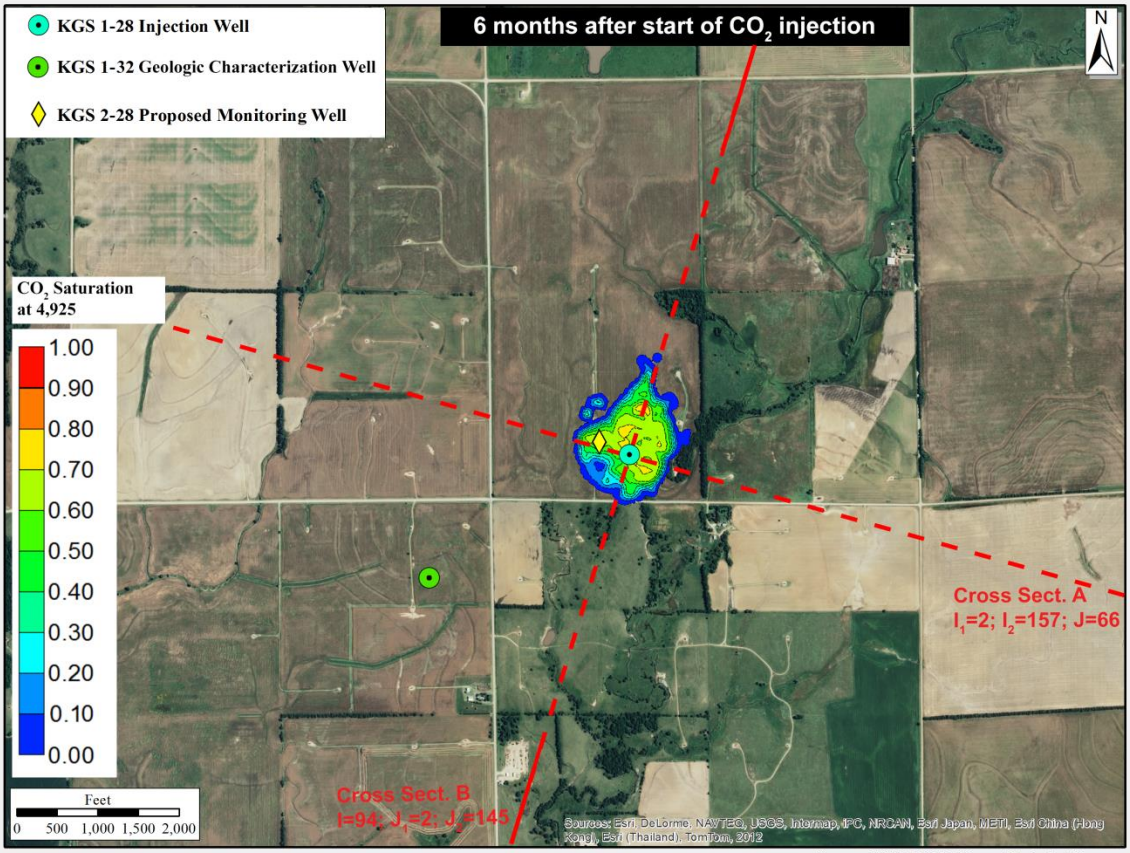

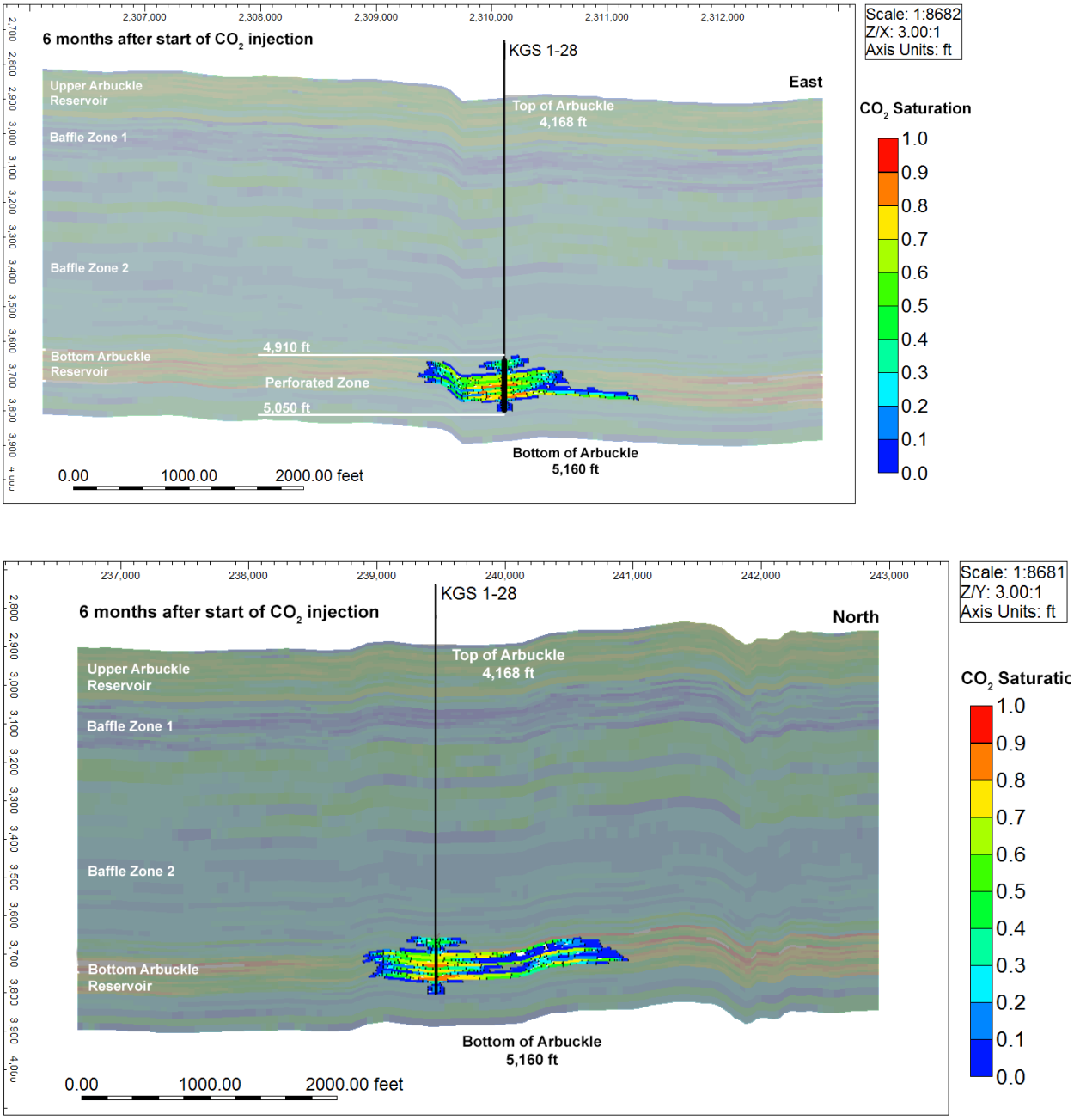

Figure 5.14a—Free-phase CO_2 plume in aerial and cross-sectional view for the largest migration alternative model (k-1.25/phi-0.75) at six months from start of injection.

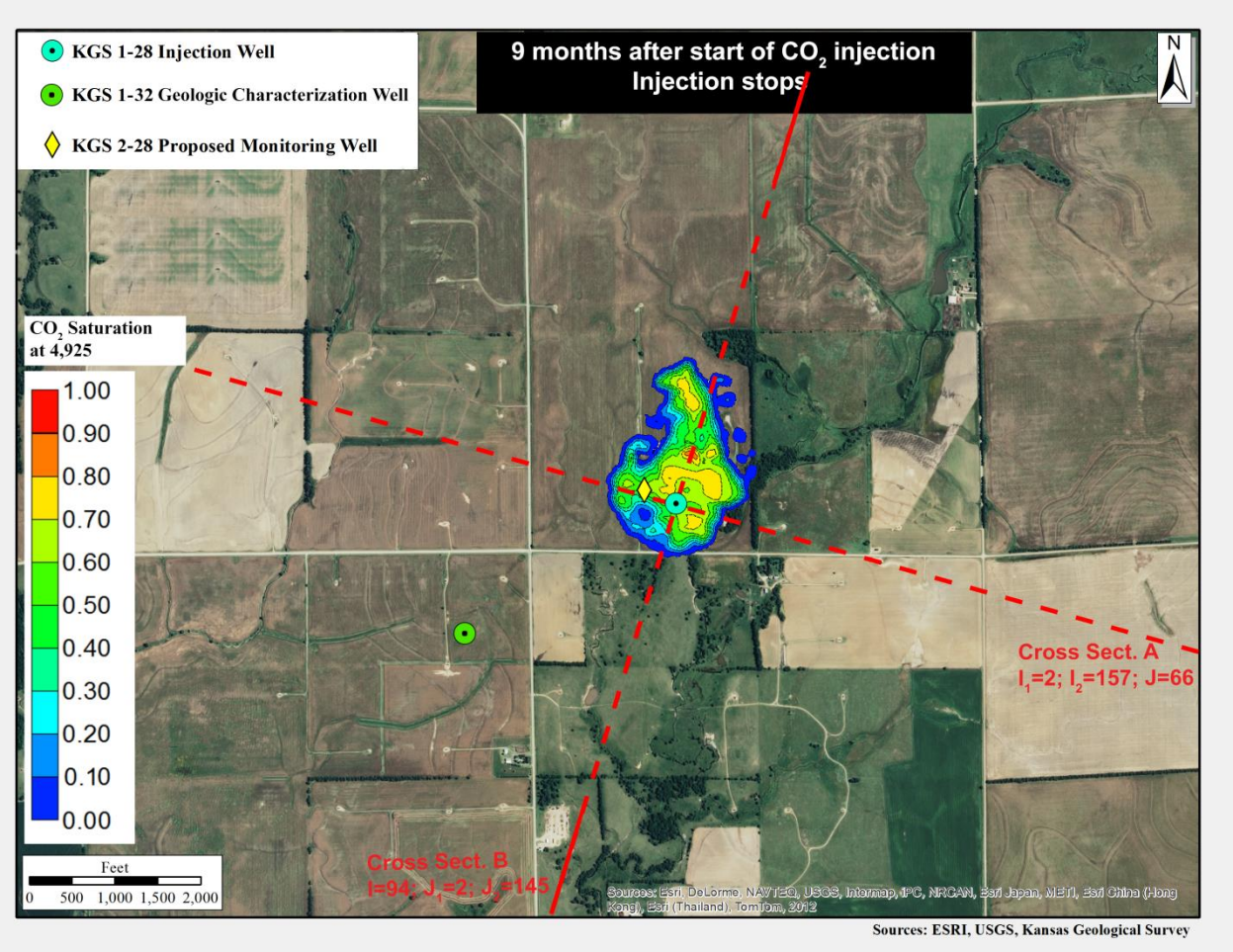
KGS 1-28 Injection Well
KGS 1-32 Geologic Characterization Well
KGS 2-28 Proposed Monitoring Well
9 months after start of CO2 injection
Injection stops
N
CO2 Saturation at 4,925
1.00
0.90
0.80
0.70
0.60
0.50
0.40
0.30
0.20
0.10
0.00
Feet
0 500 1,000 1,500 2,000
Cross Sect. A
I1=2; I2=157; J=66
Cross Sect. B
I=94; J1=2; J2=145
Sources: Esri, DeLorme, NAVTEQ, USGS, Intermap, iPC, NRCAN, Esri Japan, METI, Esri China (Hong Kong), Esri (Thailand), TomTom, 2012
Sources: ESRI, USGS, Kansas Geological Survey

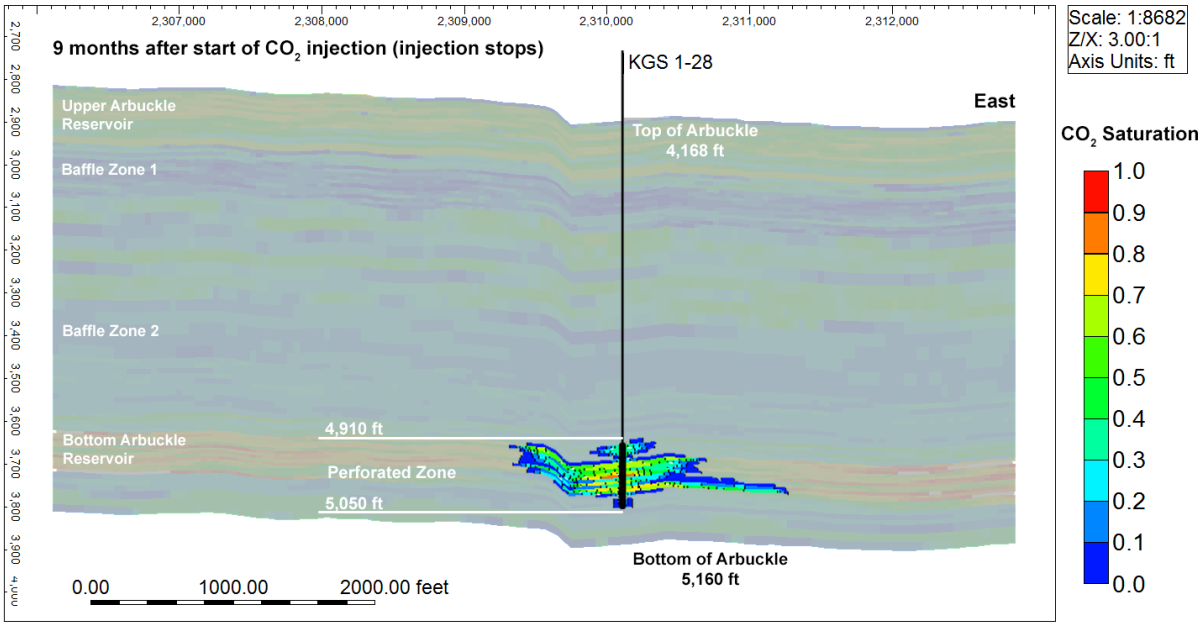
2,307,000
2,308,000
2,309,000
2,310,000
2,311,000
2,312,000
9 months after start of CO2 injection (injection stops)
KGS 1-28
East
Upper Arbuckle Reservoir
Top of Arbuckle
4,168 ft
Baffle Zone 1
Baffle Zone 2
Bottom Arbuckle Reservoir
4,910 ft
Perforated Zone
5,050 ft
Bottom of Arbuckle
5,160 ft
0.00
1000.00
2000.00 feet
Scale: 1:8682
Z/X: 3.00:1
Axis Units: ft
CO2 Saturation
1.0
0.9
0.8
0.7
0.6
0.5
0.4
0.3
0.2
0.1
0.0

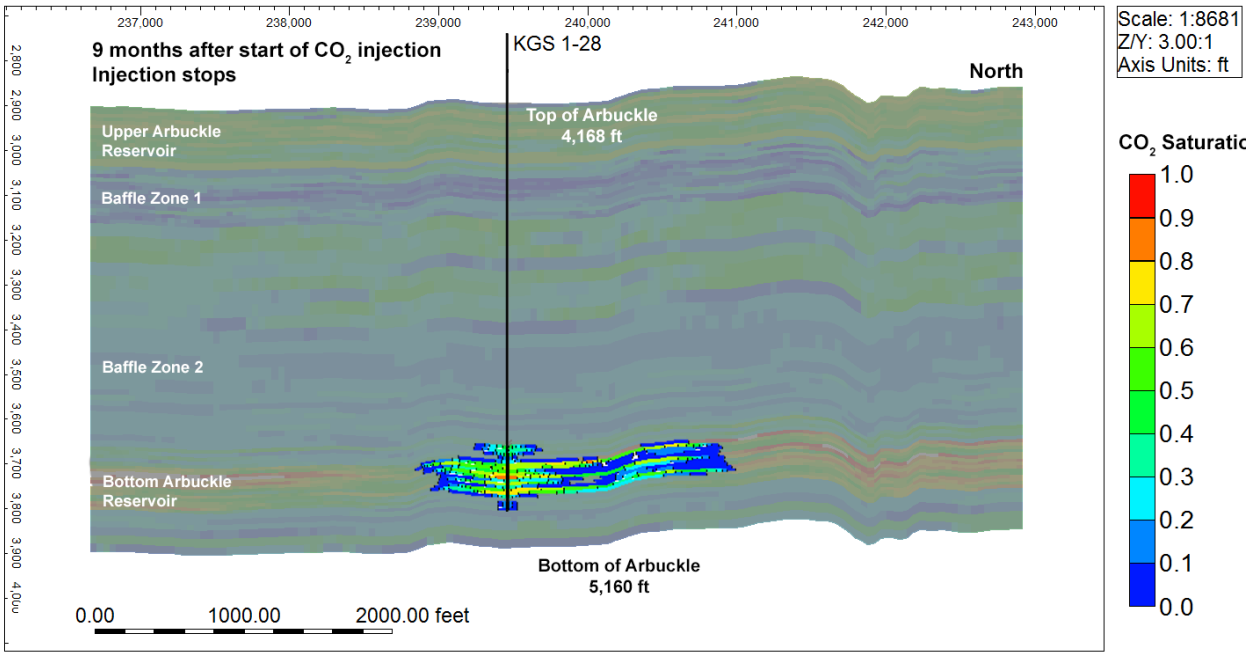

Figure 5.14b—Free-phase CO_2 plume in aerial and cross-sectional view for the largest migration alternative model (k-1.25/phi-0.75) at nine months from start of injection.

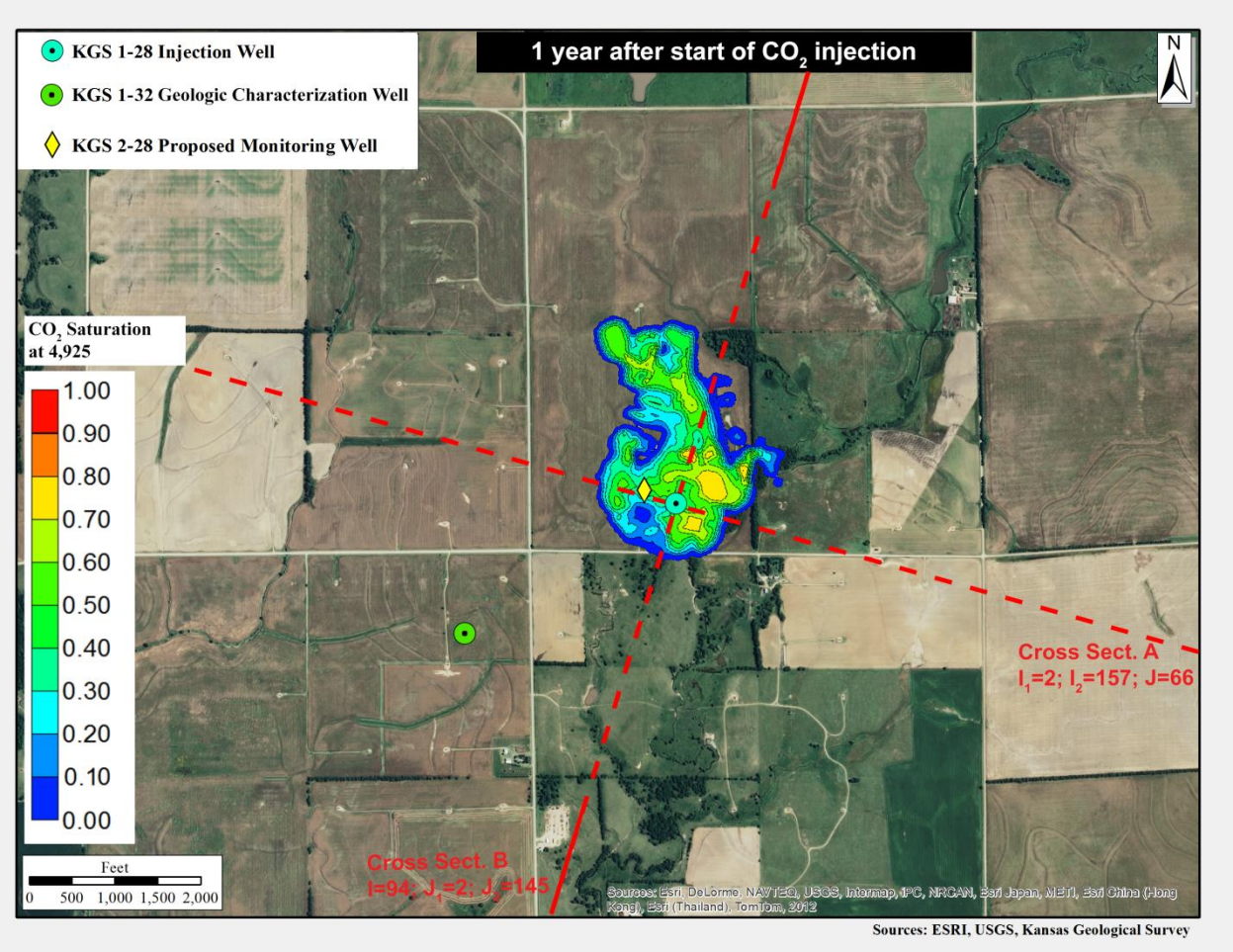

Sources: ESRI, USGS, Kansas Geological Survey

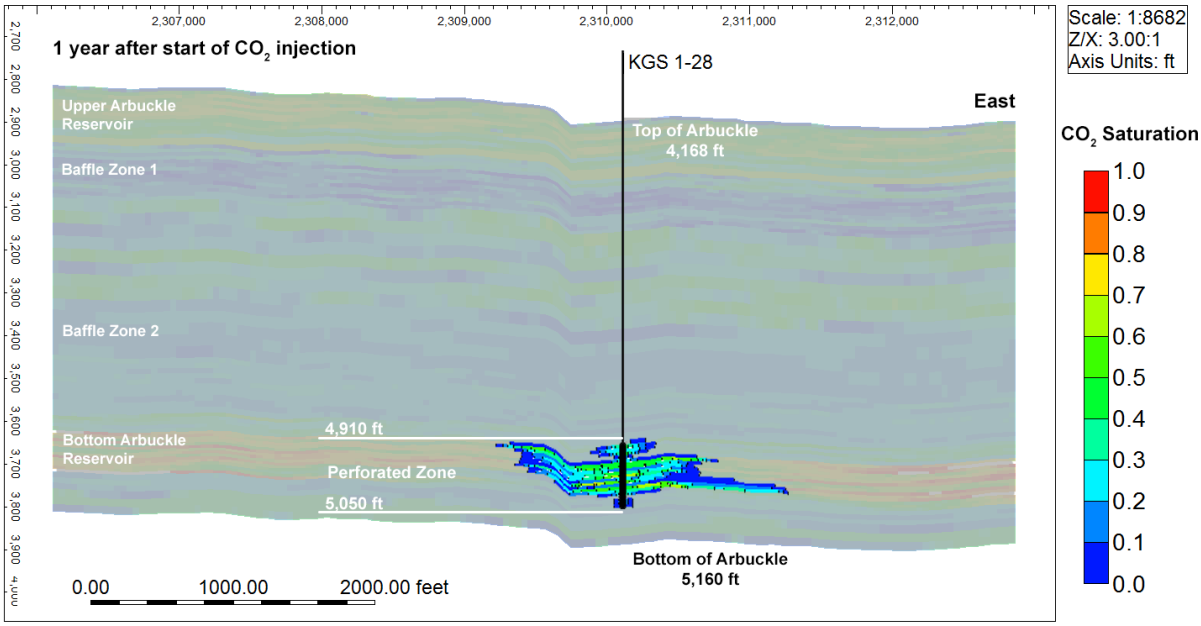

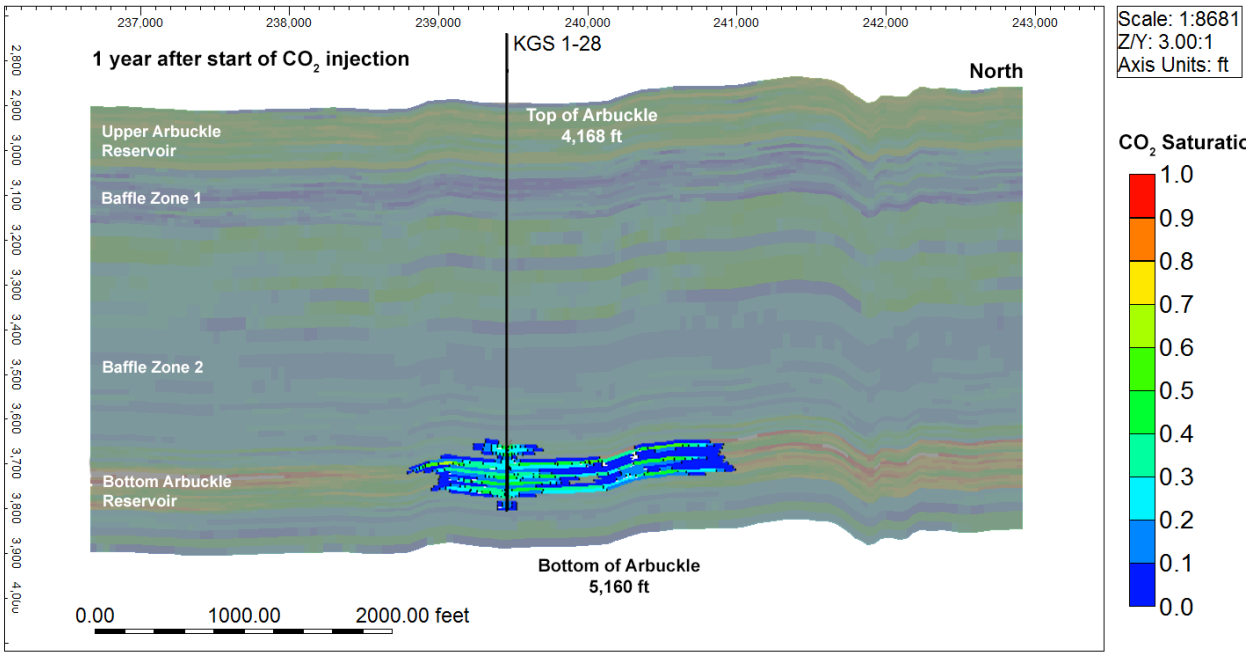

Figure 5.14c—Free-phase CO_2 plume in aerial and cross-sectional view for the largest migration alternative model (k-1.25/phi-0.75) at one year from start of injection.

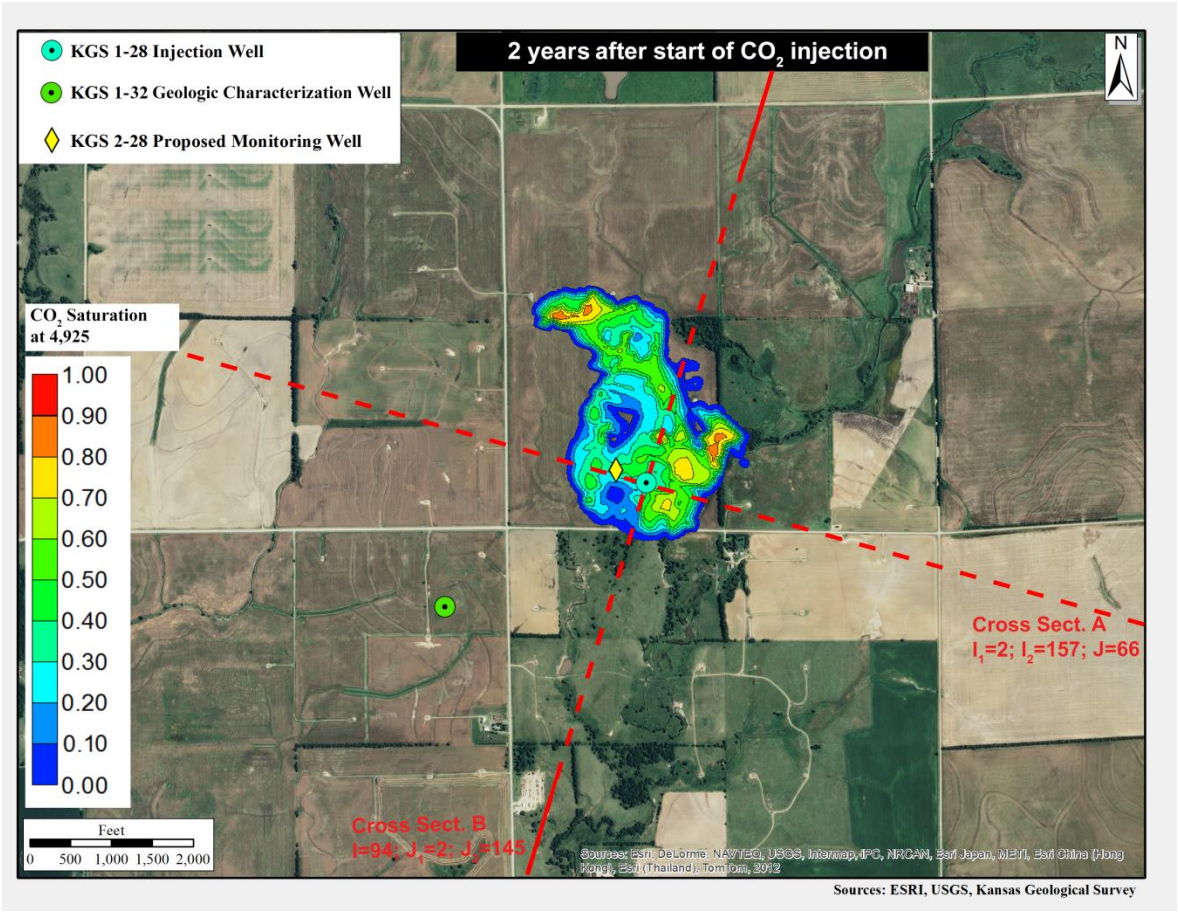

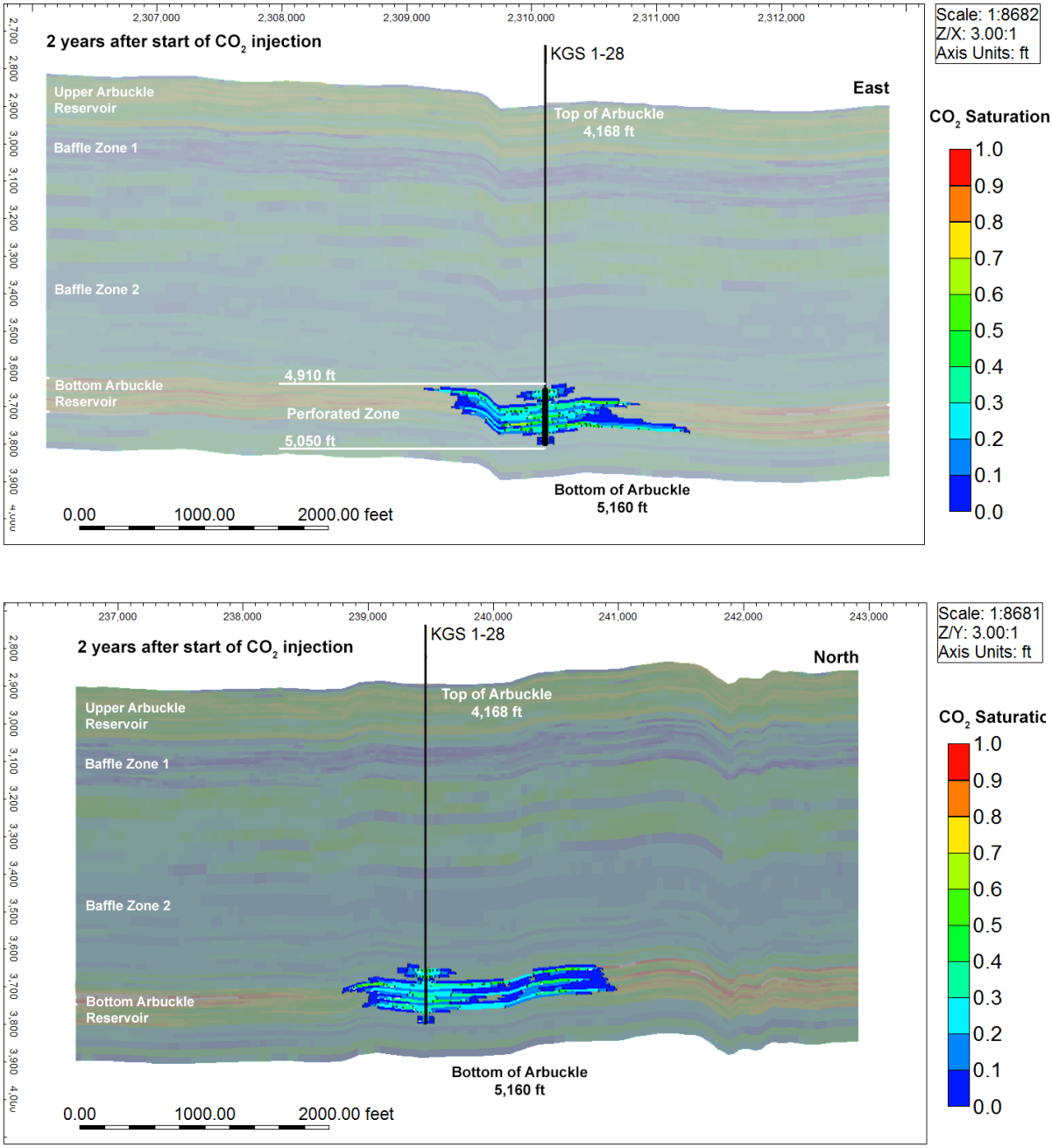

Figure 5.14d—Free-phase CO_2 plume in aerial and cross-sectional view for the largest migration alternative model (k-1.25/phi-0.75) at two years from start of injection.

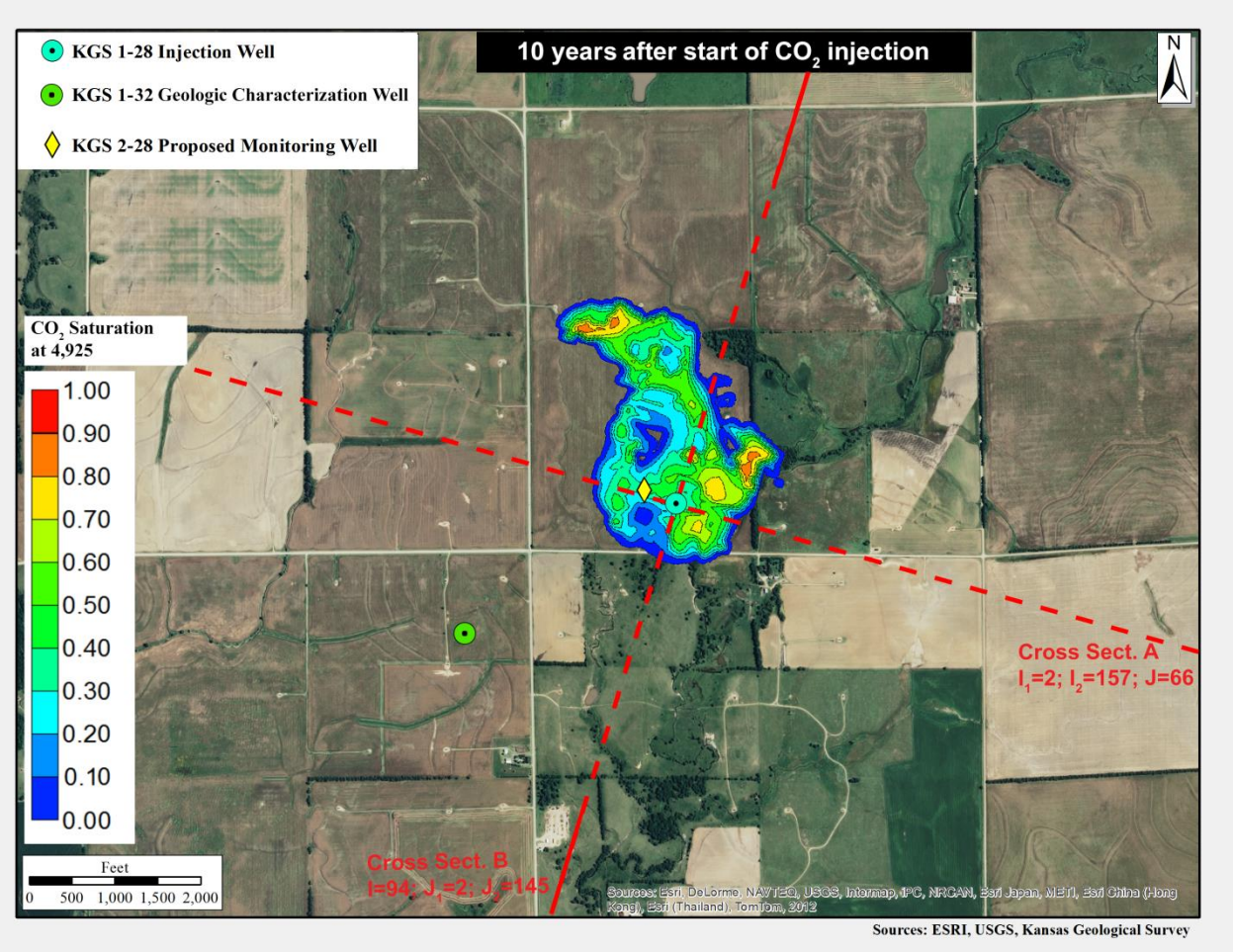
KGS 1-28 Injection Well
KGS 1-32 Geologic Characterization Well
KGS 2-28 Proposed Monitoring Well
10 years after start of CO2 injection
N
CO2 Saturation at 4,925
1.00
0.90
0.80
0.70
0.60
0.50
0.40
0.30
0.20
0.10
0.00
Feet
0 500 1,000 1,500 2,000
Cross Sect. A
I1=2; I2=157; J=66
Cross Sect. B
I=94; J1=2; J2=145
Sources: Esri, DeLorme, NAVTEQ, USGS, Intermap, iPC, NRCAN, Esri Japan, METI, Esri China (Hong Kong), Esri (Thailand), TomTom, 2012
Sources: ESRI, USGS, Kansas Geological Survey

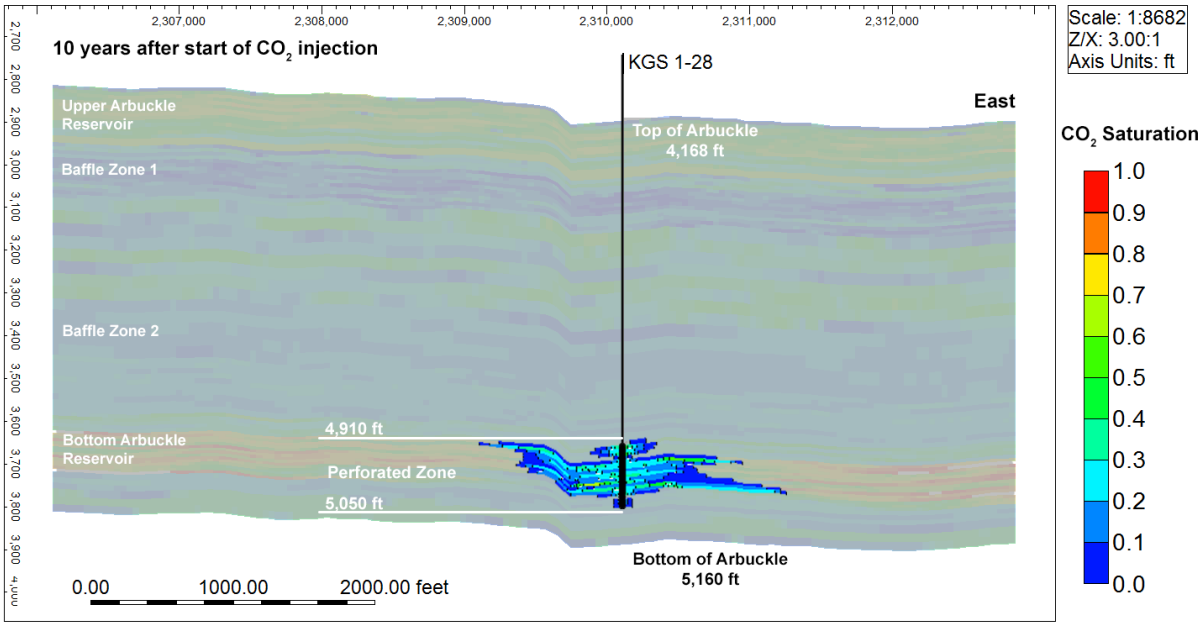
2,307,000
2,308,000
2,309,000
2,310,000
2,311,000
2,312,000
10 years after start of CO2 injection
KGS 1-28
East
Upper Arbuckle Reservoir
Top of Arbuckle 4,168 ft
Baffle Zone 1
Baffle Zone 2
Bottom Arbuckle Reservoir
4,910 ft
Perforated Zone
5,050 ft
Bottom of Arbuckle 5,160 ft
0.00 1000.00 2000.00 feet
Scale: 1:8682
Z/X: 3.00:1
Axis Units: ft
CO2 Saturation
1.0
0.9
0.8
0.7
0.6
0.5
0.4
0.3
0.2
0.1
0.0

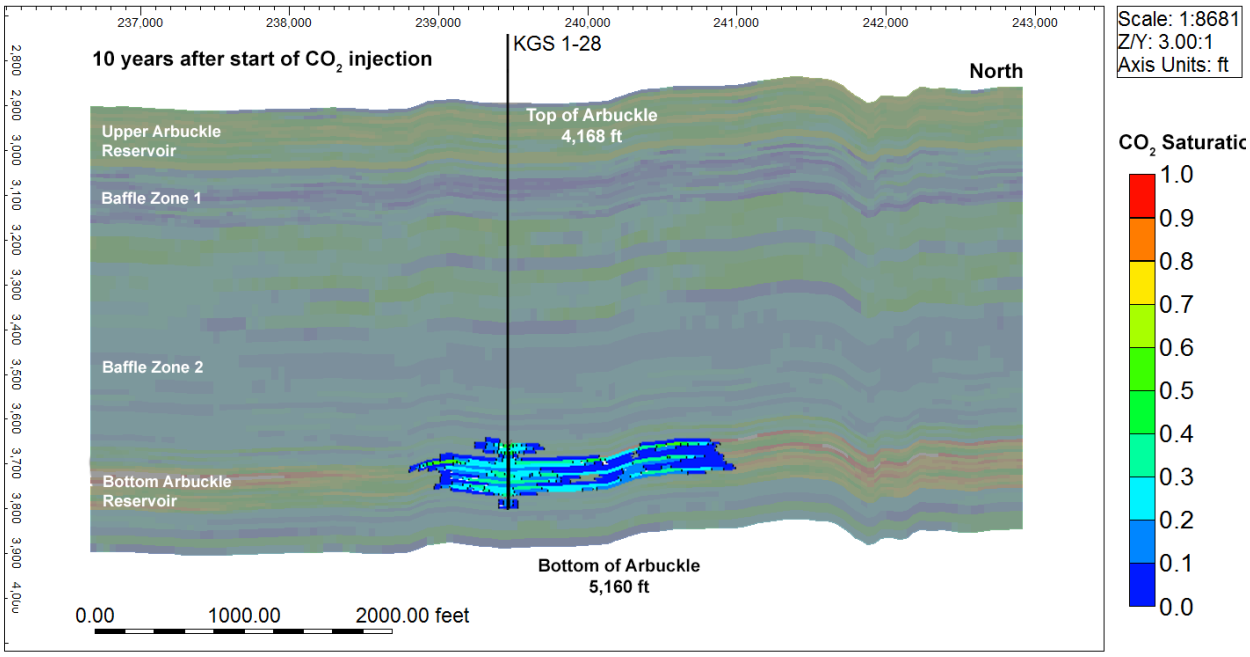

Figure 5.14e—Free-phase CO_2 plume in aerial and cross-sectional view for the largest migration alternative model (k-1.25/phi-0.75) at ten years from start of injection.

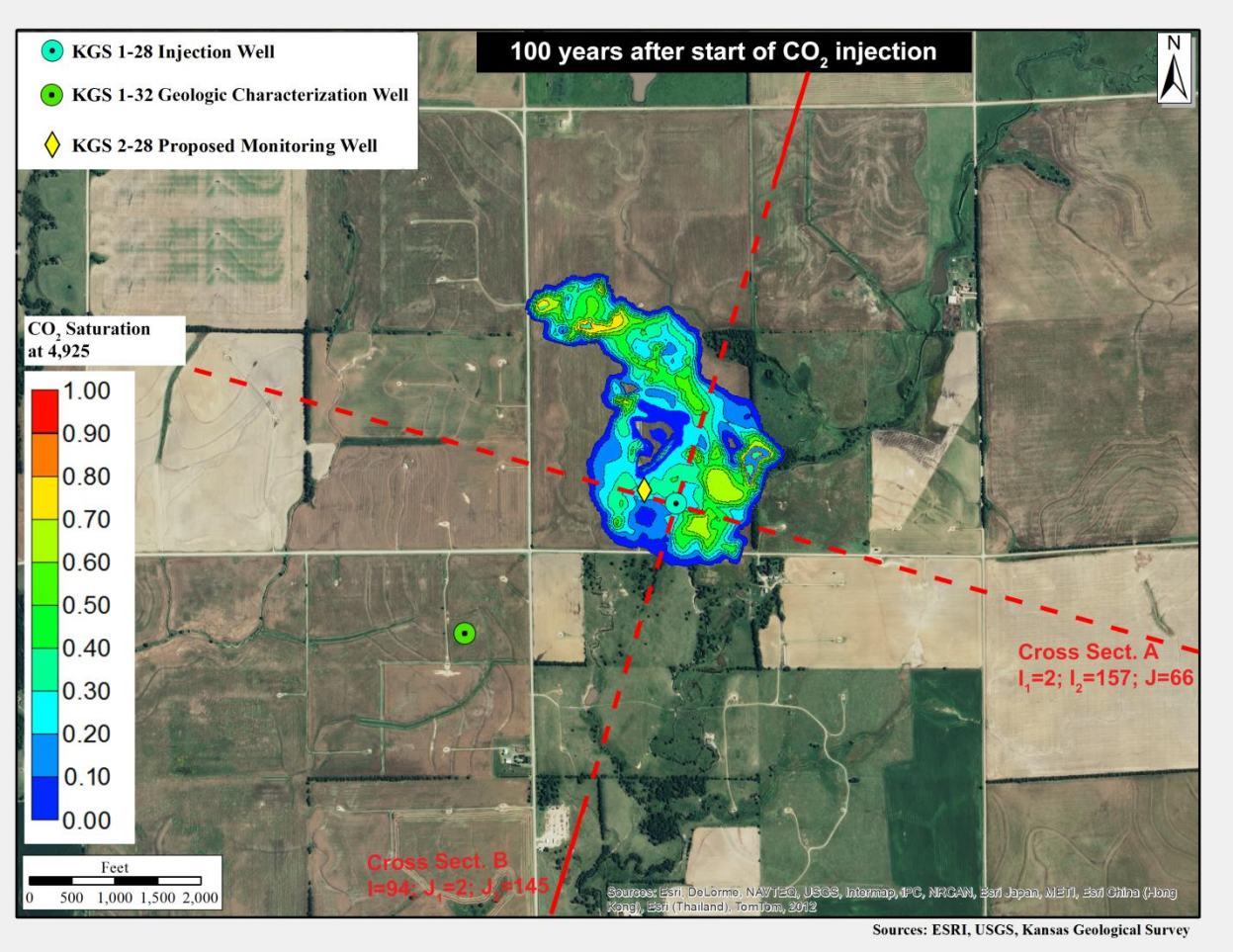
KGS 1-28 Injection Well
KGS 1-32 Geologic Characterization Well
KGS 2-28 Proposed Monitoring Well
100 years after start of CO2 injection
N
CO2 Saturation at 4,925
1.00
0.90
0.80
0.70
0.60
0.50
0.40
0.30
0.20
0.10
0.00
Feet
0 500 1,000 1,500 2,000
Cross Sect. A
I1=2; I2=157; J=66
Cross Sect. B
I=94; J1=2; J2=145
Sources: Esri, DeLorme, NAVTEQ, USGS, Intermap, iPC, NRCAN, Esri Japan, METI, Esri China (Hong Kong), Esri (Thailand), TomTom, 2012
Sources: ESRI, USGS, Kansas Geological Survey

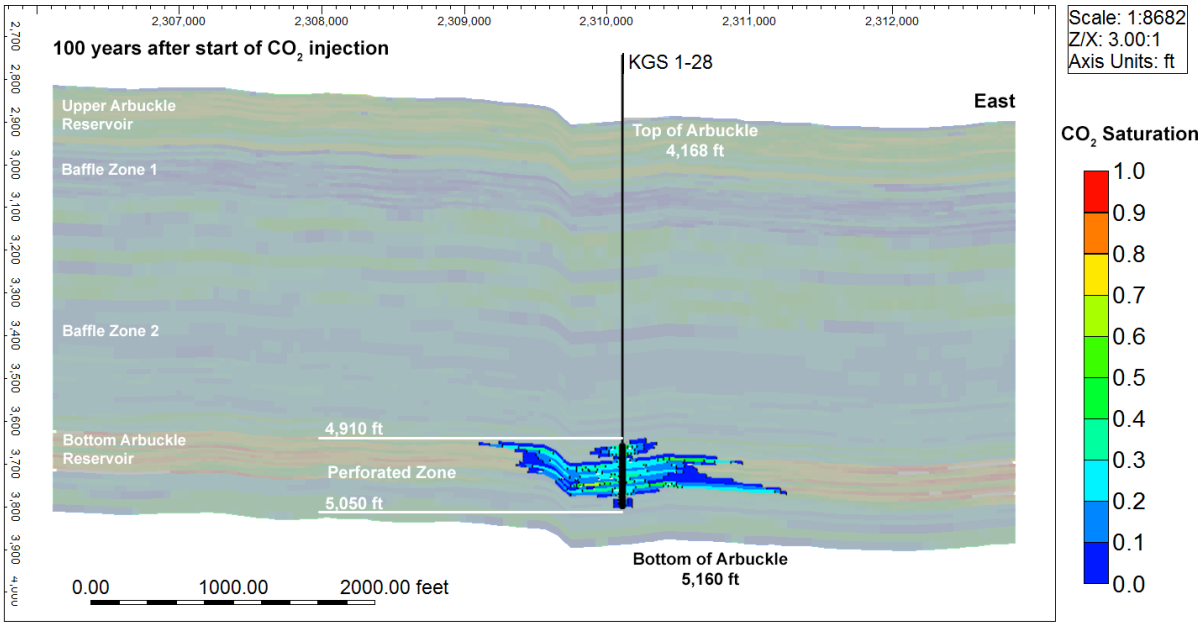
2,307,000
2,308,000
2,309,000
2,310,000
2,311,000
2,312,000
100 years after start of CO2 injection
KGS 1-28
East
Upper Arbuckle Reservoir
Baffle Zone 1
Baffle Zone 2
Bottom Arbuckle Reservoir
Top of Arbuckle
4,168 ft
4,910 ft
Perforated Zone
5,050 ft
Bottom of Arbuckle
5,160 ft
0.00
1000.00
2000.00 feet
Scale: 1:8682
Z/X: 3.00:1
Axis Units: ft
CO2 Saturation
1.0
0.9
0.8
0.7
0.6
0.5
0.4
0.3
0.2
0.1
0.0

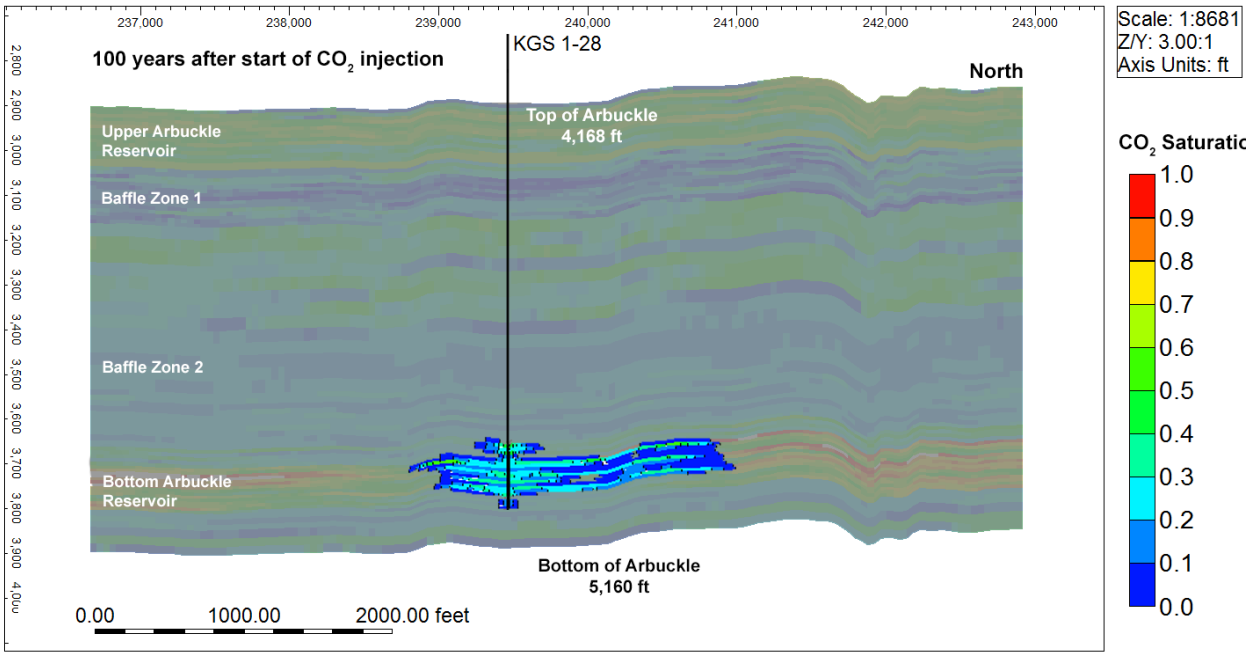

Figure 5.14f—Free-phase CO_2 plume in aerial and cross-sectional view for the largest migration alternative model (k-1.25/phi-0.75) at hundred years from start of injection.

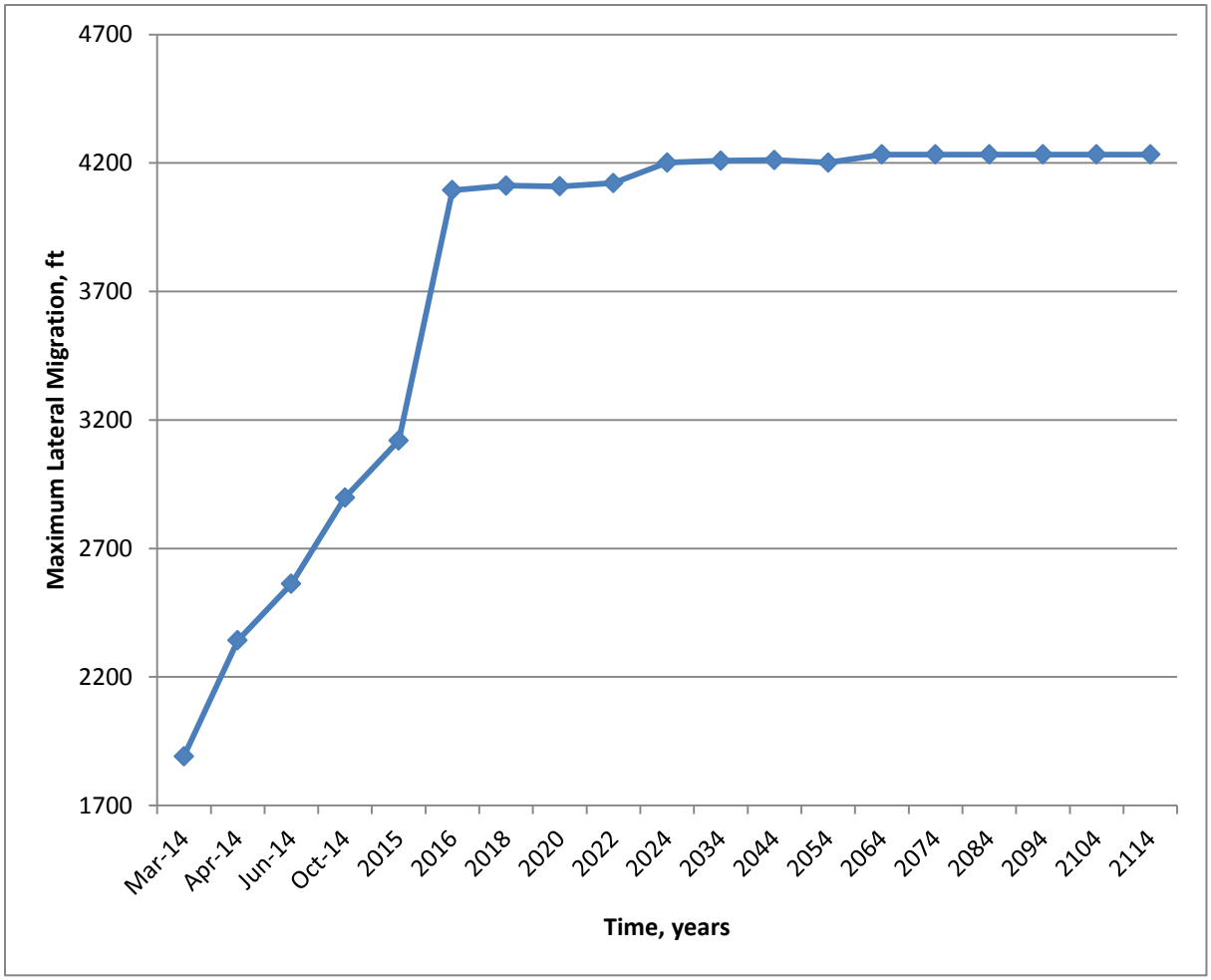

Figure 5.15—Maximum lateral extent of CO_2 plume migration (as defined by the 0.5% CO_2 saturation isoline) for the largest plume migration case k-1.25/phi-0.75.

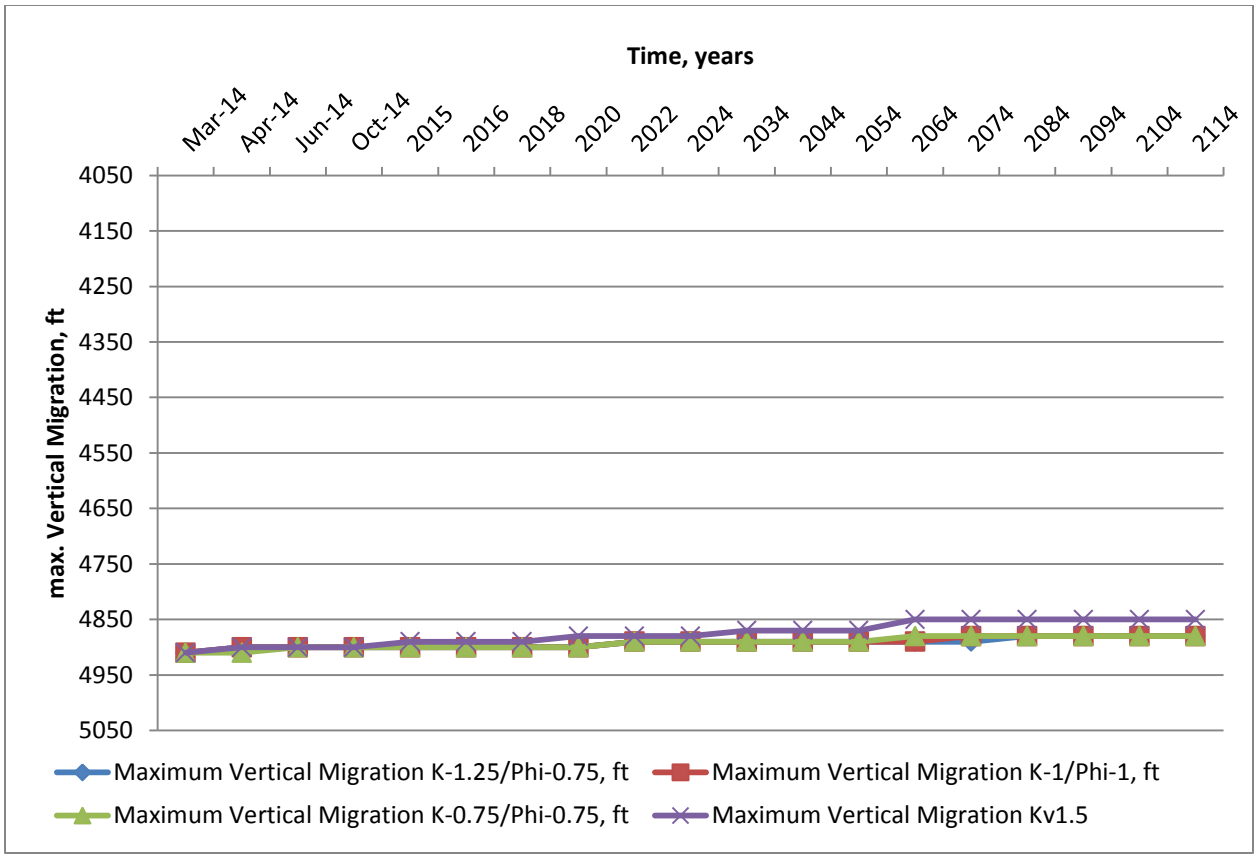

Figure 5.16— Maximum vertical extent of free-phase CO_2 migration for the two alternative cases that result in the maximum plume spread (k-1.25/phi-0.75) and the maximum induced pressure (k-0.75/phi-0.75) along with base case (k-1.0/phi-1.0) and vertical permeability sensitivity case (k-1.25/phi-0.75).

5.4.10.2 Simulated Pressure Distribution

Figure 5.17 presents the bottom hole pressure (at a reference depth of 5,050 ft) for the highest pressures alternative model (k-0.75/phi-0.75). The pressure increases to 2,485 psi on commencement of injection and then gradually drops during the injection period as the capillary effects are overcome. The pressure decreases to pre-injection levels on cessation of injection. The rise in pressure to 2,485 psi on commencement of injection represents an increase of 392 psi over pre-injection levels and results in a pressure gradient of 0.515 psi/ft, which is less than the maximum allowable pressure gradient of 0.675 psi/ft corresponding to 90% of the fracture gradient (0.75 psi/ft) as documented in Section 4.6.9.

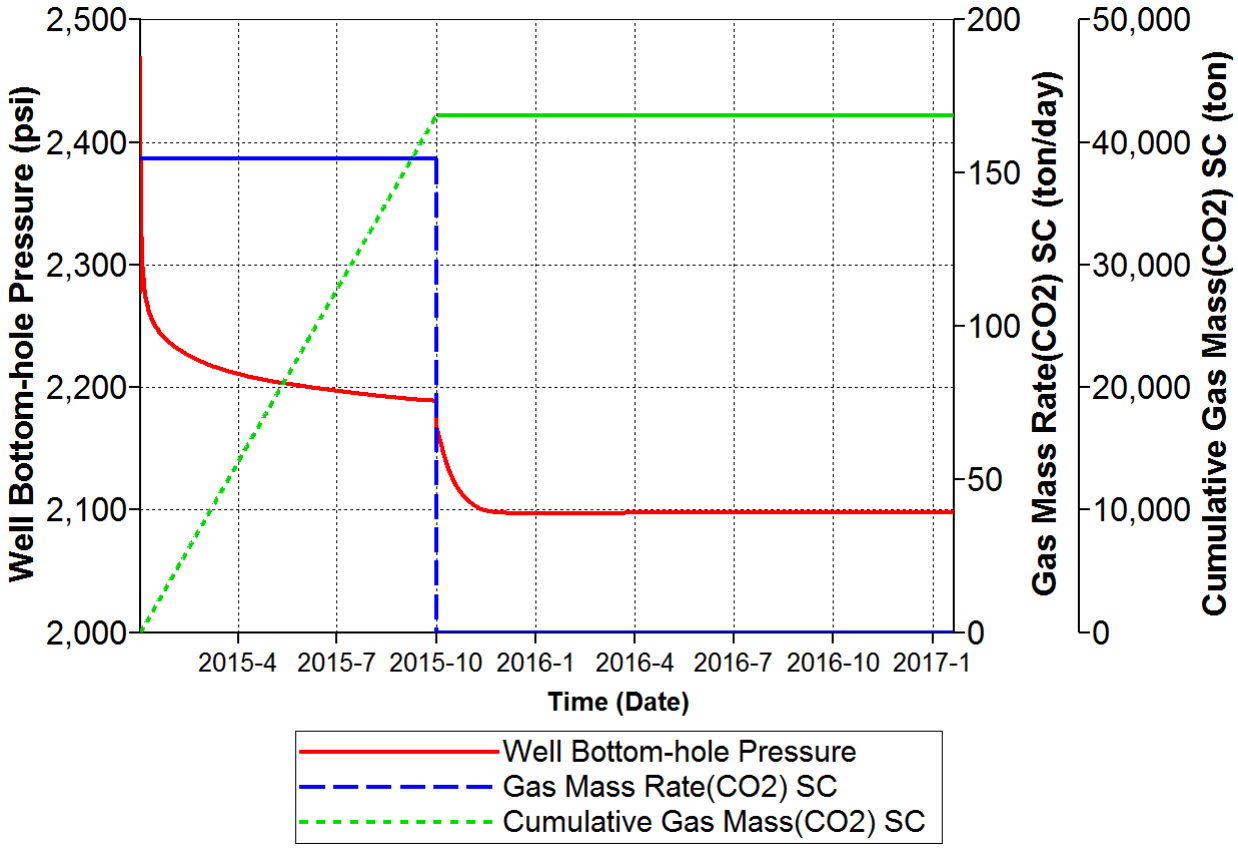

Figure 5.17—Maximum well bottom hole pressure at the depth of 5,050 ft for minimum porosity and minimum permeability case (k-0.75/phi-0.75) case.

Figure 5.18 presents the change in pore pressure at the base of the confining zone (Simpson Group) for the k-0.75/phi-0.75 alternate model that resulted in the highest pressures. The maximum pressure increase at the end of the injection period of approximately 1.15 psi is fairly small and well below the entry pressure of 956 psi for the confining zone estimated in Section 4.7.4.

Figure 5.19a–e presents the lateral distribution of pressure in the Arbuckle injection interval (at an elevation of 4,960 ft) for the k-0.75/phi-0.75 case, which resulted in the maximum induced pore pressures. The pressures increase from commencement of injection to nine months and then drop significantly by the end of the first year (three months after operations stop). The pressures also drop very rapidly at short distances from the injection

well at the end of the nine- month injection period, as shown in Figure 5.20. The pressures at the end of the nine-month injection period drop from about 120 psi a short distance from the injection well to less than 15 psi at the geologic characterization well, KGS 1-32, which is approximately 3,500 ft southwest of the injection well. The maximum induced pressure at the model boundary is only 7-12 psi.

Figure 5.18a–d also shows the vertical pressure distribution for the maximum induced pressure case (k-0.75/phi-0.75). The confining effect of the mid-Arbuckle baffle zones is evident in the plots as the large pressure increases are mostly restricted to the injection interval. The pressures decline rapidly at a short distance from the injection well. The pressures throughout the model subside to nearly pre-injection levels soon after injection stops, as shown in the one-year pressure plot in Figure 5.19e.

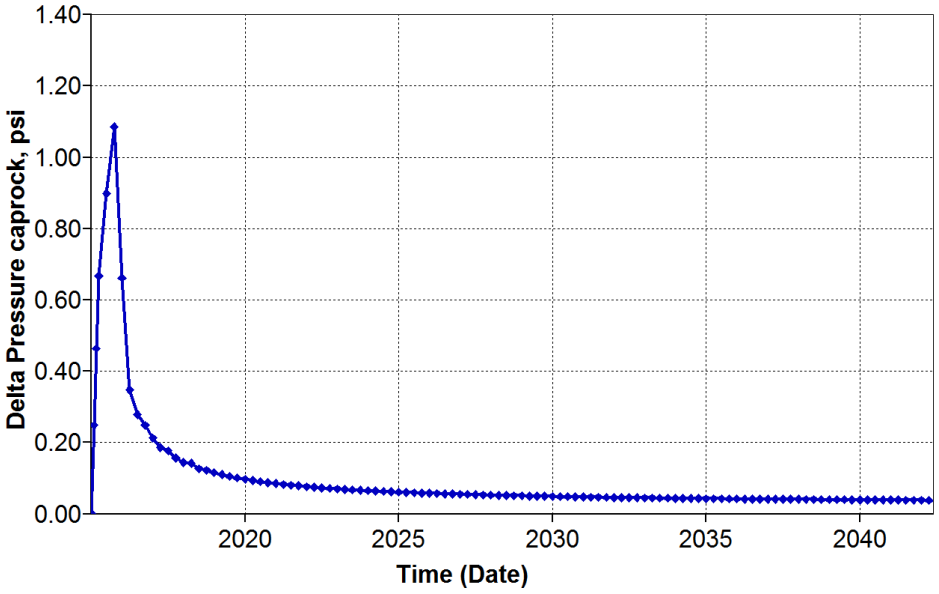

Figure 5.18—Change in pore pressure at the base of the confining zone (i.e., base of Simpson Group) at the injection well site for the maximum induced pressure (k-0.75/phi-0.75).

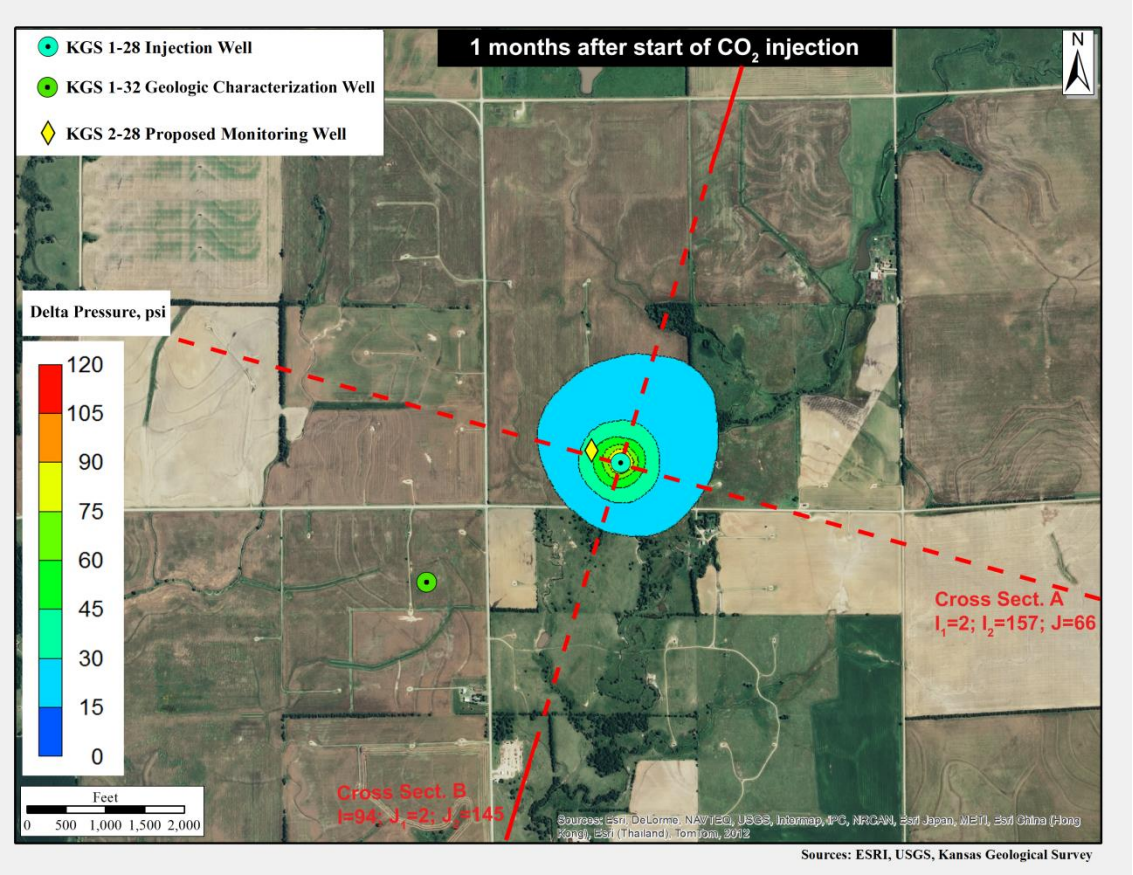
KGS 1-28 Injection Well
KGS 1-32 Geologic Characterization Well
KGS 2-28 Proposed Monitoring Well
1 months after start of CO2 injection
N
Delta Pressure, psi
120
105
90
75
60
45
30
15
0
Feet
0 500 1,000 1,500 2,000
Cross Sect. A
I1=2; I2=157; J=66
Cross Sect. B
I=94; J1=2; J2=145
Sources: Esri, DeLorme, NAVTEQ, USGS, Intermap, IPC, NRCAN, Esri Japan, METI, Esri China (Hong Kong), Esri (Thailand), TomTom, 2012
Sources: ESRI, USGS, Kansas Geological Survey

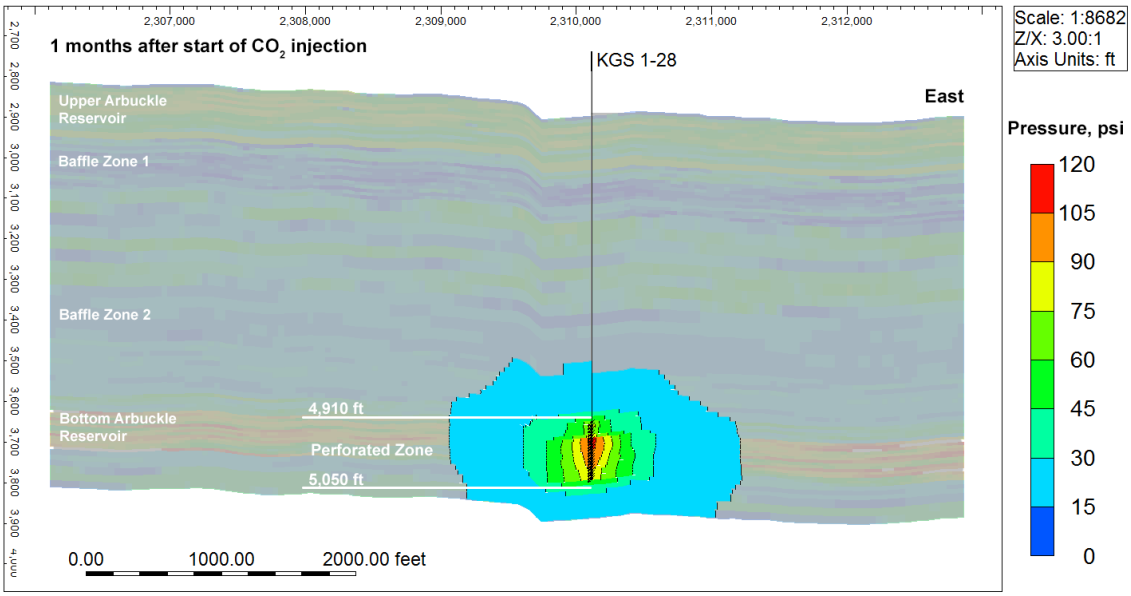
2,307,000
2,308,000
2,309,000
2,310,000
2,311,000
2,312,000
1 months after start of CO2 injection
KGS 1-28
East
Upper Arbuckle Reservoir
Baffle Zone 1
Baffle Zone 2
Bottom Arbuckle Reservoir
4,910 ft
Perforated Zone
5,050 ft
0.00
1000.00
2000.00 feet
Scale: 1:8682
Z/X: 3.00:1
Axis Units: ft
Pressure, psi
120
105
90
75
60
45
30
15
0

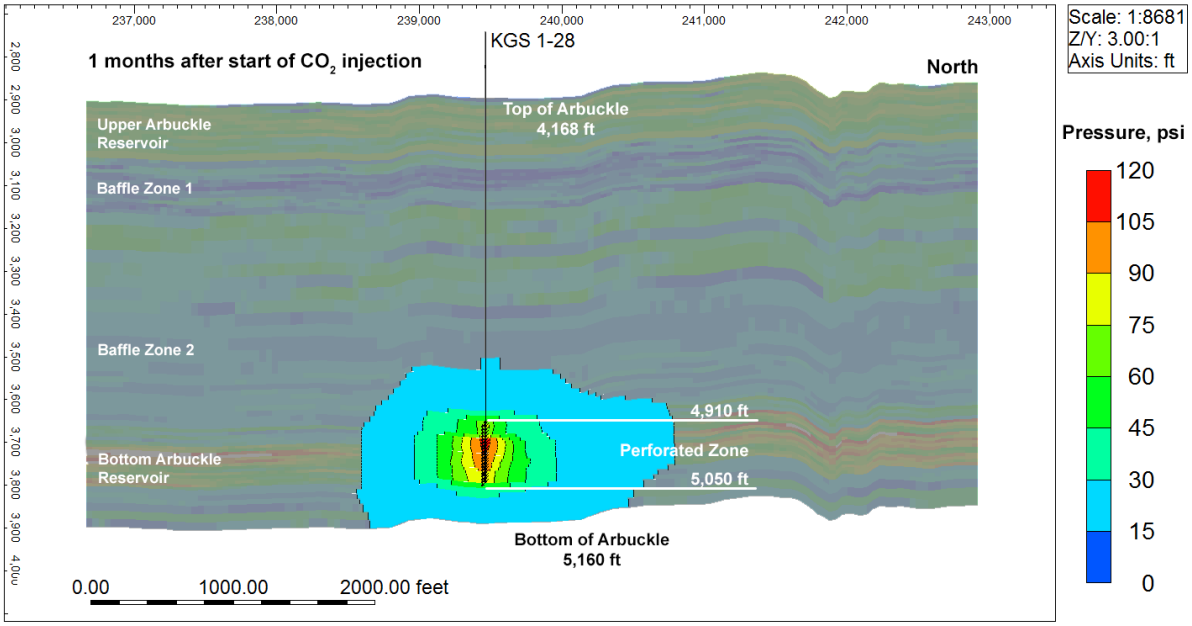

Figure 5.19a—Simulated increase in pressure in plan and cross-sectional view at one month from start of injection for the low permeability–low porosity (k-0.75/phi-0.75) alternative case, which resulted in the largest simulated pressures.

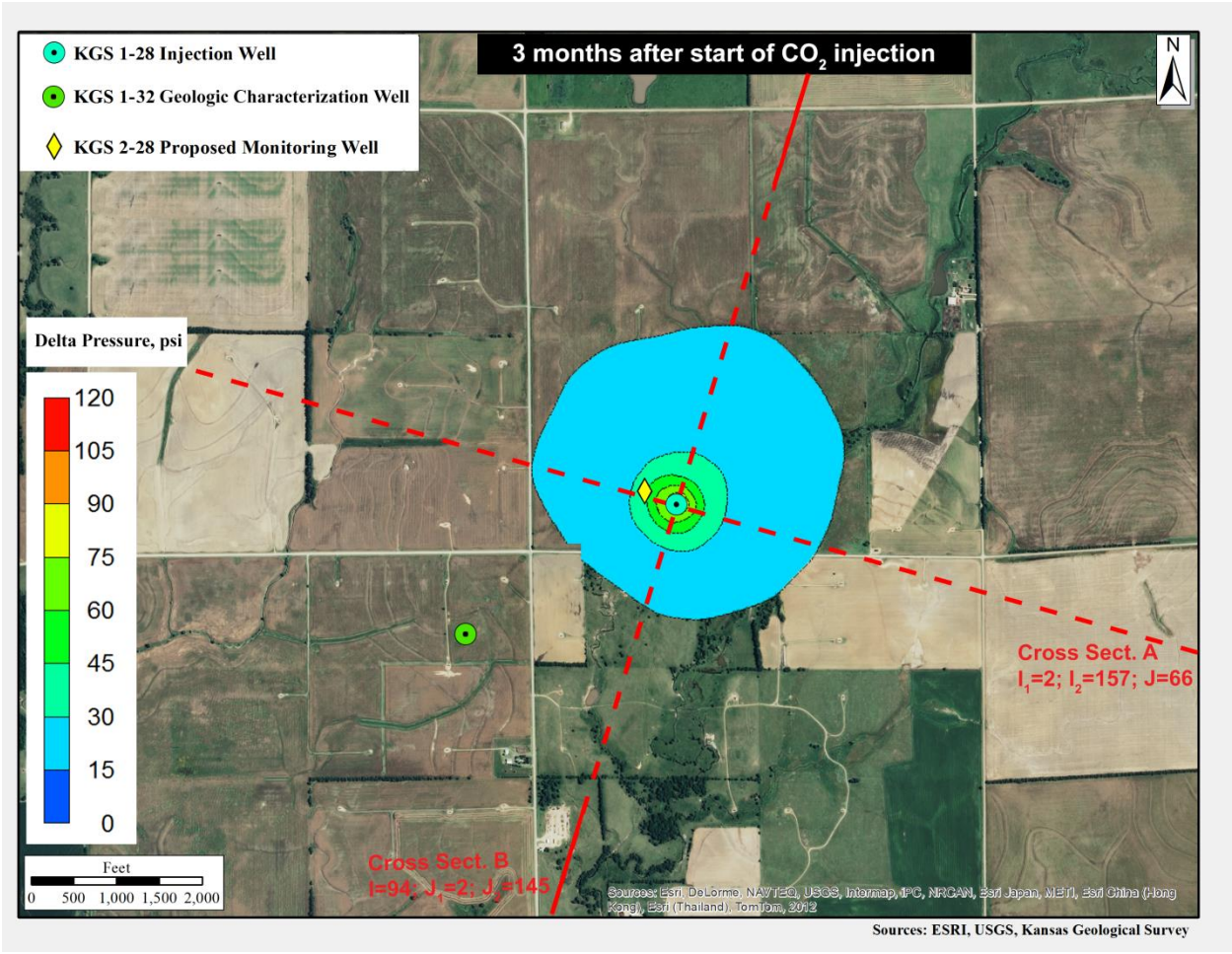

Sources: ESRI, USGS, Kansas Geological Survey

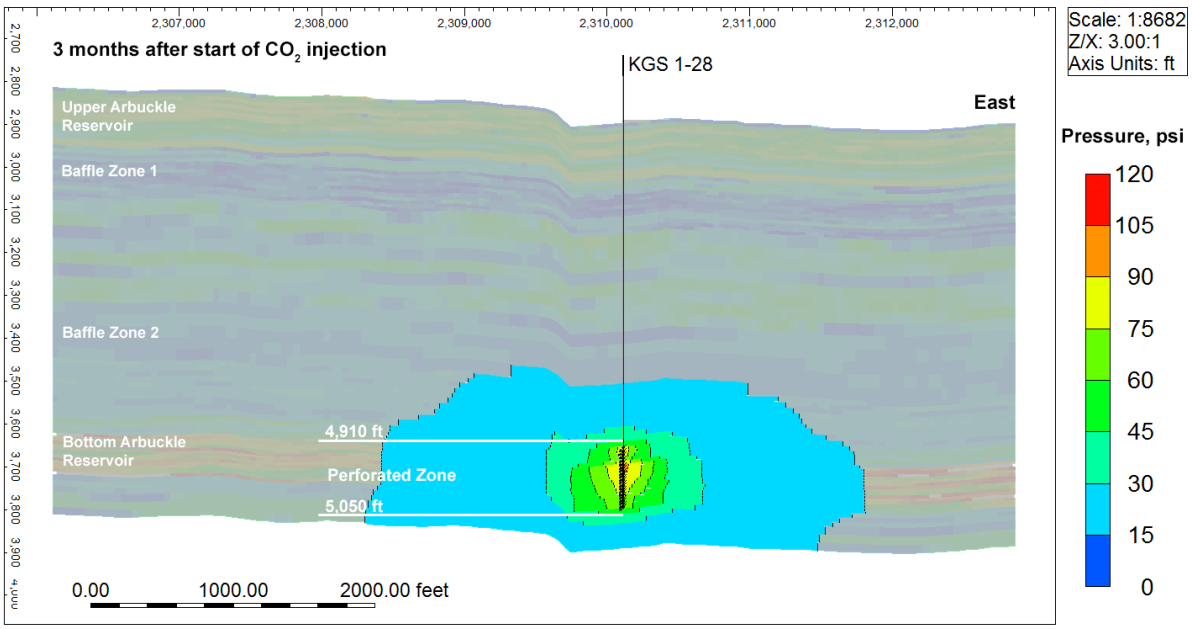

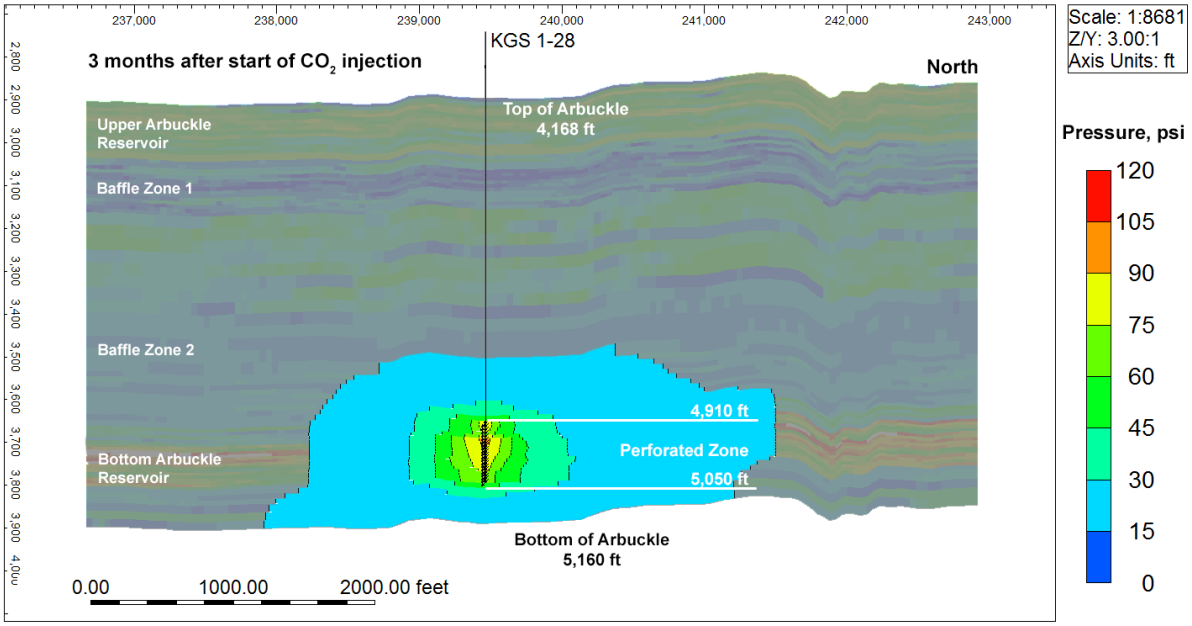

Figure 5.19b—Simulated increase in pressure in plan and cross-sectional view at three months from start of injection for the low permeability–low porosity (k-0.75/phi-0.75) alternative case, which resulted in the largest simulated pressures.

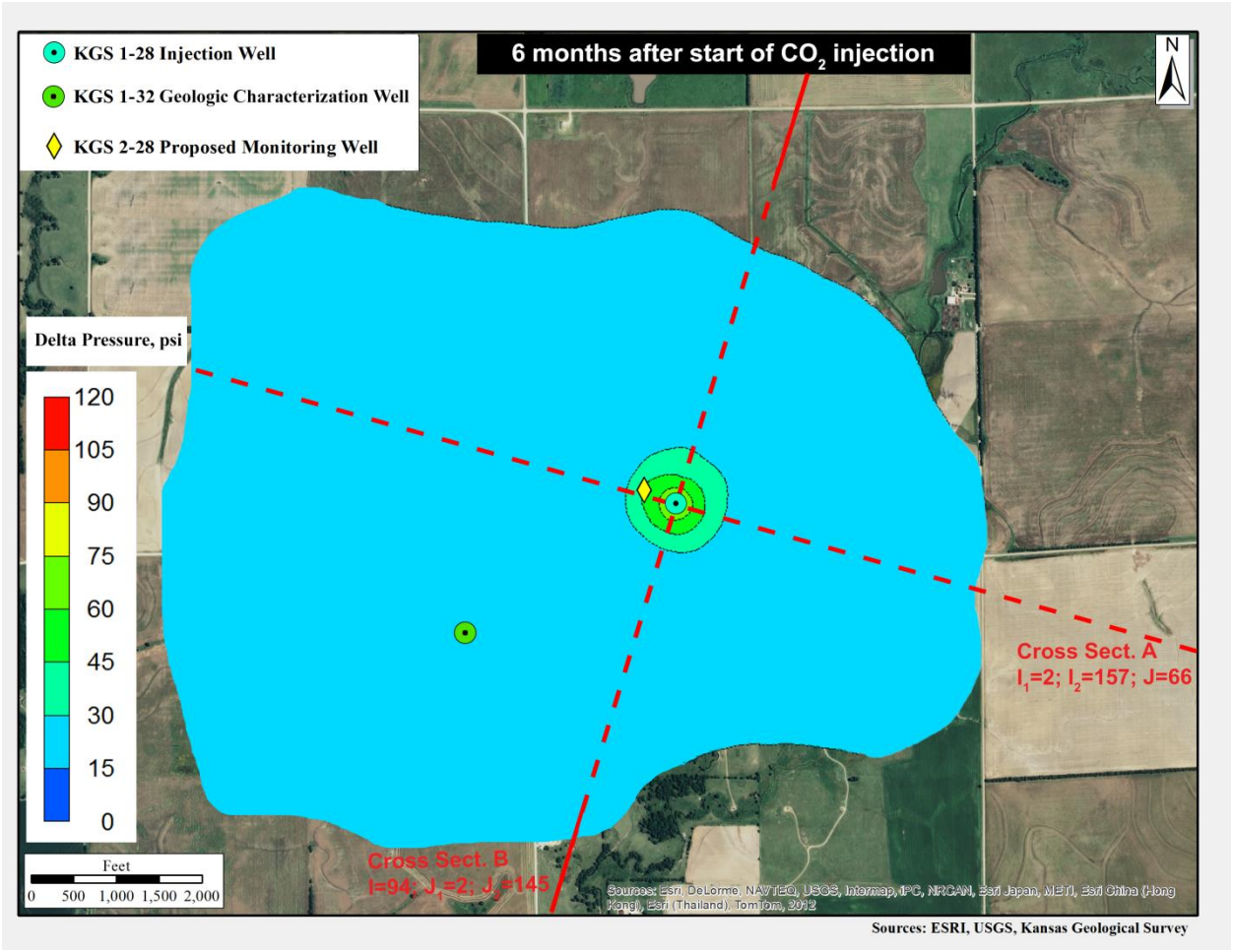
KGS 1-28 Injection Well
KGS 1-32 Geologic Characterization Well
KGS 2-28 Proposed Monitoring Well
6 months after start of CO2 injection
N
Delta Pressure, psi
120
105
90
75
60
45
30
15
0
Feet
0 500 1,000 1,500 2,000
Cross Sect. A
I1=2; I2=157; J=66
Cross Sect. B
I=94; J1=2; J2=145
Sources: Esri, DeLorme, NAVTEQ, USGS, Intermap, iPC, NRCAN, Esri Japan, METI, Esri China (Hong Kong), Esri (Thailand), TomTom, 2012
Sources: ESRI, USGS, Kansas Geological Survey

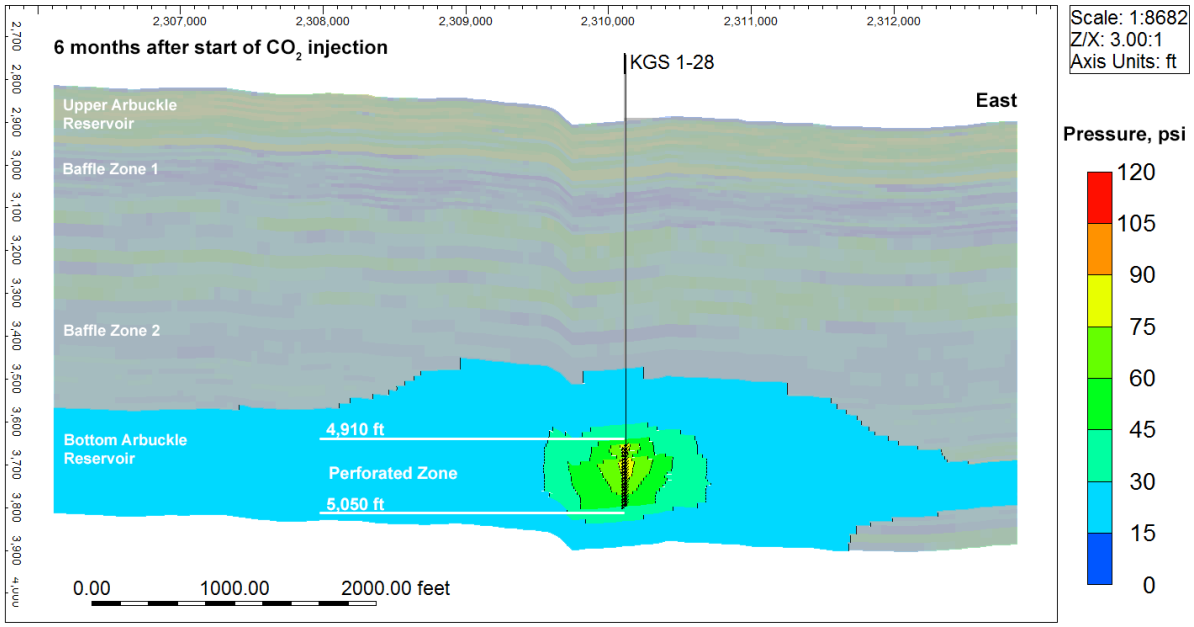
2,307,000
2,308,000
2,309,000
2,310,000
2,311,000
2,312,000
6 months after start of CO2 injection
KGS 1-28
East
Upper Arbuckle Reservoir
Baffle Zone 1
Baffle Zone 2
Bottom Arbuckle Reservoir
4,910 ft
Perforated Zone
5,050 ft
0.00
1000.00
2000.00 feet
Scale: 1:8682
Z/X: 3.00:1
Axis Units: ft
Pressure, psi
120
105
90
75
60
45
30
15
0

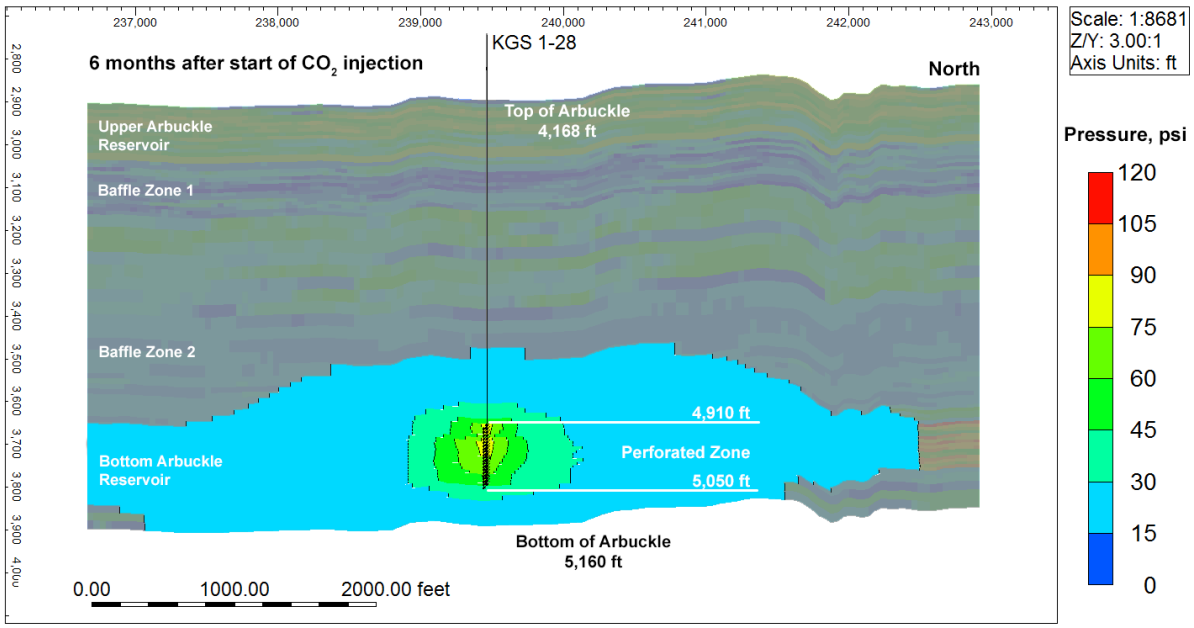

Figure 5.19c—Simulated increase in pressure in plan and cross-sectional view at six months from start of injection for the low permeability–low porosity (k-0.75/phi-0.75) alternative case, which resulted in the largest simulated pressures.

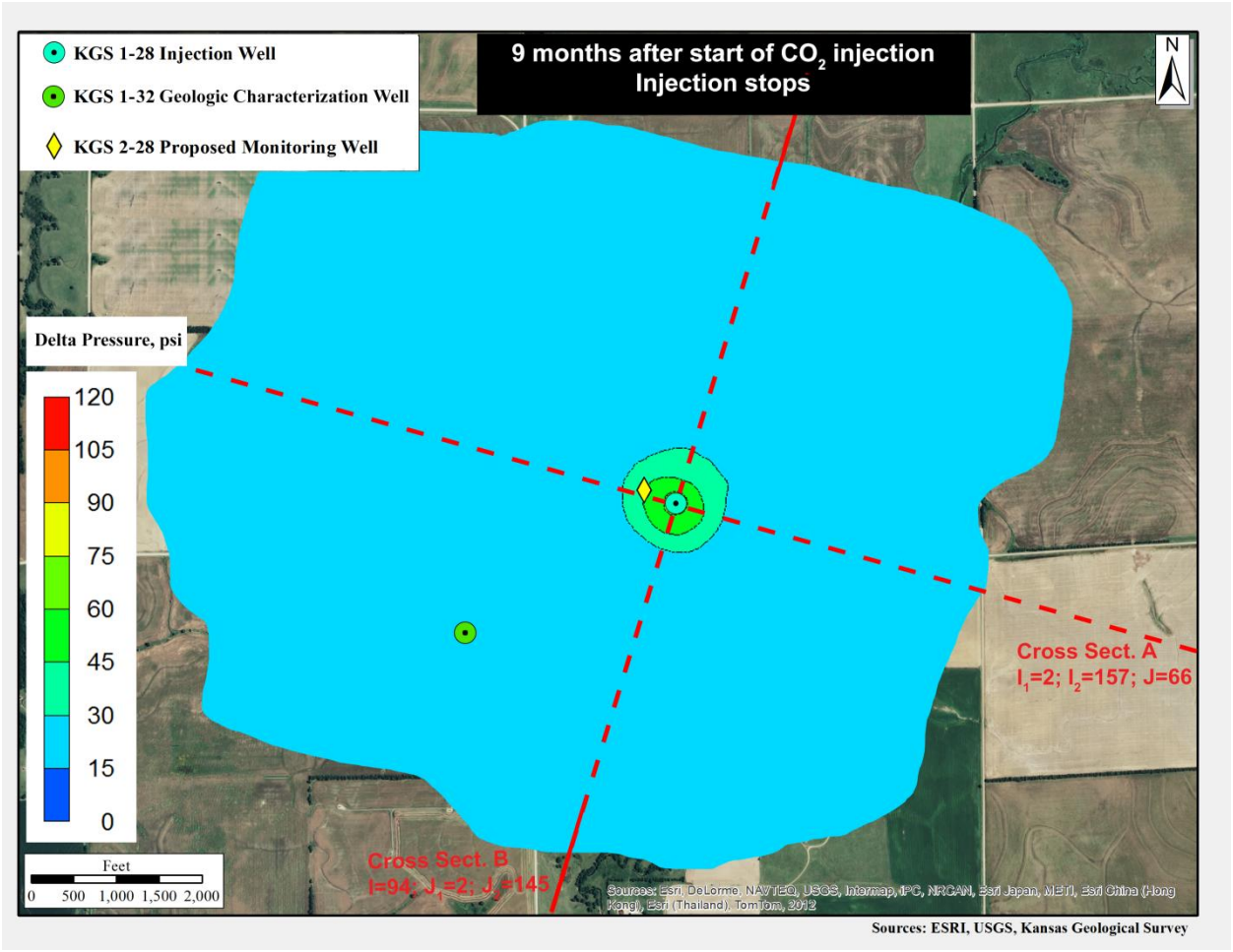
KGS 1-28 Injection Well
KGS 1-32 Geologic Characterization Well
KGS 2-28 Proposed Monitoring Well
9 months after start of CO2 injection
Injection stops
N
Delta Pressure, psi
120
105
90
75
60
45
30
15
0
Feet
0 500 1,000 1,500 2,000
Cross Sect. A
I1=2; I2=157; J=66
Cross Sect. B
I=94; J1=2; J2=145
Sources: Esri, DeLorme, NAVTEQ, USGS, Intermap, iPC, NRCAN, Esri Japan, METI, Esri China (Hong Kong), Esri (Thailand), TomTom, 2012
Sources: ESRI, USGS, Kansas Geological Survey

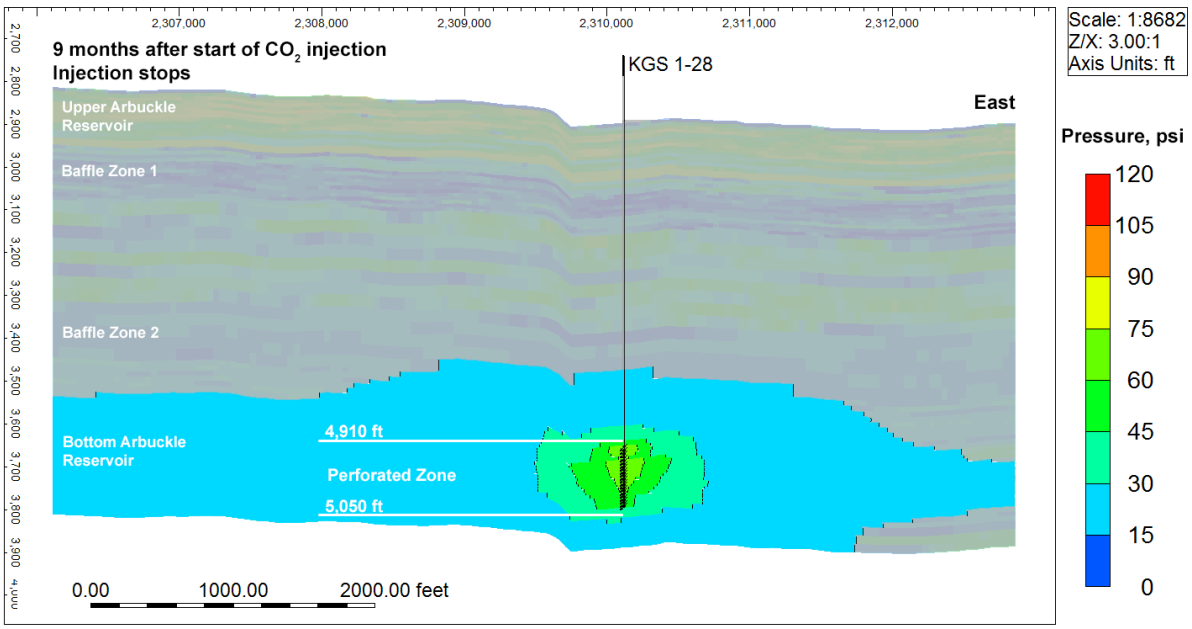
2,307,000
2,308,000
2,309,000
2,310,000
2,311,000
2,312,000
9 months after start of CO2 injection
Injection stops
KGS 1-28
East
Upper Arbuckle Reservoir
Baffle Zone 1
Baffle Zone 2
Bottom Arbuckle Reservoir
4,910 ft
Perforated Zone
5,050 ft
0.00
1000.00
2000.00 feet
Scale: 1:8682
Z/X: 3.00:1
Axis Units: ft
Pressure, psi
120
105
90
75
60
45
30
15
0

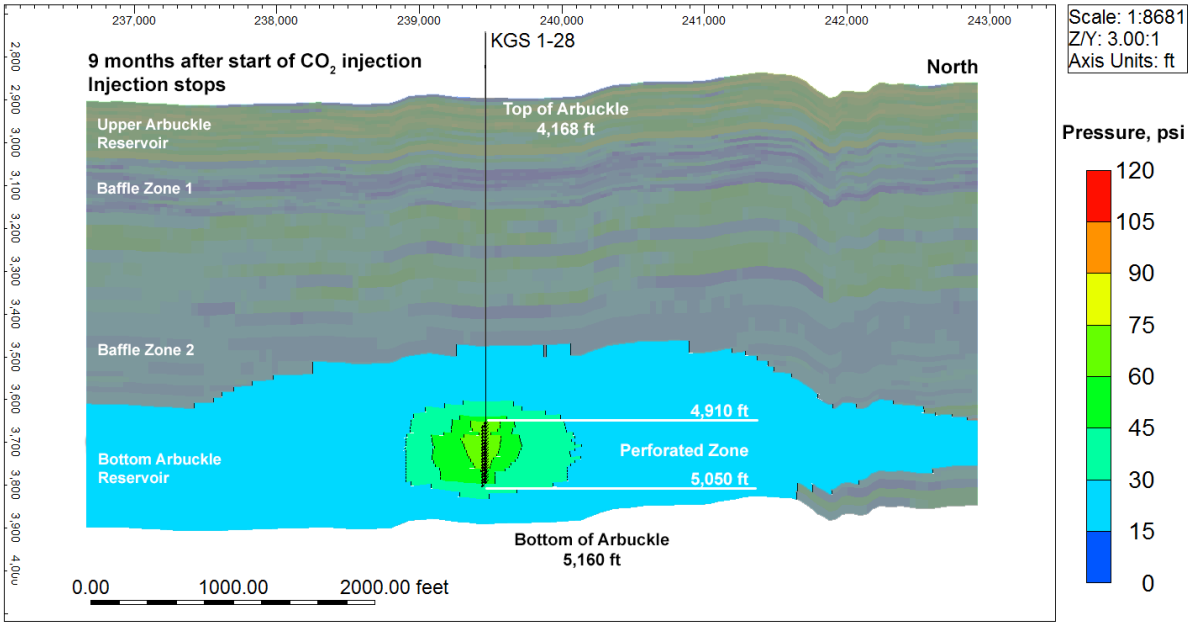

Figure 5.18d—Simulated increase in pressure in plan and cross-sectional view at nine months from start of injection for the low permeability–low porosity (k-0.75/phi-0.75) alternative case, which resulted in the largest simulated pressures.

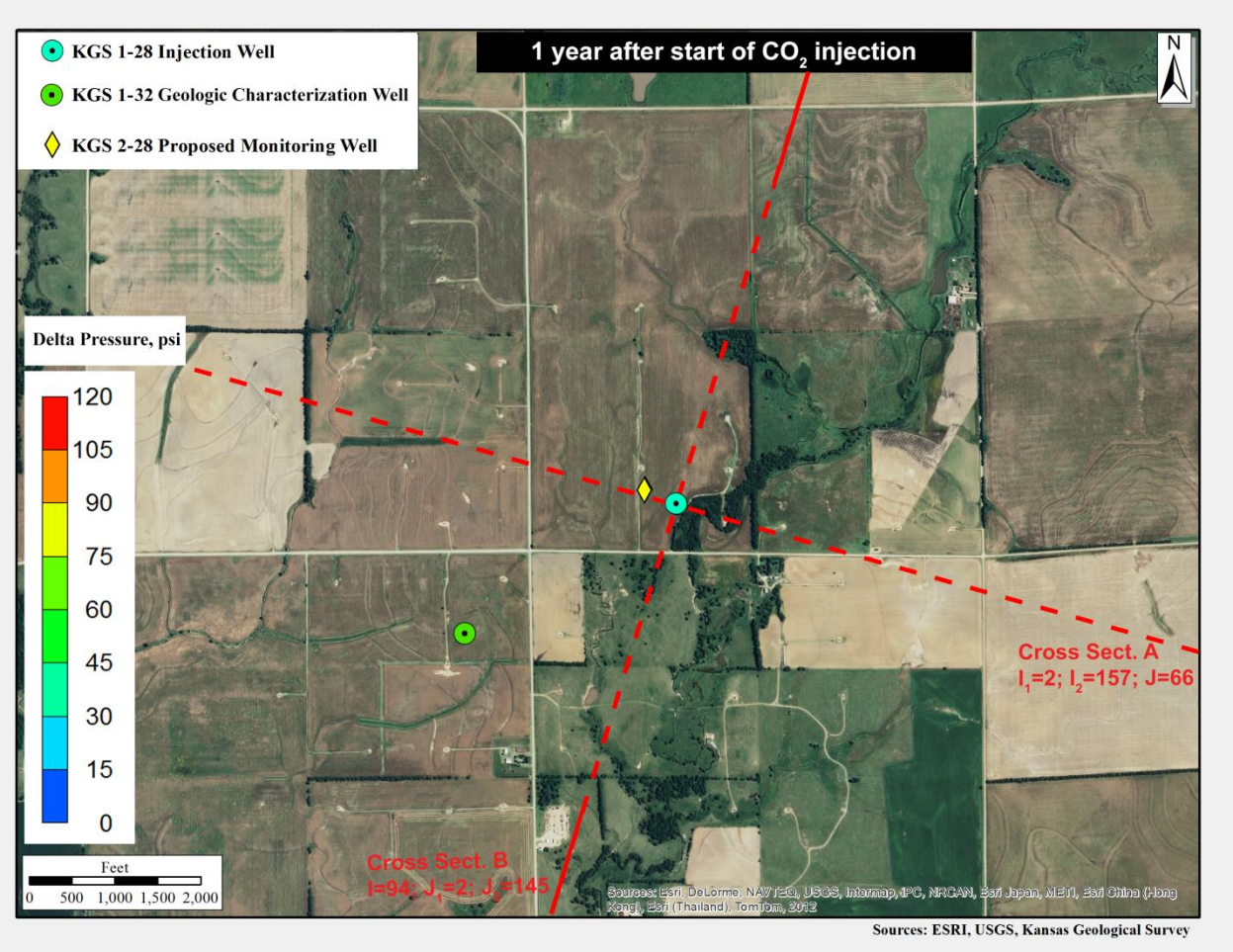

Sources: ESRI, USGS, Kansas Geological Survey

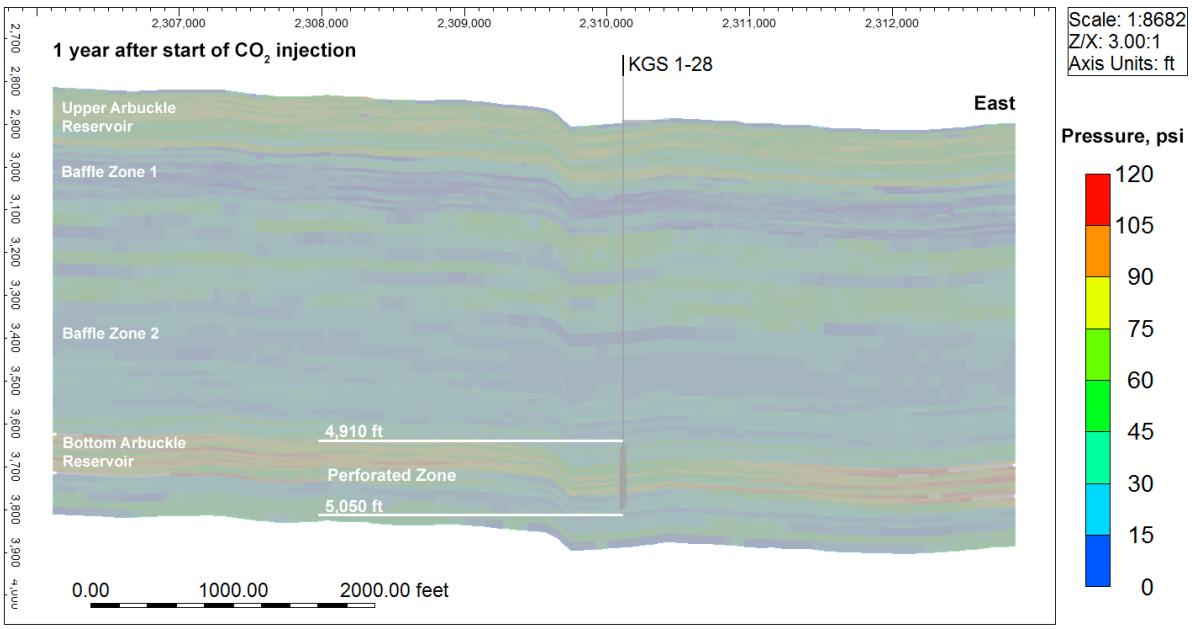

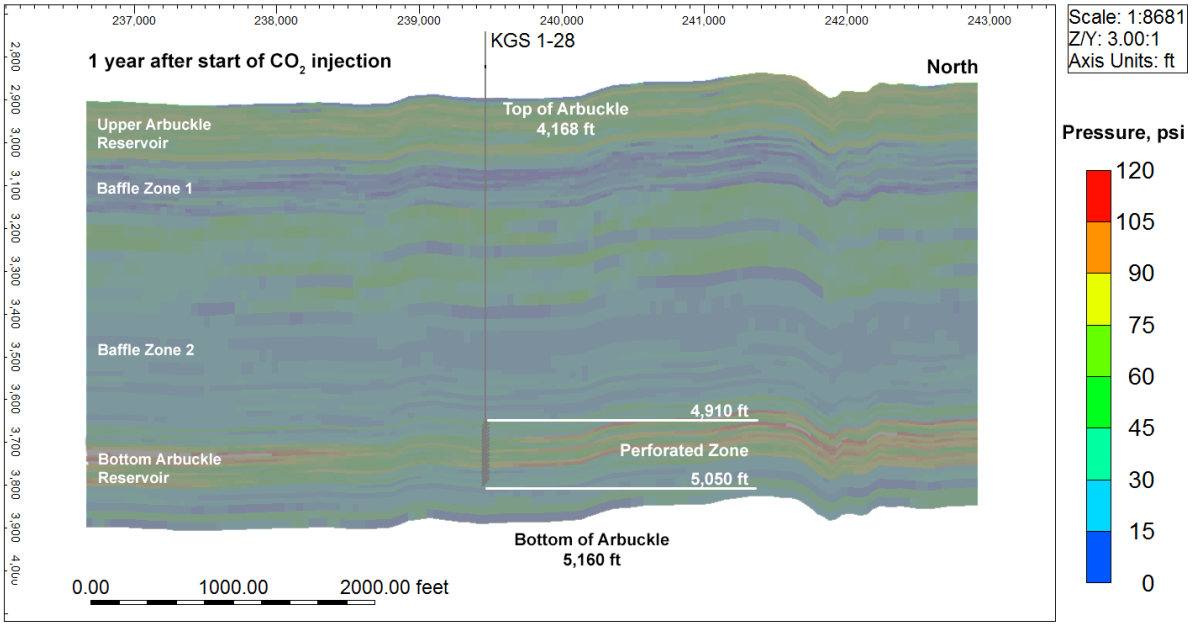

Figure 5.18e—Simulated increase in pressure in plan and cross-sectional view at one year from start of injection for the low permeability–low porosity (k-0.75/phi-0.75) alternative case, which resulted in the largest simulated pressures.

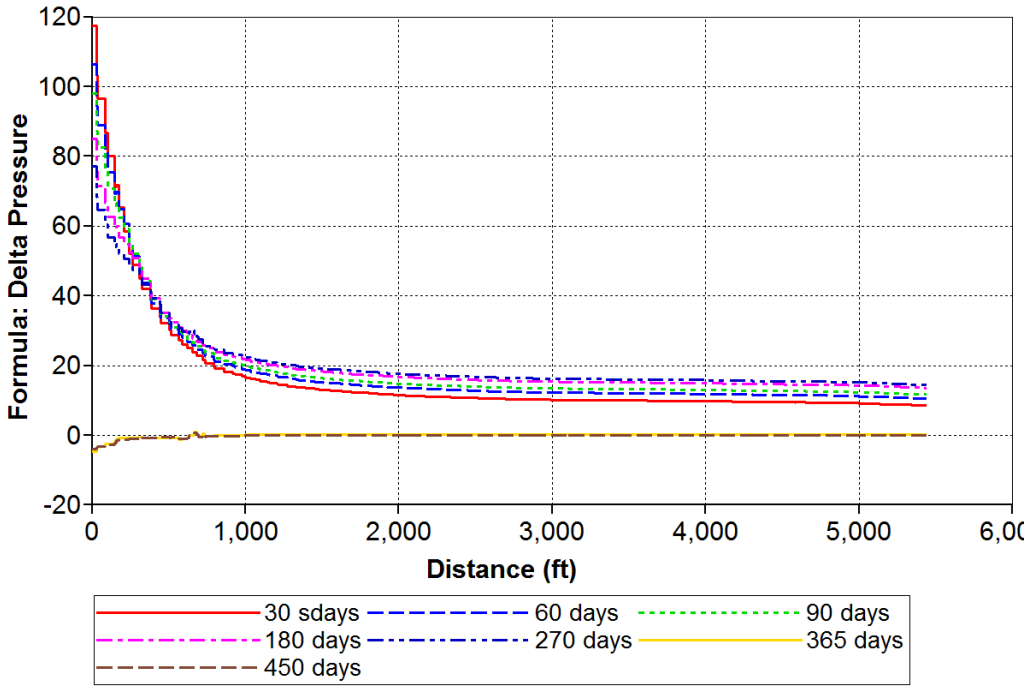

Figure 5.20—Pore pressure as a function of lateral distance from the injection well (KGS 1-28) at 7 time intervals for the highest induced pressure case (k-0.75/phi-0.75).